RESPONSES OF MURINE KERATINOCYTES TO OXIDATIVE STRESS

by ADRIENNE T. BLACK

A Dissertation submitted to the

Graduate School-New Brunswick

Rutgers, The State University of New Jersey

and

The Graduate School of Biomedical Sciences

University of Medicine and Dentistry of New Jersey

in partial fulfillment of the requirements

for the degree of

Doctor of Philosophy

Joint Graduate Program in Toxicology

written under the direction of

Jeffrey D. Laskin

and approved by

_____

_____

_____

_____

_____

_____

New Brunswick, New Jersey

May, 2007

ABSTRACT OF THE DISSERTATION

Responses of murine keratinocytes to oxidative stress

By ADRIENNE T. BLACK

Dissertation Director:
Jeffrey D. Laskin

Oxidative stress is well recognized as a major contributing factor in the development of cutaneous disease. The generation of reactive oxygen intermediates (ROI) damage cellular macromolecules, causing mutagenic DNA lesions, altered enzyme function, lipid peroxidation and inappropriate signaling. Induction of oxidative stress is associated with the onset of inflammation through production of arachidonic acid-derived lipid mediators including prostaglandins and leukotrienes although the mechanisms linking these two processes are unclear at this time. As the protective barrier of the body, the skin is exposed to many oxidants. Two such potent inducers of oxidative stress are the high energy wavelengths of the ultraviolet B (UVB) spectra (290-320 nm) and the redox-cycling herbicide paraquat (1,1'-dimethyl-4,4'-bipyridinium). In the present studies, we compared the effect of UVB and paraquat on the expression of antioxidant and arachidonic acid metabolism enzymes in undifferentiated and calcium-differentiated primary mouse keratinocytes. Using enzyme assays, we found that both UVB (2.5-25 mJ/cm^2) and paraquat (100 μM) generated ROI and were effective inducers of oxidative stress in these cells and that paraquat readily undergoes redox-cycling. Both agents

upregulated the expression of several antioxidant enzymes, measured using realtime PCR although a greater number of enzymes were induced by paraquat. UVB and paraquat equally upregulated eicosanoid enzyme expression; these enzymes included the cyclooxygenases, prostanoid synthases, lipoxygenases and leukotriene synthetic enzymes as well as the prostaglandin and leukotriene receptors. Using HPLC with fluorescence detection, UVB was found to modulate prostaglandin production. In both cell types, UVB caused a dose-dependent activation of the p38 and JNK MAP kinases. Akt kinase, however, was found to be activated only in undifferentiated cells with constitutive phosphorylation in differentiated cells. Inhibition of these enzymes markedly inhibited mRNA expression of several eicosanoid enzymes while other enzymes other were unaffected. Taken together, these data demonstrate that UVB light and paraquat effectively induce both antioxidant and eicosanoid biosynthetic enzymes in mouse keratinocytes and that activation of these pathways are regulated by MAP and Akt kinase activity. The elucidation of the keratinocyte response to oxidative stress is a necessary step to a better understanding of the effects of oxidants on the skin.

ACKNOWLEDGEMENTS

I want to thank the many people who helped and guided me through this project. I wish to thank my advisor, Dr. Jeffrey Laskin, for his support, encouragement and guidance throughout my thesis work. I also wish to thank my committee members, Dr. Donald Gerecke, Dr. Marion (Emmy) Gordon, Dr. Debra Laskin and Dr. Diane Heck for their support. I would like to acknowledgment the encouragement that I have received from all the JGPT faculty members over the years with a special recognition to Dr. Michael Gallo and Dr. Kenneth Reuhl. I wish also like to especially thank Dr. Michael Shakarjian at UMDNJ for his willingness to share his knowledge and skill in keratinocyte culture.

A big thank you to all my colleagues in the lab, both past and present: Josh Gray, Vladimir Mishin, Wendy Yang, Ruijin Zheng, Anna Vetrano, Shannon Gentile, members of the "other" Laskin lab: Carol Gardner, Vasanthi Sunil, Laurie Joseph, Li Chen, Agnes Connor and Kinal Patel as well as the other residents of the 4th floor: Rita Hahn, Yoke-Chen Chang and Ming-Wei Chao.

This project could not have been completed without the wonderful assistance of the administrative staff. Toni Myers, Bernadine Chmielowicz, Rosemary Hayes and Sandi Selby were exceptional their willingness to help negotiate the bureaucracies of Rutgers and UMDNJ.

DEDICATION

These pages are dedicated to my husband, Scott, whose love and support kept me going through the years and allowed me to complete this work.

TABLE OF CONTENTS

LIST OF FIGURES

LIST OF TABLES

LIST OF ABBREVIATIONS

BLT1	leukotriene B1 receptor
BLT2	leukotriene B2 receptor
COX-1	cyclooxygenase-1
COX-2	cyclooxygenase-2
$cPLA_2$	cytosolic phospholipase A_2
CRTH2	chemoattractant receptor-homologous molecule expressed on T helper type 2 cells
CysLT1	cysteinyl leukotriene receptor 1
CysLT2	cysteinyl leukotriene receptor 2
DAG	diacylglycerol
DCFH-DA	2', 7'-dicholorofluorescein-diacetate
DP	prostaglandin D_2 receptor
DPI	diphenyleneiodonium
EP1	prostaglandin E_2 receptor 1
EP2	prostaglandin E_2 receptor 2
EP3	prostaglandin E_2 receptor 3
EP4	prostaglandin E_2 receptor 4
FLAP	5-lipoxygenase activating protein
FP	prostaglandin F_2 receptor
GST	glutathione-S-transferase
GSTA	GST alpha
GSTM	GST mu

GSTP	GST pi
GPx-1	glutathione peroxidase-1
HETE	hydroxyeicosatetraenoic acid
HO-1	heme oxygenase-1
HPETE	hydroperoxyeicosatetraenoic acid
IP	prostaglandin I_2 receptor
5-LOX	5-lipoxygenase
8-LOX	8-lipoxygenase
12-LOX-epi	12-lipoxygenase-epidermal type
12-LOX-plt	12-lipoxygenase platelet-type
15-LOX	15-lipoxygenase
LTA_4	leukotriene A_4
LTC_4	leukotriene C_4
MAG	monoacylglycerol
mPGES-1	microsomal prostaglandin E synthase-1
mPGES-2	microsomal prostaglandin E synthase-2
MT-2	metallothionein-2
NE-OTf	2-(2,3-naphthalimino)ethyl-trifluoromethanesulphonate
NQO1	NAD(P)H quinone oxidoreductase 1
PLC	phospholipase C
PGD_2	prostaglandin D_2
PGDS	prostaglandin D_2 synthase
PGE_2	prostaglandin E_2

PGF_2	prostaglandin F_2
PGFS	prostaglandin F_2 synthase
PGH_2	prostaglandin H_2
PGI_2	prostaglandin I_2 (prostacyclin)
PGIS	prostaglandin I_2 synthase
SOD	superoxide dismutase
TXA_2	thromboxane A_2
TXAS	thromboxane A_2 synthase

RATIONALE

Oxidative stress is defined as an imbalance between the production of reactive oxygen intermediates (ROI) and the cellular antioxidant defense mechanisms. An excess of ROI causes oxidative damage to cellular macromolecules including nucleic acids, proteins and lipids, resulting in many adverse effects including the formation of mutagenic lesions, altered enzyme function, lipid peroxidation and inappropriate cell signaling. This oxidative stress-induced damage is well recognized to have a significant role in the pathogenesis of many diseases and is considered to be a major contributing factor in the development of chronic inflammation. These two processes are related but the mechanisms involved are not completely understood at this time. Oxidative damage usually occurs in conjunction with the release of arachidonic acid and subsequent production of eicosanoid metabolites such as prostaglandins and leukotrienes. These metabolites are potent lipid mediators that initiate and propagate the inflammatory response and whose expression is tightly regulated through expression of several enzymes.

Ultraviolet B (UVB) light and paraquat are examples of potent oxidative stressors to which skin may be exposed. The high energy wavelengths (290-320 nm) of UVB readily generate ROI in skin and the resulting oxidative damage causes not only DNA damage but the initiation of an inflammatory response as well. The herbicide paraquat is a potent inducer of oxidative stress whose toxicity results from ROI generated by redox cycling reactions. Paraquat has been shown to cause pulmonary inflammation but little investigation has been completed on the skin at this time.

These experiments were performed using an in vitro epidermal model. Using established protocols, undifferentiated keratinocytes were isolated from neonatal murine epidermis and differentiation was induced through increased calcium concentrations in the medium. The undifferentiated and differentiated keratinocytes represent the basal and suprabasal cells of the epidermis, respectively.

The aim of this dissertation was to determine the cellular responses by keratinocytes to oxidative stress as induced by UVB light and paraquat. The general hypothesis for this work is stated as follows:

> Oxidative stress is induced by UVB light and paraquat in keratinocytes and the cell response is evidenced by upregulation of the antioxidant and eicosanoid biosynthetic pathway enzymes as well as increased eicosanoid production.

The in vitro model system consisting of undifferentiated and differentiated keratinocytes allowed a secondary hypothesis to be investigated which is:

> Keratinocyte differentiation is a major regulatory factor mediating the cellular responses to oxidative stress in regards to the expression of the antioxidant and arachidonic acid metabolizing enzymes.

These hypotheses will be investigated through four specific aims as listed below.

1. Characterization of the effects of UVB light on antioxidant enzyme expression.
2. Characterization of the effects of paraquat on antioxidant enzyme expression.
3. Determination of eicosanoid production and induction of the eicosanoid biosynthetic enzymes
4. Determination of the induction of the eicosanoid biosynthetic enzymes by paraquat enzymes by UVB light.

INTRODUCTION

A. The skin

1. Structure

The skin is composed of three layers: the epidermis, the dermis and the subcutaneous layer. The epidermis is a keratinized stratified squamous epithelium derived from ectoderm and forms the protective external surface of the body. The predominant epidermal cell type is the keratinocyte, comprising approximately 90% of the cellular population . Basal and suprabasal keratinocytes are metabolically active cells, capable of not only protein and lipid synthesis, but the production of mediators such as cytokines and arachidonic acid metabolites that are integral to the initiation and propagation of signal transduction pathways involved in such processes as wound healing and inflammatory responses . In this manner, keratinocytes maintain epidermal homeostasis. Supplementary cell types, in significantly smaller numbers, also reside within the epidermis and play a more supportive role. Interspersed among the basal keratinocytes are melanocytes (approximately 5% of the cellular total). These cells produce melanin, the molecule responsible for the pigmentation of the skin . By absorbing the energy of solar ultraviolet radiation, melanin protects the skin from damage . Langerhans cells (2-5%) are dendritic cells within the suprabasal layers whose function is to process and present antigens acquired in the epidermis to lymphoid T cells as a component of the dermal immune response . Merkel cells (6-10%) are located within the basal layer and maintain contact with nerve endings for tactile sensory control .

The epidermis is supported by the dermis, a fibro-elastic dense connective tissue containing blood vessels from which nutrients and oxygen diffuse upwards through the

basement membrane to the cells of the epidermis . The primary cell type of the dermis is the fibroblast and these cells are responsible for fibrillar protein synthesis . The dermis provides the support basis and dermal elasticity of the skin through the deposition of collagen and elastin fibrils, respectively . Neural processes are also abundant throughout the dermis and the ends of these processes may extend into the lower layers of the epidermis in some areas . The dermis is attached to the subcutaneous layer or hypodermis, a loose connective tissue containing large numbers of adipocytes . This adipose tissue serves not only as a storage material for future energy needs but provides much of the thermoregulatory function of the skin. Additional epithelial structures including hair follicles, sweat and sebaceous glands, and nails arise from the dermis and subcutaneous layer and exit through the epidermis .

The epidermis is composed of a basal layer of undifferentiated keratinocytes overlaid with successive layers of cells in varying stages of terminal differentiation . The basal layer, the stratum germinativum, is a single cell layer of undifferentiated keratinocytes attached to the basement membrane by hemidesmosomes . These cells are cuboidal in shape with large nuclei with highly basophilic-staining cytoplasm. Functionally, these cells are the proliferative component of the epidermis and are responsible for the continuous renewal of the skin. Cell division is asynchronous with one daughter cell preserving its undifferentiated state and remaining in the basal layer while the other daughter cell moves into the upper layers of the epidermis . Once removed from contact with the epidermal basement membrane, keratinocytes begin the process of terminal epidermal differentiation.

Immediately above the basal layer is the stratum spinosum. These “prickle cells” form cytoplasmic projections containing keratin fibrillar proteins . These keratin filaments are anchored at desmosomes in the cell membranes and link adjacent cells to one another in a lattice formation. The differentiation process is continued in the stratum granulosum. These cells are squamous in shape and are characterized by the presence of keratohyalin granules in the cytosol . The granule cells also synthesize lipids and fatty acids as well as acid hydrolases and proteases which are stored in membrane-bound vesicles known as lamellar bodies . These lamellar bodies are extruded into the intercellular spaces at which time, the membranes are lysed, releasing the lipids to form a water-insoluble barrier . As the cells move into the outermost layer of the stratum granulosum, lysosomal membranes rupture, effectively killing the cells and finalizing keratin synthesis. In areas of thick skin such as the soles or palms, an additional layer is present, the stratum lucidum. This is a transitional layer with translucent cells characterized by their loss of nuclei and cytoplasmic organelles.

The outermost epidermal layer is the stratum corneum and is comprised of cornified or keratinized cells (corneocytes). Although corneocytes are dead cells without nuclei or organelles, the cell membranes remain intact, enclosing the keratins and lipids synthesized during differentiation. These cells are fused and flattened and form an impermeable barrier due to filament cross-linking . As the cells move through the stratum corneum, the lipid content decreases and the connections between the cells are eroded. Ultimately, the corneocytes are sloughed off the external surface as squames.

2. <u>Differentiation process</u>

Perhaps the best investigated component in the differentiation process has been the successive changes that occur in protein synthesis. Of primary importance are the keratin proteins for their role as structural proteins as well as their use as differentiation markers. Undifferentiated keratinocytes produce keratin 5 and keratin 14 . As the cells begin to differentiate, these keratins are replaced by the newly synthesized keratins 1 and 10 which are formed as thin filaments . The spinous cells also produce involucrin which is cross-linked by transglutaminases to form a scaffold for the assembly of the cornified envelope directly beneath the cell membrane . Transglutaminases are a family of calcium-dependent activated enzymes that form ε-(γ-glutamyl) lysine bonds between adjacent proteins, thereby cross-linking the molecules . As the process progresses, the keratins associate with profilaggrin, the precursor of filaggrin, in the keratohyalin granules . Filaggrin binds the keratin filaments into tight macrofibers and these fibers are added to the developing cornified envelope. As a consequence of the rearrangement of the keratin filaments, the keratinocyte is forced into its characteristic squamous shape. The cells of the upper granular layer now synthesize loricrin, the primary component of the cornified envelope . Loricrin is stored in granules , released in the upper regions of the granular layer and cross-linked by transglutaminases . With the disintegration of the cell membrane by proteases, the formation of the corneocyte is complete.

Additionally, several classes of lipids including fatty acids, cholesterol and ceramides are synthesized by the cells of the stratum granulosum. Once produced, lipids are stored in granules known as lamellar bodies which are then extruded into the intercellular spaces within the scaffold of the cornified envelope . Additionally, some of these lipids, ceramides in particular, are also cross-linked with the proteins of the stratum

corneum. This crosslinking of fibers and proteins with lipids filling the spaces has been described as the “bricks and mortar” structure of the epidermis.

The initial signal setting a keratinocyte on the path of terminal differentiation is not known. However, numerous transcription factors have been shown to play critical roles in this process. Activator protein 1 (AP-1) has been shown to play a critical role in keratinocyte differentiation by regulating the expression of keratins 5 and 14 , involucrin and profilaggrin . The expression of the subunits of AP-1, c-fos and c-jun, is differentiation-dependent with c-fos localized in the basal and spinous layers while c-jun was detected in the granular layer . This increase in c-jun expression correlates with AP-1 DNA binding following calcium-induced activation of protein kinase C (PKC) . Additional transcription factors involved in the differentiation process include CCAAT/enhancer binding protein beta (C/EBPbeta) for upregulation of keratin 1 and keratin 10 expression and Notch 1 for keratin 1 and involucrin expression . These transcription factors may also act in concert to upregulate the expression of differentiation markers. For example, in differentiated keratinocytes, loricrin transcription is upregulated in response to of c-Jun, SP-1 and p300/CBP DNA binding . In addition, activation of nuclear receptors, particularly those of the peroxisome proliferators-activated receptor (PPAR) family, is also a key element in the differentiation process .

3. Culture of keratinocytes

Several models systems are available to investigate the actions of xenobiotics on the skin. The effects on the entire skin may be determined in situ using whole animals or dermal explants from either humans or animals. While these studies are useful in

analyzing the global effects of a particular agent on the skin, they can not provide detailed mechanistic information for a particular cell type such as the keratinocyte. By culturing these cells, it is possible to examine the alterations induced at the molecular and cellular levels. Thus, cultured keratinocytes serve as an effective in vitro model system of the epidermis for determination of the cellular responses to xenobiotic toxicity.

Keratinocyte isolation is accomplished by removing the skin and dissociating the epidermis from the dermis usually by incubation with trypsin. The epidermis is then minced to release individual cells. At the same time, fibroblasts are isolated from the dermis, grown to confluency and changed to a low-calcium medium. This medium is then harvested as the fibroblast-conditioned medium and contains assorted growth factors secreted by the fibroblasts. Mouse keratinocytes, unlike their human counterparts, require extracellular matrix and do not grow directly on the plastic of routine culture vessels**.** In general, this requirement is met by coating the flasks with either collagen I or collagen IV.

Once seeded, keratinocytes are grown in the low-calcium fibroblast-conditioned medium. Keratinocytes that are cultured in a low calcium (> 0.1 mM) medium are phenotypically similar to the undifferentiated cells of the basal layer . As differentiation results in the loss of proliferative capability, this procedure ensures that the cultures will be composed of only undifferentiated keratinocytes. Additionally, the optimum medium for keratinocytes does not meet the requirements for either melanocytes or fibroblasts, thereby excluding these cells from the cultures.

Differentiation is then induced through the addition of calcium to the medium. Increased calcium concentrations (< 0.1 mM) result in the rapid differentiation of the

keratinocytes at both the morphological and biochemical levels . Keratinocytes in higher calcium medium assume a squamous morphology, become stratified, form desmosomes and adherens junctions and undergo growth arrest . Additionally, these cells may express such differentiation-associated proteins as keratins 1 and 10, filaggrin, involucrin and loricrin, depending upon the degree of differentiation .

B. Oxidative Stress

1. Introduction

A consequence of aerobic metabolism is the generation of reactive oxygen intermediates (ROI) through the reduction of molecular oxygen. Oxidative stress is generally defined as an imbalance between the levels of ROI and endogenous antioxidants where the ROI concentrations are in excess of the detoxification capacity of the antioxidants . This imbalance alters the metabolic regeneration of antioxidants, initiates signal transduction pathways and causes intracellular damage and, ultimately, may lead to reduced mitochondrial function and apoptosis or DNA damage, mutations and initiation of carcinogenesis .

2. Formation of reactive oxygen intermediates (ROI)

The formation of ROI results from the incomplete reduction of molecular oxygen. In this series of reactions, molecular oxygen undergoes a four-electron reduction to water and, in the process, superoxide anion ($O_2^{-\cdot}$), hydrogen peroxide (H_2O_2) and hydroxyl radical ($^{\cdot}OH$) are formed as shown in the following reactions.

1) $O_2 + e^- + H^+ \longrightarrow O_2^{-\bullet} + H^+$ Superoxide anion

2) $O_2^{-\bullet} + e^- + H^+ \longrightarrow H_2O_2$ Hydrogen peroxide

3) $H_2O_2 + e^- + H^+ \longrightarrow H_2O + {}^{\bullet}OH$ Hydroxyl radical

4) ${}^{\bullet}OH + e^- + H^+ \longrightarrow H_2O$

The reactivity of these radicals is determined by their half-life . The hydroxyl radical is extremely reactive, having a half-life of 10^{-9} seconds, and, therefore, is able to diffuse only approximately only two molecular diameters from its point of origin before reacting with any cellular macromolecule at hand . Superoxide anion is less reactive with a half-life of 10^{-6} seconds. Although not as reactive as other radicals, superoxide production is a critical event as it leads to the formation of additional ROI as shown in Figure 1, including hydrogen peroxide and hydroxyl radicals .

Hydroxyl radicals can also be generated through the interaction of metal ions with superoxide anion or hydrogen peroxide. Transition metals such as iron or copper have been identified as catalysts in these reactions . Iron, in particular, is known to generate hydroxyl radicals through reduction of hydrogen peroxide when present in its free form, Fe^{2+}, as described in the Fenton reaction :

$$Fe^{2+} + H_2O_2 + H^+ \longrightarrow Fe^{3+} + {}^{\bullet}OH + OH^-$$

In order to prevent the formation of the highly reactive hydroxyl radicals, the state of iron is tightly controlled so that Fe^{2+} is not found in the cell and iron is sequestered in ferritin as Fe^{3+} . Increases in the concentration of free intracellular iron (Fe^{2+}), however, may result from either the oxidation of Fe^{3+} by superoxide anion or by the release of Fe^{2+} through the degradation of iron-containing enzymes and ferritin .

Although hydrogen peroxide is not a radical, it is still considered a potent oxidant. Due to its lack of charge, it can diffuse great distances from its point of origin and

traverse cell membranes . As mentioned previously, hydrogen peroxide can be reduced to the very dangerous hydroxyl radical in the presence of redox-active metals. It is this potential for hydroxyl radical generation that forms the basis for the inclusion of hydrogen peroxide in the list of reactive oxygen intermediates.

There are also several radicals, produced in subsequent reactions, which are important in generating oxidative stress. These molecules include the alkoxyl radical ($RO^{\cdot}$), the peroxyl radical ($ROO^{\cdot}$) and the organic hydroperoxide (ROOH). These radicals are formed primarily in the lipid peroxidation and chain propagation reactions. Singlet molecular oxygen ($^1O_2$) is produced through photosensitized chemical reactions and is a very reactive radical important in the oxidation of lipid and other cellular macromolecules .

3. Sources of ROI

a. Endogenous sources

The majority of endogenously ROI is generated as by-products of the reduction of oxygen by cytochrome *c* oxidase in the mitochondrial electron transport chain . It is has been estimated that up to 4% of the total oxygen delivered to the mitochondria is incompletely reduced due to leakage of electrons , forming superoxide anion and hydrogen peroxide .

Other enzymes are also involved in the generation of ROI. Electron leakage from cytochrome P450 reductase generates superoxide anion in the endoplasmic reticulum . In the liver, P450-mediated superoxide generation has been shown to constitute a substantial percentage of the total endogenous ROI production . Xanthine oxidase-catalyzed

reduction of cytochrome *c* also generates superoxide which has been implicated in the resulting oxidative damage following ischemic injury . ROI are produced by neutrophils during the respiratory burst as part of the normal functioning of the immune system . In this process, NADPH oxidase reduces oxygen to superoxide which, in turn, is reduced to hydrogen peroxide. Myeolperoxidase uses hydrogen peroxide to oxidize chloride to form hypochlorous acid which can chlorinate amines or be reduced by superoxide to generate hydroxyl radicals .

b. Exogenous sources

Reactive oxygen intermediates are readily produced by environmental sources such as ionizing radiation and ultraviolet light. Ionizing radiation includes gamma and X-rays as well as nuclear fission by-products such as alpha and beta particles. These high energy particles are ionize intracellular water molecules, inducing radiolytic fission and generating hydroxyl radicals .

$$H_2O \longrightarrow 2 \cdot OH$$

Ultraviolet (UV) light is defined as those wavelengths from 200 to 400 nm of the electromagnetic spectrum with ultraviolet A (UVA) (320-400 nm) and ultraviolet B (UVB) (280-320 nm) as the UV components of sunlight. Both UVA and UVB are known to generate reactive oxygen intermediates (ROI) although by different mechanisms. The higher energy wavelengths of UVB light can generate ROI directly with hydrogen peroxide as the primary product formed . Hydrogen peroxide molecule is then reduced to hydroxyl radical as previously described.

Additionally, the photon energy may be absorbed by molecules in the skin referred to as chromophores or photosensitizers. These molecules may be endogenously produced or absorbed either through ingestion as in phytochemicals or pharmaceuticals or through application as in cosmetics . DNA is a known chromophore for UVB light, efficiently absorbing the ultraviolet energy and causing the production of hydroxyl radicals leading to nucleic acid oxidation .

The longer UVA wavelengths, however, are less energetic than those of UVB and can not directly generate ROI and requires the use of chromophores to indirectly produce ROI . Nucleic acids do not absorb energy in the UVA regions but many other molecules such as porphyrins, quinones and flavins are effective photosensitizers . These molecules are excited through absorption of the UVA photons and transfer this energy to oxygen, thereby generating singlet oxygen .

A common mechanism by which metals and chemicals produce ROI is through redox cycling . Redox cycling occurs when the parent compound is reduced or oxidized by one electron with that electron being transferred to an intermediate compound. The intermediate immediately transfers the electron to molecular oxygen, forming superoxide anion and regenerating the parent compound. In the presence of an unlimited supply of oxygen and reducing equivalents, the compound is continuously reduced and re-oxidized with an unremitting generation of superoxide anion.

The herbicide paraquat (1,1'-dimethyl-4,4'-bipyridinium) is a prime example of a redox cycling compound that generates oxidative stress through the production of superoxide anion. Initially, paraquat undergoes a single electron reduction in the presence of cellular reducing equivalents such as NADPH or glutathione, forming the paraquat

radical via NAD(P)H oxidase . In the presence of oxygen, the paraquat radical is rapidly oxidized back to the parent compound with the concomitant transfer of the extra electron to oxygen, forming superoxide anion . This, in turn, can generate additional reactive oxygen intermediates (ROI) including hydrogen peroxide and hydroxyl radicals .

4. Oxidative damage

At low concentrations, ROI act as mediators and signaling molecules in numerous pathways essential to cellular homeostasis including proliferation, differentiation and apoptosis . At higher concentrations, however, oxidative stress is induced, resulting in DNA damage and mutation, lipid peroxidation, inappropriate or altered signal transduction pathways and protein degradation .

Oxidation of DNA results in the formation of lesions that are recognized as mutagenic and serve contributing factors in the initiation of carcinogenesis. Hydroxyl radicals react with DNA bases to form the adducts of which, 8-oxo-7,8 -dihydrodeoxyguanosine (8-oxo-dG) is the most common . 8-oxodG induces A-T → C-G transversions which cause mispairing during replication and result in amino acid substitutions . These lesions have proven to be mutagenic and, in ultraviolet B-induced skin cancers, are known as the "UVB signature" mutations . Additional DNA-hydroxyl radical reactions result in the formation of pyrimidine glycols and hydroperoxides . Hydroxyl radical-mediated hydrogen abstraction from the deoxyribose backbone can result in single strand breaks .

Protein oxidation results in either a loss of or altered function . These effects may be due to conformational changes resulting from covalent binding of ROI to the side

chains of amino acid residues , most commonly cysteine, tyrosine and methionine . For example, the sulfhydryl groups of cysteines may undergo oxidation, leading to disulfide bond formation. Additionally, protein radicals, formed due to hydrogen abstraction, may crosslink with each other, altering the structure of the molecule . At the same time, the functional groups of these protein radicals may undergo oxidation, forming protein carbonyls . Quantification of these carbonyl modifications has served as an useful indicator of the level of oxidative damage in affected proteins .

Lipid peroxidation has long been recognized as the prevalent characteristic of oxidative damage . During this process oxygen reacts with unsaturated fatty acid to form lipid hydroperoxides which react with other lipids . These lipid hydroperoxides may also undergo metal-catalyzed reactions, forming alkoxyl and peroxyl radicals . Peroxidation of the lipids within the cell membrane increases the intracellular calcium concentration, thus activating endonucleases with ensuing DNA damage . In particular, membrane phospholipid peroxidation causes a significant increase in the externalization of phosphatidylserine, initiating the apoptotic process and marking the cell for phagocytosis .

5. ROI-induced signal transduction

Another avenue by which ROI mediates cellular toxicity is through alterations in signal transduction pathways. This effect occurs either through direct interactions with signaling kinases and transcription factors as well as affecting redox-sensitive proteins . The pathways affected in some way by ROI are very numerous and quite complex and only a few examples will be described at this time.

The mitogen-activated protein (MAP) kinases are known to be activated in response to oxidative stress . For example, hydrogen peroxide-mediated activation of the MAP kinases induced apoptosis . Similarly, hydroxyl radical formation also activated the MAP kinases, ultimately causing DNA damage .

ROI also regulate the activity of many transcription factors . Activation of both AP-1 and NF-κB, two major signal transduction pathways, is a well recognized cellular response to oxidative stress . AP-1 activation, however, appears to be a downstream effect of oxidative stress while NF-κB is directly activated by ROI . It has, therefore, been proposed that ROI may act as second messengers in the activation of these transcription factors .

Upregulation of gene expression following oxidative stress is known to involve transcription factor binding to the antioxidant response element (ARE). ARE's are present in the promoter regions of genes encoding for many antioxidant enzymes such as heme oxygenase-1 (HO-1) , glutathione S-transferases (GST) and NAD(P)H:quinone oxidoreductase 1 (NQO1) , to name a few. Although the ARE is known to have binding sites for AP-1 and NF-kB , the NF-E2-related factor 2 (Nrf2) transcription factor is recognized as the key regulator for ARE-mediated gene expression . In fact, Nrf2 activity has been shown to provide protection from ROI-induced damage through the upregulation of such antioxidant enzymes as NQO1 and GST .

6. Cellular defense mechanisms

In order to prevent oxidative damage, removal or detoxification of ROI is crucial.

As result, several antioxidant enzymes exist in order to convert ROI into less harmful molecules . Enzymes such as superoxide dismutase, catalase and glutathione peroxidase form the primary antioxidant defense through ROI scavenging and detoxification. Additional ROI removal is performed by heme oxygenase and metallothionein. However, these enzymes are not completely efficient and any ROI not initially removed may interact with and damage cellular macromolecules, resulting in oxidized lipids and proteins. These oxidation products are removed by the secondary antioxidant defense system comprised of the glutathione S-transferases

a. Superoxide dismutase

Superoxide dismutase (SOD) catalyzes the univalent reduction of superoxide anion to oxygen and hydrogen peroxide .

$$O_2^{-\bullet} + O_2^{-\bullet} + 2H^+ \longrightarrow O_2 + H_2O_2$$

These ubiquitous enzymes contain a transition metal at their active site and are thus classified into three types: copper-zinc SOD (CuZnSOD or SOD1), manganese SOD (MnSOD or SOD2) and iron SOD (FeSOD) . CuZnSOD and FeSOD are characteristic of eukaryotes and prokaryotes, respectively. MnSOD was originally classified as a prokaryote enzyme but is also now recognized as a mitochondrial SOD in eukaryote systems.

SOD activity provides the primary defense against oxidative stress by reducing superoxide anion to hydrogen peroxide, thus preventing the generation of further ROI.

SOD biosynthesis has been shown to be regulated by oxygen concentration . However, overexpression of CuZnSOD has been shown to increase lipid peroxidation , possibly due to the elevated hydrogen peroxide-induced hydroxyl radical formation that would occur.

b. Catalase

Catalase is a tetrameric heme-containing enzyme that catalyzes the reduction of hydrogen peroxide to water and molecular oxygen .

$$H_2O_2 + H_2O_2 \rightarrow O_2 + 2\ H_2O$$

This process occurs in two distinct reactions . First, catalase is oxidized by hydrogen peroxide to an intermediate known as Compound I. In the second reaction, Compound I oxidizes the second hydrogen peroxide molecule and the enzyme molecule is returned to its resting state. This reaction occurs very rapidly and is energy efficient in that hydrogen peroxide acts as both an electron donor and acceptor, removing the requirement for cellular reducing equivalents . Thus, catalase has the ability to decompose high concentrations of hydrogen peroxide that would otherwise be toxic to the cell. In addition, catalase is, for the most part, generally localized in peroxisomes in conjunction with many hydrogen peroxide-producing enzymes . This proximity allows catalase to act upon and detoxify the hydrogen peroxide prior to its diffusion throughout the cell.

c. Glutathione peroxidase

Glutathione peroxidase (GPx) catalyzes the reduction of hydrogen peroxide or organic hydroperoxides to water with a concomitant oxidation of reduced glutathione .

$$2GSH + H_2O_2 \rightarrow GSSG + 2\,H_2O$$

$$2GSH + ROOH \rightarrow GSSG + 2\,H_2O + ROH$$

The most well-known isoform is GPx-1, a selenium-dependent cytosolic peroxidase that is ubiquitously expressed . Other isoforms are tissue-specific and include the Se-dependent GPx-2 , GPx-3 and GPx-4 as well as the Se-independent GPx-5 . The selenium requirement dictates the substrate specificity. Hydrogen peroxide is the preferred substrate for the Se-dependent isoforms while organic hydroperoxides are metabolized by the Se-independent enzymes . The intracellular levels of hydrogen peroxide determines which peroxidase catalyzes its reduction; catalase is most effective at high concentrations while glutathione peroxidase is active at low concentrations .

d. Glutathione S-transferase

The glutathione S-transferase (GST) enzymes are a large superfamily of ubiquitous cytosolic and microsomal phase II detoxification enzymes that conjugate reduced glutathione to electrophilic compounds . Glutathione conjugation allows damaged molecules as well as xeniobiotics to be easily eliminated from the cell . GST enzymes also inhibit the continued generation of ROI through the removal of redox cycling intermediates and lipid peroxidation products, thereby preventing the propagation of further radical formation .

The cytosolic and microsomal GST gene families are both structurally and functionally distinct. The cytosolic enzymes are dimeric proteins, consisting of either homo- or heterodimers formed by two subunits from within the family . The cytosolic

GST enzymes are divided into three major gene families, alpha (GSTA), mu (GSTM) and pi (GSTP), with several minor families having been identified (omega, sigma, theta, zeta and kappa) to date . Functionally, each GST family has been documented as to having preferred substrates although all members are involved in the detoxification of oxidized macromolecules .

Members of the GSTA family are known to be the primary GST enzymes involved in the prevention of lipid peroxidation. GSTA have been shown to eliminate oxidized products such as hydroperoxides and aldehydes . In the removal of these products, GSTA utilize a glutathione peroxidase-like activity, independent of their recognized conjugation function . Overexpression of the GSTA enzymes has shown to protect cells against hydrogen peroxide-induced oxidative damage , suggesting that GSTA is has peroxidase activity.

While GSTP also participates in the removal of aldehydes, these enzymes are much more effective at detoxifying DNA degradation products . Similarly, GSTM play a minor role in protection against lipid peroxidation by detoxifying hydroxyalkenes although their primary function is the removal of *o*-quinones, produced by catecholamine oxidation .

The microsomal GST enzymes are trimers that inhibit lipid peroxidation and contribute to eicosanoid synthesis . This family also contains several isoforms. The initial enzyme described was mGST1 , followed by mGST2, mGST3 . These proteins have been recently described as members of the membrane-associated proteins in eicosanoid and glutathione metabolism (MAPEG) family of enzymes . The mGST enzymes have been shown to have glutathione peroxidase activity against lipid hydroperoxides similar to that

of the cytosolic GSTA enzymes , indicating that these enzymes are important in protection from lipid peroxidation.

e. Heme oxygenase

Heme oxygenase (HO) is the primary enzyme in the degradation of heme, catalyzing the first and rate-limiting step . In the first step, heme is converted to biliverdin, free iron (Fe^{2+}) and carbon monoxide. Biliverdin is then converted to bilirubin and the iron is sequestered in ferritin . Three isoforms have been described: HO-1, HO-2 and HO-3 . HO-1 is a ubiquitous, inducible enzyme while HO-2 and HO-3 exhibit constitutive expression and are located to specific tissues .

In addition to its role in heme degradation, HO-1 is known to be induced in response to many oxidants . Increased HO-1 expression was detected following exposure to ultraviolet A (UVA) light , hydrogen peroxide , lipopolysaccharide (LPS) , paraquat and cobalt , to list but a few examples. In fact, HO-1 -/- mice were shown to have increased mortality and hepatic necrosis when given LPS as compared to the wild-type controls , indicating that HO-1 may be a vital component of the cellular response to oxidative stress.

f. Metallothionein

Metallothioneins (MT) are zinc-containing proteins that are important in the regulation of zinc homeostasis and protection from cadmium toxicity . Over the last several years, these enzymes have come to be recognized as part of the cellular repose to

oxidative stress due to their ability to function in an antioxidant capacity by acting as free radical scavengers .

To date, four MT isoforms have been described: MT-1, MT-2, MT-3 and MT-4. MT-1 and MT-2 are widely expressed and are induced in response to metals, inflammatory mediators and oxidative stress . These enzymes have shown to inhibit oxidation of DNA scavenging of hydroxyl radicals . MT-3 is primarily found in the brain was originally referred to as growth inhibitory factor due to its ability to inhibit neuronal growth . MT-4 is located mainly in stratified squamous epithelium and its function is not yet known. It has been proposed that the antioxidant ability of MT resides in its capacity to increase intracellular zinc concentrations in response to oxidants . Zinc, thusly mobilized, activates the metal response element-binding transcription factor 1 (MTF-1), thereby initiating the transcription of and synthesis of MT as well as possibly other zinc finger transcription factors .

C. Arachidonic Acid Metabolism

1. Introduction

Metabolism of arachidonic acid is complex process with intersecting and interconnecting pathways, resulting in the production of numerous metabolites, that are referred to as the eicosanoids (see Figure 2) . Eicosanoids are potent lipid mediators that are involved in inflammation, cell proliferation and apoptosis and whose expression is tightly regulated through expression of several enzymes. These enzymes include the phospholipases, the rate-limiting enzymes for arachidonic acid production, as well as

three classes of oxygenases: cyclooxygenases, lipoxygenases and cytochrome P450 monooxygenases that generate several classes of eicosanoids.

2. Arachidonic acid mobilization

Arachidonic acid is a 20-carbon polyunsaturated fatty acid within the phospholipid layer of the cellular membrane. In response to a variety of signals, phospholipases are phosphorylated and these activated enzymes catalyze the release of arachidonic acid from the membrane. The phospholipase A_2 (PLA_2) family of enzymes are a diverse group and are responsible for the majority of arachidonic acid mobilization . The PLA_2 family is further divided into cytosolic ($cPLA_2$) and secretory ($sPLA_2$) enzymes although each member has the same function: hydrolysis of the *sn*-2 ester bond of phospholipids, forming free fatty acids that include arachidonic acid as well as lysophospholipids . $cPLA_2$ is an ubiquitous calcium-dependent enzyme, activated through phosphorylation by mitogen-activated protein (MAP) kinases . Studies with $cPLA_2$ knockout mice have shown that this enzyme is crucial for the release of arachidonic acid . Although the $sPLA_2$ enzymes also participate in arachidonic acid release, their biological role is not clear known at this time and may represent a functionality localized to specific tissues or cell types .

Alternatively, arachidonic acid mobilization may be catalyzed by phospholipase C (PLC) or phospholipase D (PLD). PLC hydrolyzes phosphoinositol-4,5-biphosphate (PIP2) to 1,2 diacylglycerol (DAG) and inositol-1,4,5-triphosphate (IP3) . DAG is then hydrolyzed by diacylglycerol lipase to monoacylglycerol (MAG) which is, in turn, hydrolyzed by monoacylglycerol lipase to form glycerol and arachidonic acid .

Phosphatidylcholine hydrolysis by PLD generates phosphatidic acid and choline . Phosphatidic acid may be further metabolized to produce DAG, thereby generating arachidonic acid through the action of PLD. Additionally, both DAG and IP3 are also potent signaling molecules, activating enzymes such as protein kinase C (PKC) and releasing Ca^{2+} from intracellular stores, respectively .

3. Production of prostaglandins, prostacyclin and thromboxane

a. Cyclooxygenase

The cyclooxygenases (COX) mediate the generation of prostaglandins as well as prostacyclin and thromboxanes and are the rate-liming enzymes in this process. The COX enzymes were originally known as prostaglandin H_2 (PGH) synthases as their activity mediated the oxidation of arachidonic acid to prostaglandin H_2 (PGH_2) . PGH_2 production occurs in two sequential reactions (Figure 3). In the first reaction, two oxygen molecules are inserted into the arachidonate backbone, forming prostaglandin G_2 (PGG_2) . The hydroperoxyl group of PGG_2 is then reduced to hydroxyl, generating PGH_2 . Specific prostanoid synthases then convert PGH_2 into the prostaglandins, PGD_2, PGE_2, $PGF_{2\alpha}$, as well as prostacyclin, PGI_2, and thromboxane A_2 (TXA_2) (Figure 3).

Two COX isoforms have been described: cyclooxygenases-1 and –2 (COX-1 and COX-2, respectively) . Both isoforms mediate the production of PGE_2. COX-1 is constitutively expressed and is involved in maintaining renal homeostasis, platelet aggregation and protection of the gastric mucosa . COX-2 is not expressed under normal conditions but is readily inducible in response to proinflammatory and mitogenic stimuli .

In addition, upregulation of COX-2 has also been well recognized as a key factor in the initiation and development of carcinogenesis .

In normal mouse skin, COX-1 expression localized to the basal keratinocytes while COX-2 is barely detectable . Increased COX-2 expression has been detected in keratinocytes in response to ultraviolet B (UVB) , phorbol ester and incisional injury . Interestingly, COX-2 also appears to play a role in keratinocyte differentiation. Overexpression of COX-2 caused hyperplasia due to basal keratinocytes moving into upper epidermis with a concomitant decrease and keratin 1 and keratin 10 expression . This involvement of COX-2 in early keratinocyte differentiation was confirmed when COX-2 -/- mice were shown to have increased keratin 1 and keratin 10 expression in the basal cells which causes premature differentiation . Moreover, studies with cultured human keratinocytes have shown that increased calcium concentrations not only cause differentiation but induce COX-2 expression as well .

b. Prostaglandin D

The production of PGD_2 is catalyzed by prostaglandin D_2 synthase (PGDS). PGDS occurs in two forms: a lipocalin-type PGDS (L-PGDS) that is a secreted enzyme and a cytosolic hematopoeitic PGDS (H-PGDS) with glutathione S-transferase activity . PGD_2 plays a major role in allergic and inflammatory responses as well as acting as a potent sleep inducer , regulating vascular homeostasis, and modulating nociception.

PGD_2 may also spontaneously convert to the cyclopentenone prostaglandins of the J series, namely PGJ_2 and 15-deoxy-$\Delta^{12,14}$- prostaglandin J_2 (15d-PGJ_2) . 15d-PGJ_2 is most well known for its role in the resolution of inflammation . This activity may result

from the ability of 15d-PGJ_2 to bind and activate PPARγ , an important negative regulator of inflammatory cytokine biosynthesis . Additionally, 15d-PGJ_2 inhibits microsomal prostaglandin E synthase, thereby suppressing a prostaglandin E_2-induced inflammatory response .

Prostaglandins work by binding to G-protein-coupled transmembrane receptors to activate intracellular signaling pathways. Two PGD_2 receptors exist: DP and (chemoattractant receptor-homologous molecule expressed on T helper type 2 cells) CRTH2 . Interestingly, CRTH2 binds 15-dPGJ_2 with equal affinity as PGD_2 and with much greater affinity than does PPARγ . Increased PGD_2 expression is known to be involved in dermal allergic reactions and sleep induction . Although the role of CRTH2 signaling is not completely known, PGD_2 has been shown to mediate allergic reactions via activation of this receptor .

c. Prostaglandin E

The formation of prostaglandin E_2 (PGE_2) is mediated by the action of microsomal prostaglandin E synthase (mPGES) which catalyses the conversion of PGH_2 to PGE_2 in a glutathione-dependent manner . Two isoforms of this enzyme exist: an inducible form, mPGES-1 and an constitutively expressed form, mPGES-2 . Expression of mPGES-1 is upregulated during inflammation , carcinogenesis and bone resorption . Upregulation of mPGES-1 activity has been functionally coupled with increased COX-2 expression during the production PGE_2 . In contrast to mPGES-1, mPGES-2 is considered to be constitutively expressed in most tissues but has been shown to be

induced in colorectal carcinoma cells. In addition, mPGES-2 has no glutathione requirement for its activity

PGE_2 is a potent mediator of inflammation and pain perception and is known to be involved in tumorigenesis and vasodilation . PGE_2 signaling occurs through four receptors: EP1 , EP2 , EP3 and EP4 , all of which are involved in mediating numerous physiological functions. In general, the EP1 receptor is recognized as having a major role in inflammation and pain perception as well as the initiation of carcinogenesis . EP2 is also involved in the development of fever as well as maintaining hypertension by control of salt concentrations . Activation of EP3 is required for the lipopolysaccharide- or cytokine-induced inflammatory febrile response as well as pain perception . The EP4 receptor is involved in bone remodeling through osteoclast induction and promotion of Langerhans cell migration during the dermal immune response .

Although all four PGE_2 receptors are expressed in skin , their activation induces varied effects. For example, UVB- and phorbol ester-induced inflammation and tumorigenesis was shown to require PGE_2-mediated activation of the EP1 and EP2 . At the same time, tumorigenesis was unaffected by EP3 receptor signaling .

Interestingly, mPGES-1 is also a member of the membrane-associated proteins involved in eicosanoid and glutathione metabolism (MAPEG) superfamily of enzymes . Included in this superfamily are the arachidonic acid metabolizing enzymes 5-lipoxygenase activating protein (FLAP) and leukotriene C_4 (LTC_4) synthase as well as the microsomal glutathione S-transferases 1, 2 and 3 (mGST1, 2, 3). These enzymes are linked by structural and sequence homology and, except for FLAP, are glutathione-dependent with glutathione S-transferase activity .

d. Prostaglandin F

$PGF_{2\alpha}$ can be generated via distinct three pathways: PGF synthase (PGFS) or PGH 9,11 endoperoxide reductase, PGD 11-ketoreductase, and PGE 9-ketoreductase. In the first reaction, PGFS or with glutathione S-transferase activity that uses PGH2 as its substrate . In the second reaction, PGD 11-ketoreductase catalyzes the reduction of PGD_2 to $PGF_{2\alpha}$ in a NADPH-dependent reaction . In the third reaction, PGE 9-ketoreductase that mediates the conversion of PGE_2 to $PGF_{2\alpha}$ in the presence of NADH or NADPH . $PGF_{2\alpha}$ binds to the FP receptor , leading to increased intracellular calcium through PLC-mediated IP3 generation .

$PGF_{2\alpha}$ is a potent mediator involved in parturition as well as in maintaining renal function and regulation of intraocular pressure . $PGF_{2\alpha}$ is known to be expressed at low levels in mouse skin and recent studies have indicated that it may play a protective role against neoplastic dermal conversion. Recent studies have shown that expression of the FP receptor, while transiently increased following phorbol ester treatment, is decreased in papillomas . Moreover, FP activation resulted in increased melanin production in human melanocytes both in vitro and in vivo in response to UVB light .

e. Prostaglandin I (prostacyclin)

Prostacyclin (PGI_2) is catalyzed by prostaglandin I_2 synthase (PGIS) , a member of the cytochrome P450 family . This product is unstable and is rapidly hydrolyzed to the stable, 6-keto-$PGF_{1\alpha}$. PGI_2 is well recognized for its role in vasodilatation and anticoagulation, pain perception, inflammation and embryonic development and, more

recently, its role in carcinogenesis . PGI_2 acts through two signaling pathways: a receptor-dependent pathway via binding to the prostacyclin (IP) receptor and a receptor-independent pathway involving the activation of PPARδ . Interestingly, prostacyclin function appears to be divided between these modes of action. Pain perception as part of the inflammatory response and maintenance of vascular homeostasis are mediated through PGI_2-binding to the IP receptor while mediation of embryo implantation and apoptosis occur through PGI_2-activation of PPARδ .

To date, there is little known regarding the function of PGIS and PGI_2 in the skin. However, prostacyclin analogs have been shown to inhibit phorbol ester-induced transformation and to induce differentiation in keratinocytes .

f. Thromboxane

Thromboxane synthase (TXAS) converts PGH_2 to thromboxane (TXA_2) through peroxide group cleavage and cyclization . TXA_2 stimulates vasoconstriction through induction of smooth muscle contraction and platelet aggregation . Thus, TXA_2 and PGI_2 expression are coordinately regulated to maintain vascular homeostasis . Activation of the TXA_2 receptor, TP, results in platelet aggregation , bronchiole constriction and T-cell activation ..

g. Isoprostanes

The isoprostanes are prostaglandin-like compounds that are formed from ROI-mediated oxidation of arachidonic acid . These molecules have been used as indicators of oxidative stress and may be useful as biomarkers in the future . Additionally, isoprostanes

have recently been reported to possess innate biological activity, acting as the causative agents in the initiation of oxidative injury .

4. Production of leukotrienes, HETE's and lipoxins

a. Introduction

The lipoxygenase (LOX) enzymes are responsible for the production of leukotrienes, hydroxyeicosatetraenoic acids (HETE's) and lipoxins (Figure 4). The 5-, 8-, 12-, and 15-lipoxygenases (5-LOX, 8-LOX, 12-LOX and 15-LOX) incorporate one oxygen molecule to the respective carbon on the arachidonic acid backbone, producing an intermediate molecule, hydroperoxyeicosatetraenoic acid (HPETE). Each HPETE is reduced to the corresponding HETE and, in some pathways, is further oxidized to a leukotriene.

b. 5-Lipoxygenase

5-LOX is a Ca^{2+} and ATP-dependent enzyme responsible for the generation of the leukotrienes . Unlike the other lipoxygenases, 5-LOX requires an additional enzyme, 5-LOX activating protein (FLAP) that acts as a transfer protein and presents the substrate for oxidation . 5-HPETE is converted to either 5-HETE as a final product or to an unstable intermediate, leukotriene A_4 (LTA_4) . LTA_4 is further metabolized by the epoxide hydrolase, LTA_4 hydrolase , to leukotriene B_4 (LTB_4), a potent mediator of inflammation and immune cell chemotaxis . LTA_4 also may be conjugated with glutathione by LTC_4 synthase to form the cysteinyl leukotriene, LTC_4 . LTC_4 may undergo further transformation to generate the other cysteinyl leukotrienes, LTD_4 and

LTE_4. As previously discussed, both FLAP and LTC_4 synthase are members of the MAPEG family, although FLAP does not have any glutathione conjugation activity.

As with the prostaglandins, leukotrienes act through bind to specific receptors. LTB_4 activates the LTB_4 receptors, BLT1 and BLT2, while LTC_4, LTD_4 and LTE_4 bind to the cysteinyl leukotriene receptors, CysLT1 and CysLT2 .

Leukotrienes, produced through activation of the 5-LOX pathway are well recognized as proinflammatory mediators . Although it was originally thought that the skin had limited 5-LOX activity, the expression of 5-LOX has been detected in both mouse and human keratinocytes as well as LTA_4 hydrolase activity . As part of a coordinated response to inflammatory stimuli, neutrophil migration into the skin is promoted by LTB_4 while LTC_4 and LTD_4 cause vasodilation, resulting in "wheal and flare" reactions .

c. 8-Lipoxygenase

8-lipoxygenase (8-LOX) mediates the production of 8-HPETE from arachidonic acid and its subsequent transformation to 8-HETE . Additionally, 8-LOX catalyzes the conversion of 5-HPETE to LTA_4 . The murine 8-LOX gene is the orthologue of the second human 15-LOX isoforms (15-LOX-2) and, in this respect, there is no 8-LOX gene described in the human genome.

The expression of 8-LOX has been detected in many tissues . In skin, 8-LOX activity appears to be directly related to epidermal differentiation . Moreover, increased expression of 8-LOX has been associated with the development of dermatitis and tumorigenesis

d. 12-Lipoxygenase

12-LOX has three distinct isoforms named for the tissue from which they first isolated: the platelet-type , the epidermal-type 12-LOX and the leukocyte-type 12-LOX . The function of these enzymes is the same; namely, the oxidation of arachidonic acid to 12-HPETE with subsequent reduction by glutathione peroxidases to 12-HETE . Alternatively, 12-HPETE may be structurally rearranged to form hepoxilins and trioxilins .

Interestingly, upregulation of platelet-type 12-LOX has been directly correlated with melanoma progression while epidermal-type 12-LOX expression appears to be anti-tumorigenic

e. 15-Lipoxygenase

The conversion of arachidonic acid to 15-HPETE is catalyzed by the Ca^{2+}-dependent 15-LOX . 15-HPETE is then reduced by glutathione peroxidases to 15-HETE. 15-HPETE may also undergo nonenzymatic reactions to form hydroxyepoxides and dihydroxy acids. 15-HETE also acts as a substrate for 5-LOX, thereby forming LTA_4. In the mouse, there is only one 15-LOX isoform while, in humans, there two distinct 15-LOX isozymes: 15-LOX-1 and 15-LOX-2 .

Although 15-LOX metabolites are involved in inflammation , 15-HETE has been shown to inhibit LTB_4 formation and activate cytotoxic suppressor T cells . In addition, both 15-LOX-1 and 15-LOX-2 activity has been shown to inhibit cancer progression .

f. Lipoxins

The lipoxins are produced by both 5- and 15-lipoxygenase oxidation of arachidonic acid . Lipoxins are known to promote the resolution of inflammation by several mechanisms including inhibition of neutrophil migration , stimulation of phagocytosis and suppression of proinflammatory cytokines . In addition, it was recently shown that aspirin-induced lipoxins increased heme oxygenase-1 (HO-1) expression , which may another factor in the anti-inflammatory effects of lipoxins.

4. Cytochrome P450

The oxidation of arachidonic acid by cytochrome P450 is an NADPH-dependent, reaction . Epoxidation of arachidonic acid generates epoxyeicosatrienoic acids (EET) which are then hydrolyzed to dihydroeicosatrienoic acids (DHT) . At the same time, P450 catalyzes the formation of several HETE's from arachidonic acid . The expression of CYP1A and 2B P450 family members has been extensively studied in skin with CYP2B19 having been identified as the primary enzyme responsible for the production of EET's . CYP2B19-catalyzed EET production has been reported to activate transglutaminases, thereby inducing keratinocyte differentiation .

5. Relationship to oxidative stress

The metabolism of arachidonic acid and the induction of oxidative stress through the production of reactive oxygen intermediates are interconnected processes . One well known example is that increased oxidative stress can induce the production of prostaglandins and leukotrienes. Phosphorylation of $cPLA_2$ and subsequent arachidonic

acid mobilization has been shown to occur following exposure to hydrogen peroxide while pretreatment with antioxidants blocked $cPLA_2$ phosphorylation as well as COX-2 expression . Although the mechanism is not known at this time, this process is thought to occur as a result of the peroxidation of membrane phospholipids ..

An example of the interconnecting relationship between these two processes is existence of the membrane-associated proteins in eicosanoid and glutathione metabolism (MAPEG) family of enzymes. The MAPEG family include both eicosanoid production and antioxidant enzymes . With the exception of FLAP, these enzymes are glutathione-dependent with GST activity. Additionally, both PGFS and PGDS has been identified as microsomal and cytosolic GST enzymes, respectively . Although the prime function of the arachidonic acid-metabolizing enzymes is the synthesis of eicosanoids, their GST activity makes them reliant upon the availability of reduced glutathione and, ultimately, the redox state of the cell.

In the last several years it has become apparent that these glutathione-conjugated eicosanoids and, in particular, the cyclopentenone prostaglandins, are involved in modulating cellular responses to oxidative stress . Perhaps, the best example of this effect has been shown to occur with 15d-PGJ_2. While 15d-PGJ_2 has been shown to induce HO-1 expression , this metabolite has also been implicated in inducing oxidative stress through the depletion of glutathione via conjugation by GST enzymes . 15d-PGJ_2, as well as other cyclopentenone prostaglandins, are substrates for GST and conjugation allows the GST enzymes to modulate the biological effects of these metabolites. . For example, by conjugating 15d-PGJ_2 with glutathione, GST suppressed transcriptional activation by PPARγ with the extent of inhibition depending upon the level of GST activity .

Clearly, the relationship between oxidative stress and arachidonic acid metabolism is extremely complex. In recent years, it has been recognized that oxidative damage usually occurs in conjunction with arachidonic acid release and eicosanoid production as components of the inflammatory response in the pathology of many diseases. These processes are, therefore, most likely related at some fundamental level although the mechanisms involved are not completely understood at this time.

METHODOLOGY

A. Chemicals and reagents

SP600125 and Wortmannin were purchased from Calbiochem (La Jolla, CA). M-MLV Reverse Transcriptase was from Promega (Madison, WI) and collagen IV from BD Biosciences (San Diego, CA). The Western Lightning enhanced chemiluminescence kit (ECL) was from Perkin Elmer Life Sciences, Inc. (Boston, MA) and precast polyacrylamide gels were from Pierce Biotechnology, Inc. (Rockford, IL). HPLC standards were obtained from Cayman Chemical (Ann Arbor, MI). Anti-HO-1 antibodies were from Assay Designs (Ann Arbor, MI), anti-catalase antibodies were from Abcam (Cambridge, MA) and anti-COX-2 and donkey anti-goat secondary antibodies were from Santa Cruz Biotechnology (Santa Cruz, CA). Anti-p38, anti-phopho-p38, anti-JNK, anti-phospho-JNK, anti-ERK 1/2 and anti-phospho-ERK 1/2 antibodies were purchased from Cell Signaling Technology (Beverly, MA). Antibodies to keratin-1, keratin-10 and filaggrin were from Covance Research Products (Berkley, CA). Horseradish peroxidase-conjugated goat anti-rabbit secondary antibodies and detergent-compatible protein assay reagents were from Bio-Rad Laboratories (Hercules, CA). The OxyBlot Protein Oxidation Detection Kit was from Chemicon International, Temecula, CA. SYBR Green Master Mix and other PCR reagents and supplies were purchased from Applied Biosystems (Foster City, CA). All medium, 2', 7'-dicholorofluorescein-diacetate (DCFH-DA), 2-(2,3-naphthalimino)ethyl-trifluoromethanesulphonate (NE-OTf), and Amplex Red reagent (10-acetyl-3, 7-dihydroxyphenoxazine) were obtained from Invitrogen Corp. (Carlsbad, CA). Paraquat, SB203580, NADPH, protease inhibitor cocktail, and all other chemicals were from Sigma (St. Louis, MO).

B. Primary keratinocyte culture

Primary mouse keratinocytes were isolated from the skin of C57Bl/6J newborn mice following the procedure described by Hager et al. . Briefly, the epidermis was separated from the dermis following incubation with trypsin or dispase and each skin section was minced to release individual cells. Fibroblasts were isolated from the dermal pieces and grown in T-75 flasks with low-calcium Eagle's Essential Minimal Medium 0.06mM calcium (EMEM0.06) (Cambrex, Walkersville, MD) to provide fibroblast-conditioned medium. Keratinocytes were isolated from the epidermal pieces and grown to confluency on collagen IV-coated flasks in N-medium (half conditioned medium and half EMEM0.06 with 10% chelexed serum) in 4.5% CO_2. Once the cultures were established, the cells were seeded into the appropriate size collagen IV-coated plates and grown in serum-free Keratinocyte Growth Medium (Cambrex, Walkersville, MD) containing 0.05 mM calcium (KGM0.05) as a low calcium medium in order to maintain undifferentiated status. Differentiation was induced by the addition of calcium (0.15 mM) to the medium . Differentiation was confirmed by morphological changes and expression of differentiation markers including keratin 1, keratin 10 and filaggrin, as analyzed by Western blotting . In some experiments, confluent cultures of primary C57Bl/6J keratinocytes in N-medium were purchased from the Yale University Cell Culture Facility (New Haven, CT) were used. Following dissociation, the same culture procedures were practiced as described above.

C. UVB and paraquat treatments

UVB treatment of the keratinocytes was performed using a bank of 2 FS40BL bulbs calibrated using an International IL-1700 UV-radiometer. For these experiments, the cells were grown to 90% confluence and exposed to UVB in phosphate-buffered saline (PBS) as previously described . Following UVB treatment, the PBS was removed and the cells refed with Keratinocyte Growth Medium containing either low or high calcium concentrations. In some experiments, kinase inhibitors were added directly to the medium and the cells were incubated at 37°C for 3 hours prior to UVB treatment. When the cells were refed after UVB exposure, the medium contained the same concentration of inhibitors. The kinase inhibitors used were SB203580 (10 μM) for p38 MAP kinase, SP600125 (20 μM) for JNK MAP kinase and Wortmannin (0.1 μM) for PI-3 kinase . The control wells contained the vehicle, DMSO (20 μM). For the paraquat experiments, paraquat (100 μM) was added to the medium and the cells were incubated for the indicated times.

D. Western blotting

Western blotting was performed as previously described . Briefly, cell lysates were prepared using an SDS-lysis buffer (10 mM Tris-base and 1% SDS, pH 7.6 supplemented with a protease inhibitor cocktail consisting of 4-(2-aminoethyl)benzenesulfonyl fluoride, aprotinin, bestatin hydrochloride, N-(trans-epoxysuccinyl)-L-leucine 4-guanidinobutylamide, EDTA and leupeptin). Proteins (20 μg) from lysates were separated on 10% SDS-polyacrylamide gels and then transferred to nitrocellulose membranes. After incubating the membranes in blocking buffer (5% dry milk Tris-

buffered saline with 0.1% Tween 20) for 1 hour at room temperature or overnight at 4°C, the membranes were then incubated for 1-2 hours at room temperature, or overnight at 4°C, with primary antibodies followed by horseradish peroxidase-conjugated secondary antibodies for 1 hour at room temperature. Protein expression was visualized using ECL reagents.

E. Flow cytometry

Intracellular hydrogen peroxide production was measured using DCFH-DA and flow cytometry as previously described . Briefly, the cells were incubated with DCFH-DA (5 μM) in PBS for 15 minutes at 37°C, exposed to UVB (25 mJ/cm^2), and then immediately analyzed by flow cytometry using a Beckman Coulter Cytomics FC 500 equipped with a 488 nm argon laser and CXP software.

F. Eicosanoid determination by HPLC

The cells were exposed to UVB light or paraquat and incubated for the indicated times. Arachidonic acid (10μM) was added directly to the medium and incubated at 37°C for an additional 20 minutes. The reaction was stopped by the addition of an equal volume of ice-cold methanol. The cells and medium were collected, centrifuged at 12,000 x *g* for 10 minutes at 4°C and the supernatants collected. Aliquots of the extracts were evaporated to dryness under helium and fluorescence derivatized as described by Yue et al. (2004) . Briefly, the dried extracts were solubilized in anhydrous acetonitrile, *N,N*-diisopropylethylamine catalyst (dried with 5 Å molecular sieves) and NE-OTf (2mg/ml in anhydrous acetonitrile), incubated in a dessicator for 30 minutes at 4°C and then

evaporated to dryness under helium. The derivatized samples were reconstituted in methanol and analyzed by HPLC.

The prostaglandins were detected using a Shimadzu HPLC (Kyoto, Japan) fitted with a Beckman Ultrasphere C18 column (4.6 mm x 250 mm) (Fullerton, CA) in conjunction with a Shimadzu RF-551 fluorescence detector with excitation and emission set at 260 and 396 nm, respectively. Mobile phase A was acetonitrile:water:acetic acid (25:75:0.1) and mobile phase B was acetonitrile (100%). The flow rate was 1 ml/min and the mobile phase A and B gradient was as follows: 15% B for 25 minutes; 50% B for 15 minutes; and 15% B for 10 min.

G. NADPH oxidase activity assay

To prepare cell lysates for NADPH oxidase assays, cells (2 X 10^6) were suspended in PBS and sonicated on ice. Lysates were then centrifuged for 10 minutes at 12000 x *g* at 4°C and the supernatants collected. NADPH oxidase activity was quantified by the formation of hydrogen peroxide during paraquat redox cycling using the Amplex Red fluorescence assay as previously described . Briefly, reactions were run in 96-well microtiter plates at 37° C and contained 10 µM Amplex Red reagent, 50 µM NADPH and 130-150 µg/µl cell lysates in a total volume of 50 µl. The Amplex Red reagent, 10-acetyl-3, 7-dihydroxyphenoxazine, is oxidized by hydrogen peroxide, forming the fluorescent product, resorufin. The detection of resorufin was recorded over 30 minutes using an HTS 7000 Plus BioAssay Reader (Perkin Elmer Life Sciences) with a 540 nm excitation filter and 595 nm emission filter. In some experiments, the inhibitors

dicoumarol (100 μM) or diphenyleneiodonium (DPI) (10 μM), were added directly to the reaction mix.

H. NADPH depletion assay

Cell lysates from undifferentiated and differentiated keratinocytes were prepared as previously described. A reaction mix containing cell lysate (150 μg/μl protein), paraquat (100 μM) and NADPH (100 μM) was placed in a 1 ml cuvette and analyzed in a Perkin Elmer Lambda 20 UV/VIS spectrophotometer at room temperature. Absorbance (340 nm) was recorded every 2.5 minutes for 3 hours.

I. Formation of paraquat radical

Cell lysates were prepared as previously described. A reaction mix containing cell lysate (130-150 μg/μl protein), paraquat (500 μM) and NADPH (3 mM) was placed in a 1 ml cuvette and tightly sealed with Parafilm. It was then placed in the UV/VIS spectrophotometer. After 120 minutes, absorbance (500-700 nm) was recorded every 2.5 minutes. The formation of the radical was confirmed by the appearance of the blue-violet paraquat radical .

J. Superoxide anion formation by HPLC

The detection of superoxide anion as indicated by the formation of 2-hydroxyethidium from dihydroethidium was previously described by . Briefly, a reaction mix containing previously prepared cell lysate (150 μg/μl protein), paraquat (100 μM) and NADPH (0.5 mM) and dihydroethidium (40 μM) was incubated for 1 hour at 37°C. The reaction was

stopped by the addition of an equal volume of ice-cold methanol. The samples were centrifuged at 12,000 x *g* for 10 minutes at 4°C and the supernatants collected. The formation of 2-hydroxyethidium was quantified by a Shimadzu HPLC (Kyoto, Japan) fitted with a Luna C18 column (250 mm x 2.0 mm) (Phenomenex, Torrance, CA) in conjunction with a RF-535 fluorescence detector (Shimadzu) with excitation and emission set at 510 and 595 nm, respectively. The mobile phase was acetonitrile in 0.1% trifluoroacetic acid and was run by a linear increase of acetonitrile concentration from 10% to 40% in 35 minutes with a flow rate of 0.2 ml/min.

K. Protein oxidation assay

Protein oxidation was determined by quantifying carbonyl groups on protein side chains using the OxyBlot Protein Oxidation Detection Kit, following the manufacturer's protocol. In this assay, oxidative stress results in the addition of carbonyl groups to proteins . Quantification of these carbonyl modifications serves as an indicator of the oxidative protein damage . Briefly, cell lysates were prepared as previously described for Western blotting with the addition of β-mercaptoethanol (2%) to inhibit protein oxidation. The carbonyl groups on the protein side chains in cell lysates were derivatized to 2,4-dinitrophenylhydrazone (DNP-hydrazone) by mixing the cell lysates (20 μg protein) with 2,4-dinitrophenylhydrazine (DNPH). Nonderivatized samples were used as a control. Both derivatized and nonderivatized samples were separated on pre-cast 4-20% gradient SDS-polyacrylamide gels and then transferred to nitrocellulose membranes. The membranes were blocked with 1% bovine serum albumin (BSA) in PBS with 0.1% Tween 20 and incubated with

primary antibodies to DNP-modified carbonyl groups, followed by HRP-conjugated secondary antibodies. Protein expression was visualized using ECL reagents.

L. Real-time polymerase chain reaction (PCR)

RNA was isolated from the cells using Tri Reagent (Sigma) following the protocol provided by the manufacturer. RNA was converted to cDNA using M-MLV reverse transcriptase. The cDNA was diluted 1:10 in RNase-DNase-free water for PCR analysis. For each gene to be analyzed, a standard curve was generated from serial dilutions of cDNA from the samples and was used as a reference. All values were normalized to β-actin (n = 3-6, ± SE). The undifferentiated control was assigned a value of one and all other samples were calculated relative to this control. Real-time PCR was performed on an ABI Prism 7900 Sequence Detection System using 96-well optical reaction plates. SYBR-Green was used for detection of fluorescent signal and the standard curve method was used for relative quantitative analysis. The primer sequences for the genes were generated using Primer Express software (Applied Biosystems) and the oligonucleotides were synthesized by Integrated DNA Technologies, Inc. (Coralville, IA). Table 1 summarizes the primers used for realtime PCR experiments. Data were evaluated using the Student t test and differences were considered statistically significant at $p < 0.05$.

RESULTS

A. The effects of UVB light on the oxidative stress response in keratinocytes

1. Induction of oxidative stress and markers of inflammation following UVB exposure.

In our initial studies, we determined that UVB light increases oxidative stress in primary mouse keratinocytes. It is thought that reactive oxygen intermediates (ROI) including superoxide anion, hydrogen peroxide and hydroxyl radical act as mediators of UVB light-induced carcinogenesis . Once generated, these ROI cause DNA damage leading to mutations , oxidization of proteins and induction of lipid peroxidation, all of which result in inappropriate or altered cellular signal transduction and aberrant proliferation .

UVB-induced oxidative stress in keratinocytes was analyzed by quantifying intracellular hydrogen peroxide. Both undifferentiated and differentiated keratinocytes constitutively generated low levels of hydrogen peroxide (Fig. 6). UVB (25 mJ/cm^2) caused a 10- 20 fold increase in intracellular hydrogen peroxide content in both cell types. No major differences were observed between undifferentiated and differentiated cells.

Oxidative stress is also recognized to be a key component in the development of skin inflammation in conjunction with exposure to UVB light . Recent studies have reported the causal relationship between the inflammatory process and the initiation of carcinogenesis . Previous studies have shown that COX-2, the rate-limiting enzyme in prostaglandin biosynthesis, and inflammatory cytokines such as TNFα, are upregulated by UVB . We found that UVB was found to markedly increase (25- to 35-fold) expression of COX-2 mRNA (Figure 7) and protein (Figure 8). In both undifferentiated

and differentiated keratinocytes, this effect was dose-dependent (2.5 to 25 mJ/cm^2). Differentiated cells were more responsive to UVB at the higher doses (15 and 25 mJ/cm^2) with respect to mRNA expression when compared to undifferentiated cells. UVB also caused a 2-4 fold increase in TNFα mRNA expression in the cells (Figure 7).

2. Modulation of antioxidant enzyme expression

We next examined the effects of UVB on expression of antioxidant enzymes in keratinocytes. A number of enzymes have been identified as important in limiting oxidant stress including the ROI scavengers superoxide dismutase (SOD), catalase and glutathione peroxidase (GPx) ; heme oxygenase-1 (HO-1) and metallothionein-2 (MT-2) are also effective cellular antioxidants , as are secondary antioxidant defense systems such as glutathione-S-transferase (GST) . UVB was found to stimulate expression of HO-1 mRNA (Figure 9) in both undifferentiated and differentiated cells which was maximal at 15 mJ/cm^2 while differentiated cells were more responsive to UVB at lower doses (2.5-10 mJ/cm^2). Both cell types also expressed HO-1 protein and UVB increased expression of this antioxidant in both cell types to maximal levels at 5-10 mJ/cm^2 (Figure 8). At the highest dose (25 mJ/cm^2), however, expression of HO-1 protein was inhibited.

In both undifferentiated and differentiated keratinocytes UVB (2.5-25 mJ/cm^2) also increased mRNA expression of Cu,Zn-SOD, GPx-1, and GSTA1-2 (Figures 9 and 10). Responses of GSTA1-2 to UVB were greater in undifferentiated cells when compared to differentiated cells (Figure 10). UVB also induced GSTM1, but only in undifferentiated cells (Figure 10). In contrast, UVB reduced expression of Mn-SOD, MT-2, GSTA3 and mGST3 in both cell types while no major changes were observed in

catalase, GSTP1, mGST1 and mGST2 (Figures 9 and 10. Although UVB induced GSTA4 expression in undifferentiated cells, expression of this enzyme was inhibited by UVB in differentiated cells (Figure 10). Interestingly, differentiated cells expressed 4-5-fold greater constitutive levels of GSTA4 mRNA when compared to undifferentiated cells.

3. Activation of the MAP kinases and the role of p38 and JNK MAP kinases in the expression of antioxidant enzymes

UVB is known to activate MAP kinases which are important regulators of gene expression . We found that both undifferentiated and differentiated keratinocytes constitutively expressed p38, JNK and ERK1/2 MAP kinases (Figure 11). Constitutive levels of the p38, JNK and ERK1/2 kinases were greater in differentiated cells. Keratinocytes also constitutively expressed the activated phospho-p38 and phospho-ERK1/2 kinases, but not phospho-JNK kinase. In both undifferentiated and differentiated cells, UVB (25 mJ/cm^2) activated p38 and JNK (Figure 11). Greater amounts of activated p38 and JNK were evident in differentiated cells following UVB treatment when compared to undifferentiated cells. Interestingly, UVB slightly activated ERK1/2 kinases in undifferentiated cells only, while no differences were detected in the differentiated cells.

To evaluate the role of these MAP kinases in the expression of HO-1, GSTA1-2 and GSTA4, each of which was highly responsive to UVB, we used p38 and JNK MAP kinase inhibitors. These inhibitors were found to suppress UVB-induced expression of the antioxidant enzymes in both undifferentiated and differentiated keratinocytes (Figure

12). The p38 inhibitor was markedly more effective in suppressing HO-1 expression than the JNK inhibitor in both cell types. Similarly, GSTA4 expression was more suppressed due to p38 inhibition than with JNK inhibition in both cell types. At the same time, the p38 and JNK inhibitors were unable to reverse the inhibitory effects of UVB on GSTA4 in differentiated cells and in fact further suppressed expression of this enzyme. In contrast, the JNK inhibitor was more effective then the p38 inhibitor in suppressing GSTA1-2 in undifferentiated cells. The reverse effect was observed in differentiated cells; p38 inhibition suppressed UVB-induced GSTA1-2 expression while no changes were detected with the JNK inhibitor.

B. The effects of paraquat on the oxidative stress response in keratinocytes

1. Evidence of NADPH-dependent redox cycling by paraquat in keratinocytes resulting in the formation of reactive oxygen intermediates.

It is well recognized that paraquat toxicity results from the production of superoxide anion through redox cycling (see Figure 13). In this reaction, paraquat undergoes a single electron reduction via NAD(P)H oxidase activity . In the presence of oxygen, the paraquat radical is rapidly oxidized back to the parent compound with the concomitant transfer of the extra electron to oxygen, forming superoxide anion . We found that paraquat readily generated superoxide anions in lysates of undifferentiated and differentiated keratinocytes (Figure 14). HPLC analysis was used to detect the formation of 2-hydroxyethidium, the fluorescent product formed when dihydroethidium is oxidized by superoxide anion. No differences were observed between undifferentiated and

differentiated keratinocytes in the quantity of superoxide anion formed due to paraquat treatment.

The redox cycling of paraquat and subsequent generation of superoxide anion is paired to the oxidation of NADPH. As superoxide anion is rapidly converted to hydrogen peroxide, its production of hydrogen peroxide can be used as an indicator of the activity of paraquat:NADPH oxidoreductase. In lysates from undifferentiated and differentiated keratinocytes, we found that paraquat readily stimulated hydrogen peroxide production (Fig 15A and 15B). These effects were time- and concentration-dependent. Greater activity was found in differentiated cells, when compared to undifferentiated cells (Fig. 15C and 15D). We next quantified the depletion of NADPH due to paraquat redox cycling (Fig. 16). In lysates from both undifferentiated and differentiated keratinocytes NADPH was rapidly metabolized. Thus, the amount of NADPH was reduced by approximately 70% in 3 hours with no major differences between the two cell types. These data demonstrate that keratinocytes have the capacity to redox cycle paraquat and that differentiation may be an important factor in regulating this activity. We also found that the addition of either dicoumarol, an inhibitor of NAD(P)H quinone oxidoreductase 1 (NQO1) , or DPI, an inhibitor of many FAD reducing enzymes including NADPH oxidase , to keratinocyte lysates significantly reduced the rate of hydrogen peroxide production by paraquat (Fig. 17). These data indicate that paraquat redox cycling by keratinocytes is catalyzed by FAD-dependent NADPH oxidases and, in particular, NQO1.

During redox cycling paraquat is reduced to its radical with a concomitant oxidation of NADPH. The paraquat radical then immediately transfers an electron to

oxygen, forming superoxide anion and the parent paraquat molecule . Under anaerobic conditions, however, the paraquat radical is stable . We next measured the capacity of keratinocyte lysates to generate paraquat radicals under anaerobic conditions. Figure 18 shows that lysates from differentiated keratinocytes can readily generate the paraquat radical. Paraquat radical formation was time dependent (Fig. 18 inset). The presence of the paraquat radical was confirmed by the appearance of a blue-violet color in the reaction mix . No major differences were observed in paraquat radical formation between undifferentiated and differentiated keratinocytes (not shown).

2. Paraquat-induced oxidative stress results in the oxidation of cellular proteins

The oxidation of proteins by reactive oxygen intermediates is known to be an important marker of cellular oxidative stress . Using an immunoblot assay for the detection of ROI-modified proteins, we found that both undifferentiated and differentiated keratinocytes contained basal levels of oxidized proteins and that paraquat treatment caused a marked increase in the content of oxidized proteins (Fig. 19). Of particular interest was the increased oxidation of proteins (with molecular weights of 68, 75 and 98 kDa). In addition, a band of oxidized protein at 43 kDa was evident only after paraquat treatment in both cell types. These changes in protein oxidation were observed in both undifferentiated and differentiated cells.

3. Induction of mRNA and protein expression of antioxidant enzymes

We found that the mRNA expression of several antioxidant enzymes were markedly upregulated in undifferentiated and differentiated keratinocytes following

paraquat treatment (Fig 20A). Cu,Zn-SOD mRNA increased approximately 4 to 5-fold in both cells types following paraquat treatment while HO-1 increased 5 to 6-fold. Similarly, the expression of catalase mRNA increased 8 to 12-fold after paraquat treatment in the undifferentiated and differentiated cells, respectively. In addition, this difference between paraquat-treated differentiated and undifferentiated cells was statistically significant ($p < 0.03$). In both cell types, HO-1 protein was constitutively expressed was increased with paraquat treatment (Fig. 20B). No major alterations in mRNA expression of Mn-SOD, GPx-1 or MT-2 were observed (Fig. 20A).

It is well recognized that the activity of the glutathione-S-transferase (GST) enzymes are crucial in the elimination of oxidized macromolecules and xenobiotics in cells through glutathione conjugation . The major members of the GST superfamily are the alpha (GSTA), mu (GSTM) and pi (GSTP) families which are important in detoxification of lipid and protein peroxidation products . We found that the alpha family of GST's exhibited marked increases in mRNA induction in response to paraquat treatment, in particular, GSTA1-2 and GSTA4 (Fig. 21A). In addition, GSTA1-2 showed significant differential induction in the undifferentiated and differentiated cells (approximately 38- versus 60-fold, respectively). Although GSTA4 expression also shows significant differential induction (22- versus 37-fold), this is likely due to increased basal expression of the enzyme (7-fold) in the differentiated cells. GSTA3 mRNA levels were also increased, 5- and 8-fold for the undifferentiated and differentiated cells, respectively, following paraquat treatment (Fig. 21A). Paraquat also stimulated GSTP1 expression (3-4 fold) in both cell types (Fig. 21B). At the same time,

no major changes were found in the mRNA expression of GSTM1 following paraquat treatment.

C. Production of eicosanoids and induction of the eicosanoid biosynthetic enzymes by UVB light

1. Prostaglandin production by keratinocytes following UVB light.

UVB light has been shown to induce prostaglandin production in both keratinocytes and skin. Moreover, elevated concentrations of these metabolites have been associated with UVB- and chemical-induced carcinogenesis. We found that exposure to UVB altered the pattern of prostaglandin synthesis in undifferentiated keratinocytes (Figure 22). Previous studies have demonstrated that the levels of prostaglandin E_2 (PGE_2) are increased following UVB in both keratinocytes and skin. These findings correlated with the results of our studies in which UVB clearly increases the amount of PGE_2. We also detected a marked increase in the quantity of prostaglandin J_2 (PGJ_2) while the amount of prostaglandin D_2 (PGD_2) dramatically decreased. PGD_2 concentrations have been shown to be increased in skin following UVB However, PGD_2 undergoes spontaneous dehydration to PGJ_2 . Our results indicate that any excess PGD_2 that may have been produced was converted to PGJ_2. No alteration was observed in the levels of prostaglandin A_2 (PGA_2).

2. Modulation of expression of prostanoid biosynthetic pathway enzymes and receptors.

The release of arachidonic acid from the phospholipid membrane is catalyzed by several phospholipases. Cytosolic phospholipase A_2 ($cPLA_2$) activity mobilizes

arachidonic acid directly and has been shown to be crucial for its release . Alternatively, activation of phospholipase C (PLC) initiates a cascade of events, resulting in the production of diacylglycerol and monoacylglycerol and their subsequent hydrolysis by diacylglycerol lipase (DAG lipase) and monoacylglycerol lipase (MAG lipase), respectively, and ultimately generating free arachidonic acid . We found that $cPLA_2$ expression was unchanged in the undifferentiated cells and slightly increased in the differentiated cells following UVB light (Fig. 23). In contrast, UVB induced PLCβ1 expression (8-fold) in both cell types (Fig. 23). No changes in DAG lipase expression were detected in either cell type while UVB light decreased MAG lipase expression in undifferentiated cells while an increase of 4-fold was observed in differentiated cells.

Once released from the phospholipid membrane, arachidonic acid is converted to prostaglandin H_2 (PGH_2) by either COX-1 or COX-2 . PGH_2 production occurs in two sequential reactions. In the first reaction, two oxygen molecules are inserted into the arachidonate backbone, forming prostaglandin G_2 (PGG_2) . The hydroperoxyl group of PGG_2 is then reduced to hydroxyl, generating PGH_2 . COX-1 is a constitutive enzyme that participates in many homeostatic functions. In our experiments, no major changes in COX-1 mRNA expression were observed in either the undifferentiated or differentiated cells (Fig. 24). As previously described, COX-2 mRNA and protein expression is markedly upregulated by UVB light in both undifferentiated and differentiated keratinocytes (Figures 7 and 8).

The intermediate prostaglandin, PGH_2, serves as the substrate for the prostanoid synthases with each enzyme responsible for the production of one specific metabolite . The major prostaglandin in the skin, PGE_2, results from the action of one of two

isozymes, mPGES-1 and mPGES-2 . We found that the mRNA expression of both mPGES-1 and -2 is increased 4-6 fold in both cell types following exposure to UVB light (Fig 25). However, the differentiation state of the cells affected the level of induction of these two enzymes; mPGES-1 expression was greater in differentiated cells while mPGES-2 was higher in undifferentiated cells. Moreover, differentiated cells had approximately twice the constitutive expression of both mPGES enzymes as compared to undifferentiated cells. The other prostaglandins, PGD_2, $PGF_{2\alpha}$, PGI_2 and TXA_2 are produced by PGDS, PGFS, PGIS and TXAS, respectively. The expression of PGFS and PGIS were also induced by UVB in a dose-dependent manner (approximately 20- and 6-fold, respectively) in both undifferentiated and differentiated cells (Fig 25). Differentiated cells had approximately twice the PGFS constitutive expression as that of undifferentiated cells. Moreover, the expression of PGFS was consistently greater in the differentiated cells when compared to the undifferentiated cells throughout the entire range of UVB doses. We also found that UVB induced small increases in PGDS (2-fold) in both cell types (Figure 25). No major changes were observed in the expression of TXAS in either undifferentiated or differentiated cells (Fig 25).

Prostaglandins, once formed, bind specific receptors on keratinocytes . Four receptors for PGE_2 have been identified: EP1, EP2, EP3 and EP4, all of which are expressed in skin . Although all four receptors are involved in the inflammatory response, EP1 is recognized as the primary signaling pathway for the proinflammatory effects of PGE_2 in the skin . EP2, EP3 and EP4 also participate in the inflammatory process but have more specialized functions such as activation of the immune system of the skin . We found that the expression of EP1 and EP2 was induced by UVB light (approximately 6-

and 4-fold, respectively) in both undifferentiated and differentiated keratinocytes (Fig 26). No major changes were detected in mRNA expression of EP3 or EP4 in either cell type (Fig. 26). The expression of FP, the $PGF_{2\alpha}$ receptor, increased 2-3-fold in both cell types (Fig 26). Expression of the prostacyclin receptor, IP, was increased in a UVB dose-dependent fashion with the undifferentiated cells having a greater maximal response (16-fold) when compared to the differentiated cells (8-fold) (Fig. 27). PGD_2 has two receptors: DP and CRTH2. The mRNA expression of both DP and CRTH2 increased following UVB exposure (Fig. 27). DP mRNA induction was observed only at the highest UVB dose (25 mJ/cm^2) with increases of 2- and 8-fold for the undifferentiated and differentiated cells, respectively. In contrast, CRTH2 expression was increased in a UVB dose-dependent manner (10 – 25 mJ/cm^2) in both cell types. Moreover, the differentiated cells had 2-fold greater CRTH2 expression at these higher UVB doses when compared to the undifferentiated cells (10-fold versus 20-fold) (Fig. 27). No major alterations were detected in the expression of TP, the thromboxane A_2 receptor.

3. Modulation of expression of leukotriene biosynthetic pathway enzymes and receptors

Lipoxygenases catalyze the oxidation of arachidonic acid to leukotrienes and HETE's . As shown in Figure 28, the greatest induction was detected in 8-LOX expression with maximal increases of 12-fold in both undifferentiated and differentiated cells. FLAP mRNA levels increased 6-fold in both cell types even as no major changes were detected in the expression of 5-LOX. UVB also induced 15-LOX expression (4-fold) both cell types in a dose-dependent manner. Epidermal-type 12-LOX expression increased (2-fold) slightly following UVB in both cell types. Platelet-type 12-LOX was

differentiation-dependent at the higher UVB doses (10-25 mJ/cm^2) with small increases or decreases in expression in the undifferentiated and differentiated cells, respectively.

Leukotriene A_4 (LTA_4) is hydrolyzed by LTA_4 hydrolase, producing LTB_4 . LTB_4 is then glutathionylated by LTC_4 synthase to form LTC_4 . LTC_4 is the initial cysteinyl leukotriene produced and this metabolite can be converted to the other members of this group, LTD_4 and LTE_4. We found that low UVB doses (5-10 mJ/cm^2) slightly increased LTA_4 hydrolase expression while, at higher doses (15-25 mJ/cm^2), the levels of this enzyme decreased in both cell types (Figure 29). At the same time, UVB induced LTC_4 synthase expression 2- and 6-fold in the undifferentiated and differentiated cells, respectively (Figure 29).

Once formed, leukotrienes bind to specific receptors to initiate biological activity. LTB_4 has two receptors, BLT1 and BLT2, as do the cysteinyl leukotrienes, CysLT1 and CysLT2 . No changes were observed in either BLT1 or BLT2 expression following UVB (Figure 30). In contrast, UVB increased the expression of CysLT1 6-9-fold in the undifferentiated and differentiated cells, respectively (Figure 30). Similarly, CysLT2 expression was increased 6-fold in both cell types.

The membrane-associated proteins in eicosanoid and glutathione (MAPEG) enzymes include both enzymes involved in arachidonic acid (FLAP, LTC_4 synthase and mPGES-1) and glutathione metabolism (mGST1, 2 and 3) . The enzymes are linked by structural and sequence homology as well as having glutathione-dependent activity with the exception of FLAP which is glutathione independent. As shown in Figure 31, we found that UVB light induced the expression of the eicosanoid family enzymes to a much greater extent than the mGST enzymes. As previously described, FLAP and LTC_4

synthase expression increased approximately 6-fold. Similarly, mPGES-1 mRNA levels were increased 4-6 fold following UVB. In contrast, no major changes in expression of mGST1 or mGST2 were observed in either cell type. At the same time, mGST3 levels were decreased to only a fraction of that of the control in both cell types.

4. Activation of Akt by UVB light

Activation of Akt occurs through a signaling cascade starting with phosphorylation of phosphoinositol 3-kinase (PI3K) by activated growth factor receptors such as the epidermal growth factor receptor (EGFR) . Activated PI3K initiates the phosphorylation of a series of phosphoinositide products, thereby causing Akt to translocate from the cytosol to the nucleus where it is phosphorylated . In vitro studies have shown that by increasing the extracellular calcium concentrations, phosphoinositide metabolism was rapidly activated, leading to keratinocyte differentiation . The role of calcium in the activation of the PI3K/Akt pathway is now recognized as a major actor in the promotion of the differentiation process .

The Akt pathway is recognized as a pro-survival pathway . UVB is known to activate Akt in both keratinocytes and skin . We found that the undifferentiated cells exhibited a UVB dose-dependent phosphorylation of Akt while the differentiated cells had high constitutive levels of Akt phosphorylation, irregardless of the UVB dose (Figure 34). This differential expression was most likely due to the higher intracellular calcium concentrations contained within the differentiated keratinocytes.

Akt is also known to be cleaved by caspases during apoptosis . In correlation with the degree of Akt phosphorylation, the presence of these cleavage fragments at 40 and 44

kDa are evident only at the highest UVB doses (15-25 mJ/cm^2) in the undifferentiated cells but are constitutively and continuously present in the differentiated cells, irregardless of UVB dose (Fig 32).

5. Effects of p38 and JNK MAP and Akt kinase inhibitors in the expression of prostaglandin and leukotriene synthetic enzymes

We have shown that UVB is a potent activator of the p38 and JNK MAP kinases in keratinocytes. To evaluate the role of these kinases in mediating the expression of COX-2, mPGES-1 and PGIS, each of which was highly responsive to UVB, we used p38 and JNK MAP kinase inhibitors, as shown in Figure 33. These inhibitors were found to suppress UVB-induced COX-2 expression in both undifferentiated and differentiated keratinocytes. In contrast, mPGES-1 expression was decreased with JNK inhibition while p38 inhibition was slightly effective only at the highest UVB (15-25 mJ/cm^2) dose in undifferentiated keratinocytes. However, in differentiated cells, inhibition of both kinases prevented UVB-induced mPGES-1 expression. PGIS expression was unchanged with p38 inhibition while JNK inhibition caused an approximate 2-fold decrease in PGIS induction in undifferentiated cells. In contrast, in differentiated cells, no changes were detected in PGIS expression due to inhibition of either the p38 or JNK MAP kinases.

We next assessed the role of Akt in COX-2, mPGES-1 and PGIS expression using an inhibitor of phosphoinositide 3-kinase (PI3K). Phosphorylation of PI3K initiates a signaling cascade, resulting in the activation of Akt . Inhibition of PI3K, therefore, effectively prevents Akt phosphorylation . As with the MAP kinases, we found that COX-2 expression was suppressed by PI3K inhibition although this effect was more

pronounced in the undifferentiated cells than in the differentiated cells (Fig 34). Similarly, PI3K inhibition decreased mPGES-1 expression in both cell types and was more effective in undifferentiated cells versus differentiated cells (Fig 34). In contrast, PGIS expression was unchanged with PI3K inhibition in the undifferentiated cells while PGIS mRNA induction was slightly decreased in differentiated cells.

As both 8-LOX and 15-LOX expression were noticeably increased by UVB, we chose to determine the effect of kinase inhibition on the expression of these enzymes. We found that alterations in 8-LOX mRNA expression due to kinase inhibition were differentiation-dependent. As shown in Figures 35 and 36, 8-LOX mRNA levels were decreased with p38, JNK and PI3K inhibition at the higher UVB doses (10-25 mJ/cm^2) in undifferentiated cells. In differentiated cells, however, inhibition of p38 and PI3K resulted in increased 8-LOX expression at the lower UVB (2.5-10 mJ/cm^2) with decreases observed at the higher doses. JNK inhibition, however, enhanced 8-LOX expression approximately 2-fold in these cells. 15-LOX expression was unchanged by kinase inhibition in undifferentiated cells (Figures 35 and 36). In differentiated cells, however, JNK inhibition resulted in an increase in 15-LOX mRNA levels, similar to that observed with 8-LOX expression. At the same time, no major changes were detected in 15-LOX expression following p38 or JNK inhibition.

D. Induction of the eicosanoid biosynthetic enzymes by paraquat

1. Modulation of mRNA and protein expression of prostanoid and leukotriene biosynthetic pathway enzymes.

Arachidonic acid mobilization and eicosanoid metabolite production are known to be induced by oxidative stress . As paraquat is an effective generator of ROI, we determined if paraquat treatment affected the expression of the eicosanoid biosynthetic enzymes. We found that paraquat (100 μM) increased expression of $cPLA_2$ mRNA (3- and 5-fold) in undifferentiated and differentiated keratinocytes, respectively while no changes were observed in COX-1 mRNA levels in either cell type (Fig 37A). At the same time, COX-2 expression was dramatically increased following paraquat treatment in both undifferentiated and differentiated cells (approximately 35- and 70-fold, respectively) (Fig 37A). COX-2 protein was also upregulated after paraquat treatment with the differentiated cells having greater protein expression when compared to the undifferentiated cells (Fig 37B).

Prostaglandins are produced through the sequential actions of the COX enzymes and the prostanoid synthases, mPGES-1 and -2, PGFS, PGIS, PGDS and TXAS . The major prostaglandin in the skin, PGE_2, is formed by mPGES-1 and mPGES-2 . In our studies, paraquat induced mPGES-1 expression by 4-fold in both cell types even as the constitutive level of mPGES-1 mRNA in the differentiated cells was approximately twice that of the undifferentiated cells. No alteration in mPGES-2 levels was detected in the undifferentiated cells while, in differentiated cells, the expression of mPGES-2 was decreased. As with mPGES-1, the differentiated cells exhibited an almost 3-fold greater basal level of mPGES-2 when compared to the undifferentiated cells.

PGFS and PGIS are the terminal synthases responsible for the production of PGF_2 and PGI_2. Paraquat treatment induced PGFS (3- and 5-fold) and PGIS (2- and 3-fold) expression in the undifferentiated and differentiated cells, respectively (Fig 38). Similar

to the mPGES results, the differentiated cells had a 2-fold greater constitutive expression of PGFS when compared to the undifferentiated cells. In contrast, the constitutive expression of PGIS was decreased in differentiated cells versus undifferentiated cells. PGDS and TXAS levels were not changed in response to paraquat in the undifferentiated cells (Fig 38). However, in the differentiated cells, the mRNA levels of these enzymes were increased approximately 2-fold over that of the control cells. At the same time, the basal expression of both PGDS and TXAS in the differentiated cells was reduced to approximately half that of the undifferentiated cells.

The lipoxygenase (LOX) enzymes oxidize arachidonic acid, generating leukotrienes, HETE's and lipoxins . Paraquat treatment had the greatest effect on the expression of 15-LOX with increases of 7- and 15-fold in the undifferentiated and differentiated cells, respectively (Fig 39). We also found that paraquat treatment increased the expression of 5-LOX (2-fold), FLAP (4-5 fold), 8-LOX (3-5 fold), platelet type 12-LOX (2-fold) and LTC_4 synthase (2-4 fold) in both cell types (Fig 39). No major changes were observed in the expression of epidermal type 12-LOX or LTA_4 hydrolase (Fig 39).

The MAPEG enzymes are grouped by both sequence and structural homology as well as functional activity . Members of this family include enzymes involved in arachidonic metabolism (mPGES-1, FLAP and LTC_4 synthase) as well as oxidative stress response enzymes (mGST1, mGST2 and mGST3). As described previously, mPGES-1 FLAP and LTC_4 synthase expression was increased following paraquat treatment in both undifferentiated and differentiated cells (Fig 40). No major changes were observed in the expression of mGST1 or mGST2 in either cell type (Fig 40).

Paraquat increased mGST3 expression (approximately 2-fold) in the undifferentiated cells with a slight decrease in mGST3 mRNA levels in the differentiated cells (Fig 40).

DISCUSSION

A. The effects of UVB light on the oxidative stress response in keratinocytes

Oxidative stress is recognized as a key factor contributing to the development of many cutaneous diseases including cancer). In both intact skin and isolated keratinocytes, UVB induces oxidative stress. It stimulates the formation of ROI which can generate oxidized cellular material including lipid peroxidation products and oxidized DNA bases . In the skin, UVB-induced oxidative stress also generates an inflammatory response . In this regard, our studies demonstrate that in mouse keratinocytes, UVB induces gene expression for TNFα as well as COX-2, an enzyme that can generate prostaglandins. Previous studies have shown that these genes can be upregulated by ultraviolet light . Gene expression for COX-2 was greater in differentiated cells when compared to undifferentiated cells treated with UVB and this may be the result of greater amounts of activated p38 and JNK in differentiated cells. Both of these MAP kinases are known to be important in regulating COX-2 expression .

Similar levels of intracellular oxidative metabolism were noted between undifferentiated and differentiated cells in response to UVB indicating that the two cell types possess a similar antioxidant capacity. This idea is consistent with our findings that the two cell types express generally similar constitutive gene expression levels of SOD, catalase and GPx-1. In response to UVB-induced oxidative stress, we found that both undifferentiated and differentiated keratinocytes upregulate expression of several antioxidant genes including HO-1 and GPx-1. No consistent changes in catalase or Cu,Zn-SOD gene expression were noted while expression of Mn-SOD and MT-2 declined. UVB was also more effective in inducing HO-1 in differentiated cells. Like

COX-2, expression of HO-1 is regulated by the MAP kinases and increases in their activity following differentiation may account for increased expression of this antioxidant. Previous studies have suggested that HO-1 is induced primarily by UVA with little or no effects of UVB except at very high doses (50-550 mJ/cm^2) . Our studies show that HO-1 mRNA and protein expression in keratinocytes is dependent on the dose of UVB and that expression of the enzyme is inhibited at higher doses.

The mechanisms regulating gene expression of GPx-1, SOD and MT-2 in response to oxidative stress are not well understood. That GPx-1 gene expression is not increased to the same extent as COX-2 and HO-1 in response to UVB and that there are no differentiation specific effects suggests that regulation of its expression is distinct. The mechanisms mediating decreases in expression of MT-2 and Mn-SOD are also not clear. MT-2 functions to sequester metals such as zinc, a process that may be important in its antioxidant activity . Zinc and other heavy metals are known to regulate expression of metallothioneins and it is possible that UVB interferes with their ability to regulate MT-2 expression in murine keratinocytes . In this regard, Yamada et al. demonstrated that ultraviolet light blocks transcriptional activation of MT-2 in human skin-derived fibroblasts. Cu,Zn-SOD and MnSOD are distinct gene products; Cu,Zn-SOD is localized in cytosolic and lysosomal fractions of cells and in mitochondrial intermembraneous space, while Mn-SOD is found in mitochondrial matrix and inner membrane . Multiple SOD's are thought to be important in protecting different intracellular compartments from superoxide, a radical that does not readily cross membranes. UVB is known to damage mitochondria and this may trigger signals that decrease expression of Mn-SOD .

The GST enzymes are comprised of a large superfamily of ubiquitous cytosolic and microsomal phase II detoxification enzymes that conjugate reduced glutathione to electrophilic compounds. The cytosolic GST's are divided into three major gene families, alpha (GSTA), mu (GSTM) and pi (GSTP) . Each GST family has preferred substrates. Although total GST activity has been shown to increase significantly in skin following UVB exposure , there has been limited investigation on the involvement of GST isozymes in this cellular response. We found that GSTA1-2 and GSTA4 were markedly upregulated in undifferentiated keratinocytes after UVB exposure. These findings are in accord with previous studies showing that GSTA4 expression is upregulated in response to oxidative stress induced by UVB and paraquat . Overexpression of GSTA1 has also been shown to protect against hydrogen peroxide-induced oxidative stress . GSTA and, to a lesser extent, GSTP, remove lipid peroxidation products, thereby breaking radical-forming chain reactions . This activity is likely important in the antioxidant response of keratinocytes to UVB. In contrast to GST1A, GSTA3, which is involved in steroid biosynthesis , as well as GSTP1, which removes DNA and protein oxidation products , were unaffected by UVB-induced oxidative stress. GSTM1, which is also important in protecting against protein oxidation, initially declined in response to UVB and then increased. A greater increase was observed in undifferentiated cells when compared to differentiated cells. These findings demonstrate that specific cytosolic GST's are important in the response to UVB, although their precise functions in keratinocytes are not known at the present time. Interestingly, gene expression of both GSTA1-2 and GSTA4 are regulated by the differentiation status of the keratinocytes. Thus, the differentiated keratinocytes express much greater

constitutive levels of these cytosolic GST's when compared to the undifferentiated cells. This is consistent with previous work showing that differentiated cells are more resistant to oxidant-induced stress and that the differentiation process itself results in an increase in GST activity . However, the responses of GSTA1-2 and GSTA4 in differentiated cells to UVB are distinct. Thus, GSTA1-2 increases in response to UVB, although not to the same extent as in undifferentiated cells. Unexpectedly, GSTA4 decreased following UVB treatment. The mechanism for differential responsiveness of GSTA4 to UVB in undifferentiated and differentiated cells is not known. Previous studies have shown that GSTA4 can regulate proliferation and protect against apoptosis and it is possible that UVB-induced decreases in expression of the enzyme are important in promoting turnover of the differentiated epidermis during oxidative stress.

The microsomal GST (mGST) are members of the membrane-associated proteins in eicosanoid and glutathione metabolism (MAPEG) family of enzymes . Like cytosolic GSTA, these enzymes are important in protecting cells against microsomal lipid peroxidation . It appears, however, that neither expression of mGST1 nor mGST2 are significantly altered by UVB in keratinocytes. Interestingly, UVB markedly reduced expression of mGST3 in the cells and this was not differentiation specific. These data indicate that distinct mechanisms regulate expression of the microsomal GST's. At the present time, factors regulating mGST3 expression are not known. mGST3 is important in synthesizing leukotriene A_4, a proinflammatory lipid mediator and UVB-induced decreases in its expression may be important in the resolution of inflammation .

It is well recognized that ROI can activate a number of signal transduction pathways important in controlling gene expression . This is thought to occur by direct or

indirect activation of growth factors or growth factor receptors via a process referred to as "the UV response" . This response was initially characterized with respect to activation of the immediate early genes, c-fos and c-jun and the transcription factors NF-□B and AP-1 . Members of the MAP kinase family have been implicated as regulators of the UV response and are activated by UVB). In mouse keratinocytes we found that only p38 and JNK MAP kinases were activated following UVB treatment. These results are in accord with reported effects on UVB on PAM212 mouse keratinocytes and human keratinocytes . Interestingly, greater amounts of constitutive expression of total and activated forms of JNK and p38 MAP kinase were noted in differentiated relative to undifferentiated keratinocytes. Increases in activated JNK have been reported previously in suprabasal layers of human skin . This may be due to increased sensitivity of the differentiated cells to autocrine growth factor activation or a requirement for JNK in regulation of gene transcription in differentiating keratinocytes . A variety of additional growth factors including activators of MAP kinase signaling have been identified in primary mouse keratinocytes, as well as in mouse skin . It has also been suggested that activation of MAP kinases is important in promoting differentiation , although the mechanisms mediating these effects are, at present, unknown.

Our studies using MAP kinase inhibitors demonstrated that JNK and p38 were important in regulating keratinocyte expression of HO-1, GSTA1-2 and GSTA4. Moreover, with the GST's, differentiation appears to regulate cellular responsiveness to the kinase inhibitors. Previous studies have shown that both the p38 and JNK MAP kinases regulate expression of HO-1. The fact that inhibition of p38 was more effective than JNK in suppressing UVB-induced HO-1 suggests that this kinase plays a more

prominent role in regulating expression of this antioxidant. A similar pattern of inhibition was noted in the regulation of GSTA4 in undifferentiated cells. A prominent role for p38 in regulating expression of GSTA4 has also been reported in murine hepatocytes stimulated with epidermal growth factor. In contrast, JNK appeared to play a more prominent role in regulating GSTA1-2 expression in undifferentiated cells. These data indicate that regulation of expression of these antioxidants in the cells occurs via different mechanisms. While p38 and JNK inhibition did not reverse the inhibitory effects of UVB on GSTA4, only p38 inhibition was able to inhibit UVB-induced GSTA1-2 in differentiated cells. These data indicate that the differentiation process changes mechanisms regulating UVB-induced alterations in expression of the GST's. These data are consistent with studies showing that keratinocyte differentiation is associated with alterations in expression of a variety of transcription factors including AP-1, SP-1 and PPAR-gamma .

In summary, our data demonstrate that UVB light induces oxidative stress in primary cultures of undifferentiated and differentiated mouse keratinocytes by increasing the production of ROI and inflammatory mediators, activating the p38 and JNK MAP kinases, and increasing expression of critical antioxidant enzymes including HO-1, GPx-1, GSTA1-2, and, in undifferentiated cells, GSTA4. However, UVB also decreases MnSOD, MT-2, GSTA3 and mGST3. GSTA4 also decreased in differentiated cells. Whether or not these responses are important in protecting the skin from UVB will depend on the levels of expression of functional proteins for these enzymes in the different cell types and their precise roles in regulating oxidative stress and/or repairing cellular damage. Further studies are required to understand the mechanisms regulating

expression of the antioxidants, the role of differentiation in controlling responsiveness to UVB, and how these enzymes contribute to protecting the skin against oxidative stress.

B. The effects of paraquat on the oxidative stress response in keratinocytes

Paraquat is recognized as a potent oxidant whose toxicity results from the generation of reactive oxygen intermediates through a redox cycling mechanism . Numerous studies have shown that the production of these ROI causes nucleic acid damage as well as protein and lipid peroxidation in paraquat-treated tissues. In the present studies, we showed that paraquat readily undergoes redox cycling in primary mouse keratinocytes, thereby generating ROI and inducing oxidative stress. Our data showed that differentiated keratinocytes have a greater capacity for hydrogen peroxide production when compared to the undifferentiated cells. This difference occurred even as the inherent rates of NADPH depletion and paraquat radical formation were the same between the two cell types. Undifferentiated keratinocytes have been reported to be more susceptible to hydrogen peroxide-induced apoptosis than differentiated cells , indicating that the differentiated cells appear to be more tolerant of increased oxidative stress.

The question then is to what extent differentiation affects the keratinocyte response to paraquat-induced oxidative stress. Although the majority of studies have analyzed the antioxidant capacity of the epidermis as a whole, there is currently little known about the oxidative stress responses of the undifferentiated versus the differentiated cells. In one such study, Vessey et al. determined that keratinocyte

differentiation resulted in higher levels of GPx and GST activity and that this increase in the cellular antioxidant capacity provided protection from chemically-induced oxidative damage. We found that both undifferentiated and differentiated keratinocytes respond to increased oxidative stress with an upregulation in the expression of several antioxidant enzymes and also that some of these enzymes exhibit differential induction.

No major differences were observed in SOD expression between undifferentiated and differentiated keratinocytes. Interestingly, Cu,Zn-SOD mRNA levels were induced while those of Mn-SOD were unchanged. These results correlate with previous studies in which Cu,Zn-SOD activity was increased while Mn-SOD activity was decreased in paraquat-treated fibroblasts and keratinocytes exposed to UVB . Studies with transgenic mice have demonstrated that Cu,Zn-SOD expression is necessary for prevention of oxidative damage in retinal cells and in neurons . The expression of HO-1 also did not exhibit any differential effects; both cell types showed equal upregulation of HO-1 mRNA and protein. As with SOD expression, HO-1 has been shown to be upregulated in response to exposure to oxidants such as ozone , sodium arsenite and UVA and, in studies with transgenic mice, HO-1 deficiency resulted in increased ROI production and mortality . Surprisingly, catalase expression at both the mRNA and protein level was clearly differentiation dependent following paraquat treatment. The markedly higher basal catalase expression of the differentiated cells has been previously reported and may explain their greater tolerance to hydrogen peroxide-induced damage. Although increased catalase expression has been shown to occur in skin following UVA exposure , the intrinsic enzymatic activity was decreased following phorbol ester or UVB exposure.

Catalase overexpression, however, provided protection not only from hydrogen peroxide-induced damage but UVB-mediated apoptosis as well ..

The primary function of the GST enzymes is the conjugation of glutathione to electrophilic compounds in order to facilitate their detoxification and elimination. Although all GST enzymes conjugate glutathione, the specificity of the substrates differs between the GST families which may account for the variety of induction levels we observed following paraquat treatment. The cytosolic GST's are divided into three major gene families, alpha (GSTA), mu (GSTM) and pi (GSTP), with several minor families described to date . The GSTA enzymes have been shown to break lipid peroxidation chain reactions through the removal of hydroperoxides and aldehydes . This GSTA preference for lipid peroxidation products explains the striking induction of GSTA1-2 and GSTA4 as well as GSTA3 observed in our data. These findings correlate with previous work in which overexpression of GSTA1 provides protection against hydrogen peroxide-induced cytotoxicity and DNA damage in retinal pigment cells . Although total cytosolic GST activity has been shown to increase as keratinocytes differentiated , our data indicate that GSTA4 mRNA alone exhibits differential constitutive expression. The importance of GSTA4 activity in protection against paraquat-induced oxidative stress has been demonstrated using GSTA4 null mice . The increased basal GSTA4 expression in the differentiated cells may, therefore, provide additional defense against ROI-mediated damage. The small induction of GSTP1 and lack of induction in GSTM1 in keratinocytes may be due to the much diminished roles that GSTP and GSTM play in lipid peroxidation product detoxification .

The microsomal GST (mGST) enzymes, described as members of the membrane-associated proteins in eicosanoid and glutathione metabolism (MAPEG) family of enzymes , have been shown to have glutathione peroxidase activity against lipid hydroperoxides similar to that of the cytosolic GSTA enzymes . However, in keratinocytes, the expression of these enzymes does not appear to be influenced by paraquat and mGST activity has not been detected in either undifferentiated or differentiated keratinocytes .

Clearly, keratinocytes react to paraquat treatment by upregulating the antioxidant enzymes, an action critical for the prevention of ROI-induced injury. Antioxidant therapy such as the administration of SOD or N-acetylcysteine (NAc) following exposure has, therefore, been proposed as a potential treatment for paraquat poisoning. This approach, however, has had mixed results. While NAc and SOD increased the survival of treated animals , further work has shown that the protective effects of SOD are only evident with the addition of Mn-SOD and glutathione (GSH) . In the same study, Cu,Zn-SOD treatment was proven to enhance oxidative injury, primarily due to the reactivity of the copper ions. In recent experiments, however, synthetic SOD analogs have successfully prevented oxidative damage without proving toxic . Clearly, the use of antioxidants as treatments for paraquat requires further research in order to provide a safe and efficacious therapy.

At the present time, the importance of the differential responses of growing and differentiated keratinocytes to paraquat-induced oxidative stress is not known. It is well recognized that oxidative stress increases the expression of a number of antioxidant enzymes as a general keratinocyte response. The data presented in this study indicates

that the differentiation status of the cells also regulates the specific pattern of antioxidant enzyme induction in keratinocytes. It may be that this differential response to oxidative stress is key to a more complete understanding of the dermal toxicity of paraquat.

C. Production of eicosanoids and induction of the eicosanoid biosynthetic enzymes by UVB light

UVB light is known to initiate an inflammatory response in exposed skin. In the last several years, UVB-induced cutaneous inflammation has been recognized as a major contributing factor in the development of carcinogenesis. These effects are mediated by many proinflammatory mediators such as cytokines and arachidonic acid metabolites. Consequently, more focus has been placed on determining the exact role of the eicosanoids in the UVB inflammatory response in the skin in order to develop better treatment options. As with other cancer research, much of the work has focused primarily on the function and effects of COX-2. In the present studies, we took a more global approach. Using primary mouse keratinocytes, we investigated the effects of UVB light on eicosanoid production through activation of the COX and LOX branches of the arachidonic acid metabolism pathway.

The initial step of eicosanoid biosynthesis is the mobilization of arachidonic acid from the phospholipid membrane through phospholipase action. UVB is known to activate $cPLA_2$ in skin . In contrast, we found that $cPLA_2$ mRNA expression was generally unchanged following UVB light. Our data was collected 24 hours following UVB exposure while the previous studies indicated that activation of $cPLA_2$ was an early response, occurring 2-4 hours after irradiation . Although we detected an increase in

PLCβ1 expression, there was no or slight increases in the downstream enzymes, DAG and MAG lipases. This indicates that the generation of free arachidonic acid from this pathway of phosphoinositide metabolism is most likely not a significant factor in UVB exposure. However, previous studies have shown that UVB increases diacylglycerol (DAG) concentrations in keratinocytes and DAG production through PLCβ1 activity is known to activate protein kinase C (PKC) . Activated PKC initiates a signal transduction cascade through stimulation of Raf1, then MEK and finally to the MAP kinases and this activation of the MAP kinases is known to phosphorylate $cPLA_2$. It is well known that UVB activates the MAP kinases and our data shows this as well.

Although both COX-1 and COX-2 are involved in the conversion of arachidonic acid into prostaglandins, the expression and function of these two isozymes differ. COX-1 is constitutively expressed in almost all tissues and is considered a "housekeeping" enzyme while COX-2 is inducible in response to inflammatory stimuli . In agreement with our results, numerous studies have shown that COX-2 expression is upregulated by UVB light at both the gene and protein levels . Previous studies have also shown that UVB-induced COX-2 expression occurs primarily in the suprabasal keratinocytes in skin . Additional investigation using cultured human keratinocytes has shown that with increased intracellular calcium concentrations, there was an upregulation of COX-2 mRNA and protein with a concomitant induction of PGE_2 production .

Our data also shows that UVB-induced COX-2 expression is regulated through activation of the p38 and JNK MAP kinases as well as the Akt kinase as previously reported . In contrast, activation of the PI3K/Akt signaling pathway due to increased Ca^{2+} concentrations is well known and our data shows that it is clearly differentiation-

dependent. Akt is a pro-survival pathway and activation of PI3K/Akt has been shown to inhibit UVB-induced apoptosis . Akt phosphorylation in conjunction with suppression of COX-2 expression may be a mechanism for inhibition of the synthesis of potentially damaging metabolites.

Recently, research has focused more on the activity of the prostanoid synthases as modulators of prostaglandin production as opposed to solely on COX-2 activity. Early studies have shown that exposure of skin to UVB results in increased concentrations of free arachidonic acid and as well as the prostaglandins, PGE_2, $PGF_{2\alpha}$ and PGD_2 . As subsequent research demonstrated that PGE_2 was the primary prostaglandin upregulated in skin following UVB exposure , the bulk of the prostanoid synthase research has centered on mPGES-1 and mPGES-2 expression and activity. Although there have not been any reports of the expression of the mPGES enzymes being upregulated by UVB light, both isozymes are known to be upregulated during bacterial-induced inflammation . Additionally, dermal PGE_2 concentrations are increased following UVB exposure , indicating that the mPGES enzymes may be UVB-inducible. Our results clearly show that, in keratinocytes, both mPGES-1 and mPGES-2 are upregulated by UVB light. Moreover, as with COX-2, we found that that mPGES-1 expression is regulated through activation of the MAP kinases as Akt kinase. However, there appears to be a differential effect in thep38 and JNK MAP kinase-mediated induction of mPGES-1. In differentiated cells, inhibition of both kinases suppressed mPGES-1 expression while only JNK inhibition was effective in the undifferentiated cells. It is unclear at this time why differentiation should have such an effect on p38 MAP kinase-mediated mPGES-1 expression.

Previous studies have shown that UVB-induced PGE_2 production occurs through EP1 and EP2 signaling. Our data showing that mRNA expression of these two receptors was increased following UVB correlates with these findings. Recently, it has been demonstrated that the EP1 and EP2 receptors play vital roles in mediating the development and progression of skin tumors following UVB and phorbol ester treatments . Moreover, in malignant keratinocytes, increased PGE_2 production was evident and was mediated through the EP1 receptor . In contrast, EP3 and EP4 expression was not altered by UVB in our studies. Although these two receptors are involved in fever generation and pain perception, they do not appear to be responsive to UVB.

UVB light induced a marked increase in the expression of PGFS which has not yet been reported in keratinocytes. Previous studies have shown that $PGF_{2\alpha}$ expressed at low levels in mouse skin and recent studies have indicated that it may play a protective role against neoplastic dermal conversion. Expression of the FP receptor, while transiently increased following phorbol ester treatment, was decreased in papillomas . Moreover, FP activation resulted in increased melanin production in human melanocytes in vitro and in vivo in response to UVB light . We found that UVB also induces FP expression in keratinocytes, indicating that activation of this pathway may be a dermal protective measure against UVB injury.

The increased expression of PGIS and the IP receptor we observed may be another attempt by the keratinocytes to minimize UVB-induced damage. PGI_2, in conjunction with PGE_2, is recognized as a primary mediator in inflammation-related pain perception . However, PGI_2-activation of IP has also been shown to have antimitogenic effects through inhibition of G1 to S phase cell cycle progression . Moreover,

prostacyclin analogs have been shown to inhibit phorbol ester-induced transformation and to induce differentiation in keratinocytes through growth inhibition . As with mPGES-1 expression, the extent to which activation of the p38 and JNK MAP kinases and Akt kinase play a role in mediating the expression of PGIS is differentiation-dependent but the implications of this differential effect are not known at this time.

We also found that the expression of PGDS and both PGD_2 receptors, DP and CRTH2, was increased by UVB. Surprisingly, the receptors appeared to be much more responsive to UVB than PGDS itself. It may be that PGDS induction is an early response to UVB while activation of the receptors may be a late response or one of greater duration. The marked increase of CRTH2, in particular, may also be due to the binding of not only PGD_2 but of its metabolite, 15d-PGJ_2, as well. It has been shown that CRTH2 binds 15-dPGJ_2 with equal affinity as PGD_2 . As 15d-PGJ_2 is known for its role in the resolution of inflammation , 15d-PGJ_2-binding of CRTH2 may initiate the recovery from UVB-induced injury.

Although it had previously thought that keratinocytes did not have the capability to produce leukotrienes, our data indicates otherwise. Activation of the 5-LOX pathway is considered to be the primary mechanism for the synthesis of LTA_4, the initial leukotriene precursor. Recent studies, however, have shown that 8-LOX is also capable of LTA_4 production . Although we found no changes in 5-LOX expression in response to UVB, there was a marked increase in 8-LOX induction. UVB-induced leukotriene production in the skin may, therefore, occur through an increase in 8-LOX activity rather than the traditional 5-LOX pathway. As with other arachidonic acid-metabolizing enzymes, induction of 5-LOX may be an early response to UVB with a quick return to

basal levels. It is also of note, that, while 5-LOX expression was unchanged, FLAP was increased. It is unclear at this time whether FLAP has additional functions beyond its 5-LOX accessory role that would account for our observations.

It also appears that the leukotriene synthesis pathway is shunted away from LTB_4 formation in favor of cysteinyl leukotriene production. We detected a decrease in LTA_4 hydrolase expression as well as no change in the levels of the LTB_4 receptors. At the same time, UVB increased the expression of LTC_4 synthase and both cysteinyl leukotriene receptors. 15-LOX activity is known to inhibit LTB_4 production and expression of this enzyme was increased in our studies. The observed pattern of receptor expression may, therefore, be the result of a lack of LTB_4 formation due to 15-LOX activity.

The upregulation of 15-LOX may also have a dual role in the cellular response to UVB. While 15-LOX is considered pro-inflammatory in that its metabolite, 15-HETE, may be converted to LTA_4, this enzyme also has anti-inflammatory properties through inhibition of LTB_4 and catalysis of lipoxin production. Moreover, increased 15-LOX activity has been associated with an inhibition of cancer progression . The increased 15-LOX expression that we observed may be a component of a complex cellular response leading to the resolution of UVB-induced inflammation. It is also of note that, contrast to other eicosanoid synthesis enzymes, 15-LOX expression does not appear to be regulated by either MAP kinase or Akt kinase activation.

The arachidonic acid-metabolizing enzymes, mPGES-1, FLAP and LTC_4 synthase, are also included with mGST1, mGST2 and mGST3 as members of the MAPEG family of enzymes. Although these enzymes have been grouped by structural

and sequence homology and GST activity, there have not been any reports of this family functioning in a coordinated manner in response to some stimulus. As an example, in our data, we observed an upregulation in the expression of the eicosanoid synthesis members while there was little to no change in expression of the mGST enzymes. It remains to be seen whether the MAPEG family is simply a classification scheme or a block of enzymes that are regulated by and response to stimuli in a coordinated manner.

In summary, we have shown that UVB light upregulates the prostaglandin and leukotriene biosynthetic pathways in primary mouse keratinocytes. In addition, we demonstrate that the expression of several representative enzymes in these pathways is regulated through activation of the p38 and JNK MAP kinases and Akt kinase. Surprisingly, the differentiation status of the keratinocytes was, for the most part, not a major determinant in the UVB-induced enzyme expression. Our results indicate that there is most likely an overall keratinocyte response to UVB and that the differentiation state modulates only certain aspects of this reaction.

D. Induction of the eicosanoid biosynthetic enzymes by paraquat

Increased oxidative stress has recently been acknowledged as a major contributor to the inflammatory process. It is well known that reactive oxygen intermediates are effective inducers of many proinflammatory mediators such as growth factors, cytokines and arachidonic acid-derived metabolites. Numerous studies have reported a direct correlation with the presence of inflammation and the onset of disease in the affected tissue . Although reports of adverse effects on the skin due to paraquat exposure range from contact dermatitis to premalignant lesions and squamous cell carcinomas , there

has been little investigation as to the role of this herbicide in the development of the inflammatory response. As paraquat is an effective inducer of ROI, this herbicide would also most likely be efficient in producing an inflammatory response in the skin. Using primary mouse keratinocytes as an epidermal model, we investigated the role of paraquat in mediating the expression of the prostaglandin and leukotriene biosynthetic pathways.

We found that the addition of paraquat to primary keratinocytes caused an increase in the expression of $cPLA_2$ mRNA. Previous studies have shown that PLA_2 activity increased in response to superoxide anion and hydrogen peroxide . Moreover, antioxidants effectively inhibited the phosphorylation of $cPLA_2$ following UVB or tert-butyl hydroperoxide treatments . A primary function of phospholipases is remodeling of the phospholipid membrane, releasing arachidonic acid for subsequent eicosanoid production. This action also results in the removal of lipid peroxidation products and increased PLA_2 activity has been correlated with the removal of such adducts .. Whether this PLA_2 activity is an active defense mechanism or simply a beneficial by-product is unclear at this time

In either case, arachidonic acid is mobilized, thus initiating the eicosanoid synthesis cascade. The cyclooxygenases (COX-1 and -2) are the rate-liming enzymes in the production of prostaglandins, prostacyclin and thromboxane. It is well known that COX-1 is constitutively active while COX-2 is induced in response to many stimuli. Our results are in agreement with these facts. Although ROI are known to stimulate COX-2 activity , it is surprising just how effective paraquat was at inducing COX-2 expression. COX-2 mRNA and protein were shown to be readily upregulated in phorbol ester treated mouse skin but not to that extent that we observed in paraquat-treated keratinocytes.

The COX reactions produce an intermediate that serves as the substrate for the production of the prostaglandins, prostacyclin and thromboxane by the prostanoid synthases. We found that paraquat stimulated the expression of PGFS in keratinocytes. These results correlate with previous reports demonstrating that paraquat increases $PGF_{2\alpha}$ concentrations in the lung and blood plasma . Elevated $PGF_{2\alpha}$ levels, in particular, have been correlated with paraquat-induced pulmonary edema . These same studies also reported no change in PGE_2 concentrations in these tissues although we observed increases in mPGES-1 expression in keratinocytes. Previous studies have shown that the amount of PGE_2 was significantly increased in mouse skin treated with other oxidants such as phorbol esters and hydrogen peroxide which correlates with our data. Paraquat also has been to induce TXA_2 and 6-keto-$PGF_{1\alpha}$, a PGI_2 metabolite , in lung fluid and vascular endothelial cells . Our results showing increased expression of PGIS and TXAS in keratinocytes indicate that paraquat may also induce these metabolites in these cells.

Similarly, in our studies paraquat increased the expression of the lipoxygenases and leukotriene synthesis enzymes in keratinocytes. To date, little investigation has occurred in this area. One report showed that leukotriene B_4 was readily produced in alveolar macrophages of paraquat-treated rats . The authors also showed that incubation with the antioxidant, *N*-acetylcysteine, inhibited not only LTB_4 formation but release of arachidonic acid from the cells as well. Phorbol ester treatment is known to elevate the concentrations of LTB_4 as well as other LOX metabolites including 5-, 8-, 12- and 15-HETE in mouse skin . These studies, in accordance with our results, indicate that keratinocytes most likely produce LOX metabolites in response to paraquat treatment.

We found that paraquat readily induced the expression of 8- and 15-LOX in keratinocytes. 8-LOX was originally characterized in phorbol ester-treated mouse skin and antioxidant pretreatment was shown to suppress its activity . Similarly, 15-LOX activity as evidenced through 15-HPETE production was increased by hydrogen peroxide . These results indicate that upregulation of both 8- and 15-LOX may be controlled by ROI levels with correlates with our data. In contrast, we found that paraquat had little effect on the expression of 12-LOX and previous studies have shown that increased ROI concentrations inhibited both 12-LOX activity and production of 12-HETE .

Surprisingly, there was no change in the expression of mGST1, mGST2 or mGST3 following paraquat treatment. These enzymes are important in removing products of lipid peroxidation; however, in keratinocytes, they do not appear to be involved in the cellular response to paraquat.

In our experiments, we also determined whether keratinocyte differentiation affected the cellular response to paraquat. Greater levels of protein oxidation have been quantified in suprabasal cells as compared to basal cells, indicating that these populations may respond differently to paraquat. For example, COX-2 protein expression was upregulated by phorbol ester and acetone treatment in mouse skin; however, these increases were confined primarily to the basal cells with little change observed in the suprabasal cells . In our experiments, however, differentiation did not have a major impact on enzyme expression except in a few instances such as 15-LOX and PGFS. Why the expression of certain enzymes is differentiation-dependent while the expression of others is not is not known at this time.

In the past several years, it has become evident that the inflammatory process plays a major role in the carcinogenic initiation. As proinflammatory mediators, prostaglandins and the enzymes involved in their synthesis have been used as markers to distinguish between normal, neoplastic and malignant cells and tissues. For example, overexpression of COX-2 and increased PGE_2 and $PGF_{2\alpha}$ biosynthesis has been directly correlated with skin carcinogenesis in the mouse model as well as in human colorectal carcinoma . In addition, 8-HETE has been shown to be greatly increased in skin tumors . Interestingly, several studies using inhibitors of COX or LOX enzymes have shown that prostaglandins and leukotrienes themselves are involved in stimulating ROI production by phorbol ester and cumene hydroperoxide . In addition, LOX inhibitors were shown to inhibit superoxide anion-driven transformation by phorbol ester in mouse epidermal cells .

In summary, we have demonstrated that paraquat is an effective inducer of the arachidonic acid metabolism enzymes. The importance of inflammation in the toxicity of paraquat was demonstrated during a recent clinical study in which an anti-inflammatory therapy significantly reduced paraquat-induced mortality . It may be that ROI-induced production of these pro-inflammatory lipid mediators is the primary factor in the development of paraquat pathogenesis.

Concluding Remarks

The primary aim of this dissertation was to determine and compare the cellular responses of primary murine keratinocytes to oxidative stress induced by two oxidants, ultraviolet B (UVB) light and paraquat. In particular, the investigation was limited to those of the enzymes involved in the oxidative stress response and arachidonic acid metabolism. Using an in vitro epidermal model of undifferentiated and differentiated keratinocytes also allowed us to ask if the expression of any of these enzymes was differentiation-dependent.

Both UVB and paraquat were clearly effective in generating reactive oxygen intermediates (ROI), thereby inducing oxidative stress. In general, both oxidants induced the antioxidant enzymes although the patterns of enzyme expression differed following treatment with the two agents. While UVB exposure did result in induction of several of the antioxidant enzymes, paraquat was clearly much more effective in this regard. Paraquat treatment resulted in not only the upregulation of the expression of a greater number of individual enzymes but, in several instances, these increases were dramatically greater than those observed with UVB.

These differences may be due to the intrinsic nature of these two oxidants. UVB generates ROI, however, once irradiation ceases, ROI production ends as well. Paraquat, on the other hand, is a redox-cycling agent. Provided that oxygen and NADPH are not limited, paraquat will undergo continuous redox-cycling, generating an endless supply of ROI. The redox-cycling ability of paraquat is, therefore, the most likely reason for its enhanced oxidative capability as compared to that of UVB.

In regards to arachidonic acid metabolism, the keratinocyte response to UVB and paraquat were quite similar. These results indicate that, while oxidative stress is capable of inducing the inflammatory response through the upregulation of the eicosanoid biosynthetic pathways, the degree to which the cells respond is most likely dependent upon many factors. Although paraquat is a potent inducer of ROI, exposure to UVB is known to activate signaling pathways, many of which are involved in mobilization of arachidonic acid and subsequent eicosanoid production.

As to the role of differentiation in the cellular responses, our hypothesis was that when oxidative stress was induced in undifferentiated and differentiated cells, these two cell types would respond differently. Surprisingly, with a few exceptions such as COX-2 or GSTA1-2, there were no major differences between undifferentiated and differentiated keratinocytes. It appears that there is an overall keratinocyte response to oxidative stress, regardless of the oxidant, and that differentiation may modify this response in certain instances. Although our studies were performed using an in vitro model system, other researchers working with both mouse and human skin report similar results in which the differentiation state of the cells did not determine the cellular response. It is unclear at this time why a minority of the enzymes would exhibit differentiation-dependent expression.

Based on our results, it is the nature of the oxidant rather than the differentiation state of the keratinocytes that is the primary factor in determining the cellular response to oxidative stress. Further characterization of the mechanisms involved in the regulation of enzyme expression and eicosanoid production are needed to more completely understand this response and if differentiation does, in fact, have any significant role in the process.

BIBLIOGRAPHY

Figure 1. Reactive oxygen intermediates and their detoxification pathways.

Superoxide anion is converted to hydrogen peroxide by SOD. Hydrogen peroxide can be metabolized by catalase or various peroxidases including GPx-1. Hydrogen peroxide has been implicated in the mobilization of heme, an oxidizing agent, which is then degraded by the heme oxygenases including HO-1. In the presence of transition metals such as iron or copper, hydrogen peroxide can also be converted to hydroxyl radical which can be removed through the zinc-mediated free radical scavenging function of MT-2. If not removed, ROI can oxidize proteins and lipids and these oxidation products are conjugated with glutathione by the GST enzymes to facilitate cellular elimination.

Figure 1

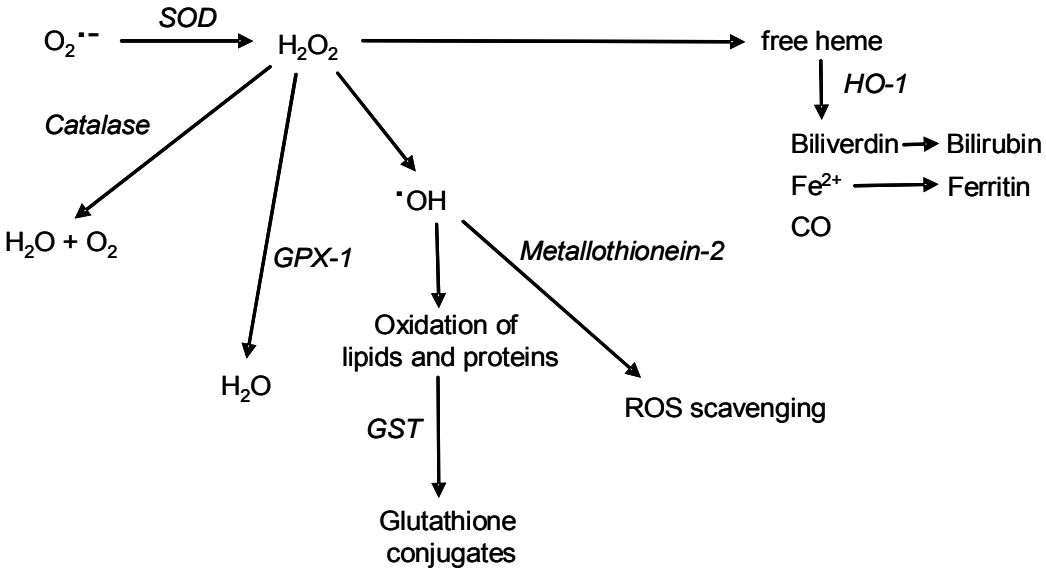
$O_2^{\bullet -}$
SOD
H_2O_2
free heme
HO-1
Biliverdin
Bilirubin
Fe^{2+}
Ferritin
CO
Catalase
$H_2O + O_2$
GPX-1
H_2O
$^{\bullet}OH$
Metallothionein-2
Oxidation of lipids and proteins
ROS scavenging
GST
Glutathione conjugates

Figure 2. Pathways of eicosanoid production.

Arachidonic acid is directly mobilized from the phospholipid membrane by phospholipase A_2 ($cPLA_2$) or indirectly through phospholipase C (PLC), diacylglycerol lipase (DAG lipase) and monoacylglycerol lipase (MAG lipase). Arachidonic acid is then oxidized by cyclooxygenases (COX), lipoxygenases (LOX) and P450 monooxygenases, producing prostaglandins, prostacyclin, thromboxane, leukotrienes, hydroperoxyeicosatetraenoic acids (HETE), lipoxins, epoxyeicosatetraenoic acids (EET) and hydroperoxides.

Figure 2

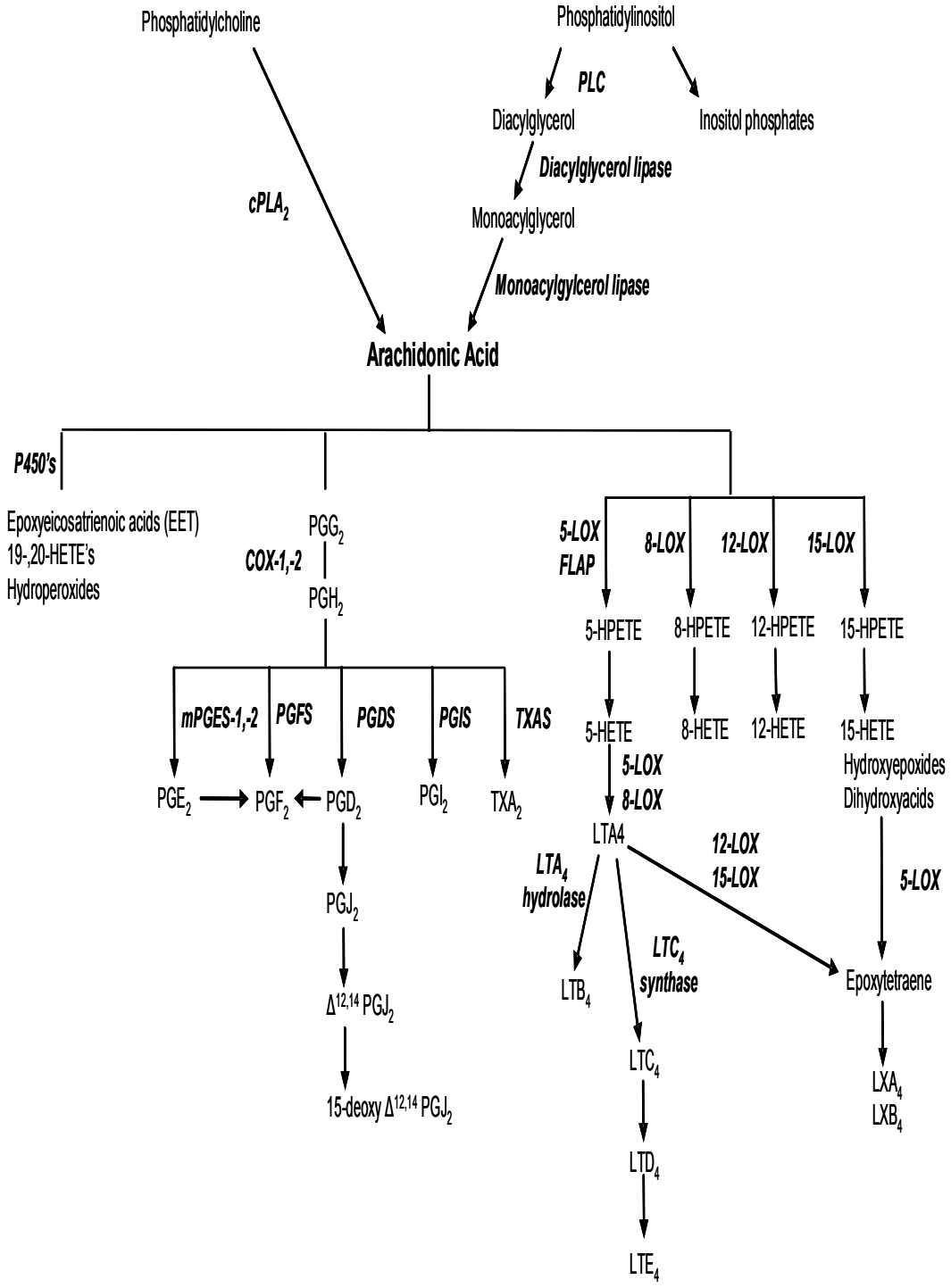
Phosphatidylcholine
Phosphatidylinositol
PLC
Diacylglycerol
Inositol phosphates
Diacylglycerol lipase
cPLA2
Monoacylglycerol
Monoacylglycerol lipase
Arachidonic Acid
P450's
Epoxyeicosatrienoic acids (EET)
19-,20-HETE's
Hydroperoxides
PGG2
COX-1,-2
PGH2
5-LOX
FLAP
8-LOX
12-LOX
15-LOX
5-HPETE
8-HPETE
12-HPETE
15-HPETE
mPGES-1,-2
PGFS
PGDS
PGIS
TXAS
5-HETE
8-HETE
12-HETE
15-HETE
Hydroxyepoxides
Dihydroxyacids
5-LOX
8-LOX
PGE2
PGF2
PGD2
PGI2
TXA2
LTA4
12-LOX
15-LOX
5-LOX
LTA4 hydrolase
LTC4 synthase
PGJ2
LTB4
Epoxytetraene
Δ12,14 PGJ2
LTC4
LXA4
LXB4
15-deoxy Δ12,14 PGJ2
LTD4
LTE4

Figure 3. Structures of metabolites produced in the cyclooxygenase branch of arachidonic acid metabolism.

Arachidonic acid is oxidized by COX-1 and COX-2 in a two-step reaction, producing first prostaglandin G_2 (PGG_2) and then prostaglandin H_2 (PGH_2). PGH_2 is the substrate for prostanoid synthase activity, generating prostaglandin D_2 (PGD_2), prostaglandin E_2 (PGE_2), prostaglandin $F_{2\alpha}$ ($PGF_{2\alpha}$), prostaglandin I_2 or prostacyclin (PGI_2) and thromboxane A_2 (TXA_2). PGD_2 is further metabolized to prostaglandin J_2 (PGJ_2) which, is converted to $\Delta^{12,14}$-prostaglandin J_2 ($\Delta^{12,14}$-PGJ_2) and finally to 15-deoxy-$\Delta^{12,14}$-prostaglandin J_2 (15d-PGJ_2).

Figure 3.

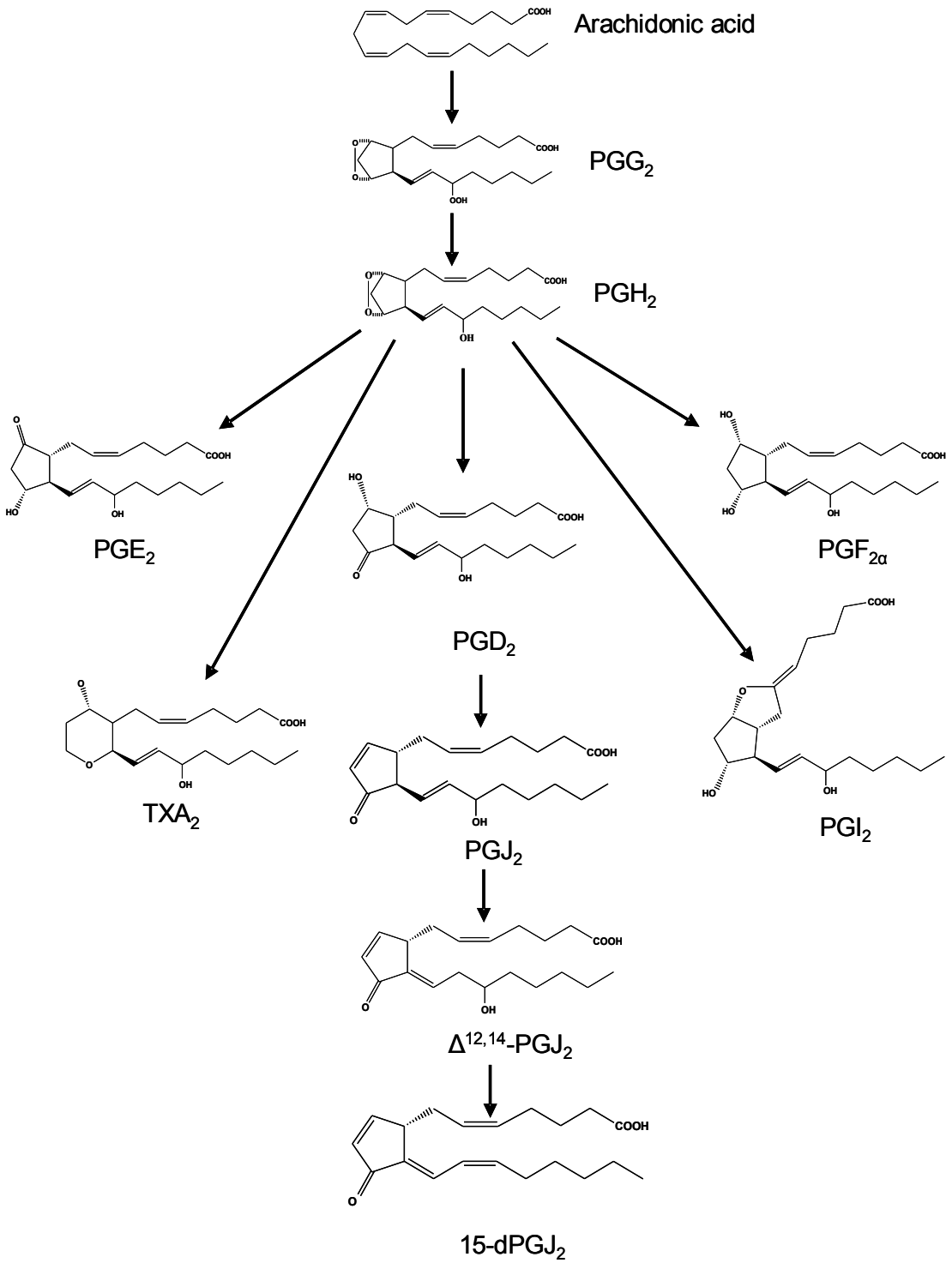
Arachidonic acid
PGG2
PGH2
PGE2
PGD2
PGF2α
TXA2
PGJ2
PGI2
Δ12,14-PGJ2
15-dPGJ2

Figure 4. Structures of metabolites produced in the lipoxygenase branch of arachidonic acid metabolism.

The lipoxygenases (5-, 8-, 12- and 15-LOX) incorporate an oxygen atom to the respective carbon of the arachidonic acid backbone. This reaction occurs in two steps, producing a hydroperoxyeicosatetraenoic acid (HPETE) which is readily converted to a hydroxyeicosatetraenoic acid (HETE). 5-HETE is metabolized to leukotriene A_4 (LTA_4) which may be converted to leukotriene B_4 (LTB_4) or conjugated with glutathione to form leukotriene C_4 (LTC_4). LTA_4 may also be converted to either lipoxin A_4 (LXA_4) or lipoxin B_4 (LXB_4).

Figure 4

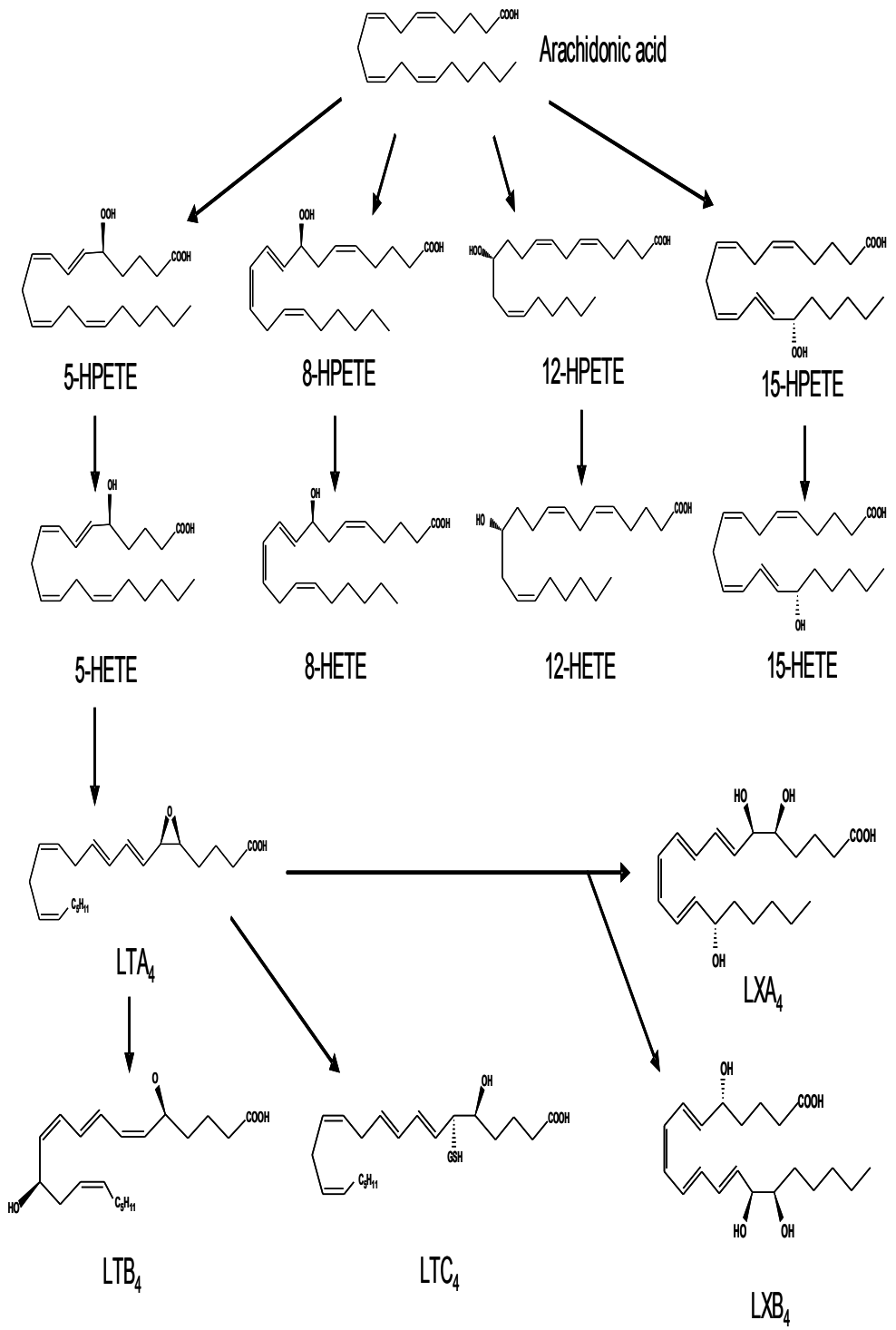
Arachidonic acid
5-HPETE
8-HPETE
12-HPETE
15-HPETE
5-HETE
8-HETE
12-HETE
15-HETE
LTA4
LXA4
LTB4
LTC4
LXB4

Figure 5. Characteristics of terminal differentiation of primary mouse keratinocytes. Keratinocytes are grown in low calcium medium (0.05 mM). The addition of calcium (0.15 mM) to the medium initiates differentiation. Panel A: Micrograph showing the surface morphology of undifferentiated cells (upper panel) and differentiated cells (lower panel). Panel B. Undifferentiated keratinocytes exhibit weak or no expression of three differentiation markers, keratin-1, keratin-10 and filaggrin. Differentiation results in upregulation of these markers.

Figure 5

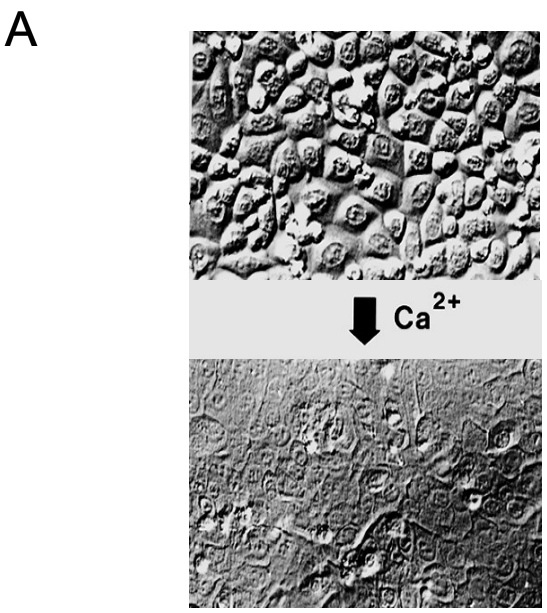

Figure 6. Exposure to UVB increases intracellular hydrogen peroxide in keratinocytes. Undifferentiated and calcium-differentiated keratinocytes were incubated with DCFH-DA (5 μM, 15 minutes), exposed to UVB light (25 mJ/cm^2) and then analyzed by flow cytometry. The data are presented on a four decade log scale.

Figure 6

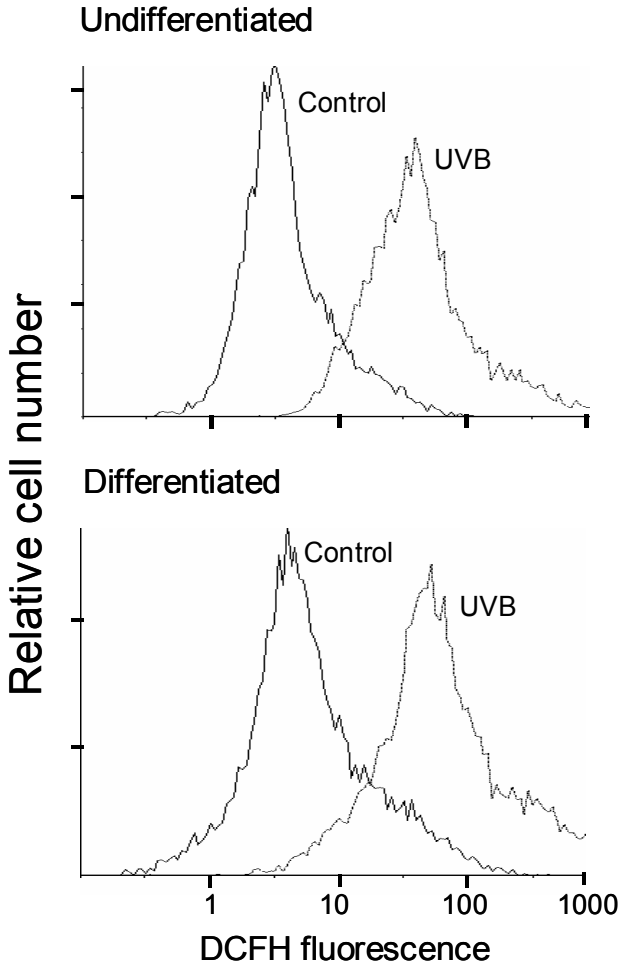
Undifferentiated
Control
UVB
Differentiated
Control
UVB
Relative cell number
1
10
100
1000
DCFH fluorescence

Figure 7. Effects of UVB on COX-2 and TNFα mRNA expression in keratinocytes.

Undifferentiated and differentiated keratinocytes were treated with UVB (0 - 25 mJ/cm^2). After 24 hours, cells were lysed and analyzed for COX-2 and TNFα gene expression by realtime PCR (n = 3-6, ± SE).

Figure 7

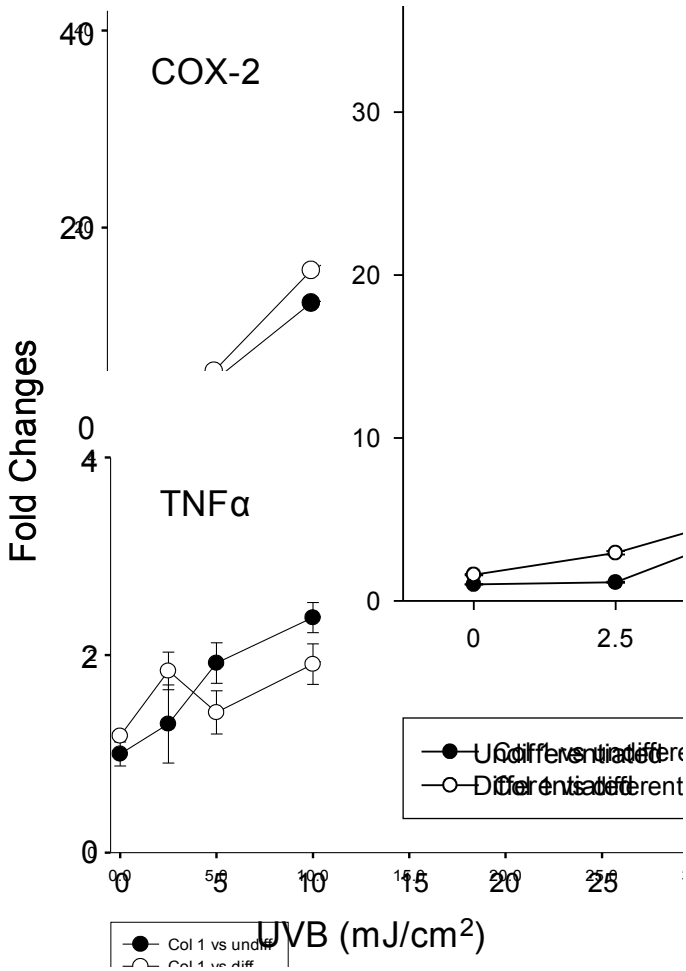
COX-2
TNFα
Fold Changes
UVB (mJ/cm2)
0
2.5
0
5
10
15
20
25
Col 1 vs undiff

Figure 8. Effects of UVB on COX-2 and HO-1 protein expression.

Cell lysates were prepared from undifferentiated and differentiated keratinocytes and COX-2 and HO-1 protein expression determined by Western blotting. Cells were analyzed 24 hours after UVB treatments (0-25 mJ/cm^2).

Figure 8

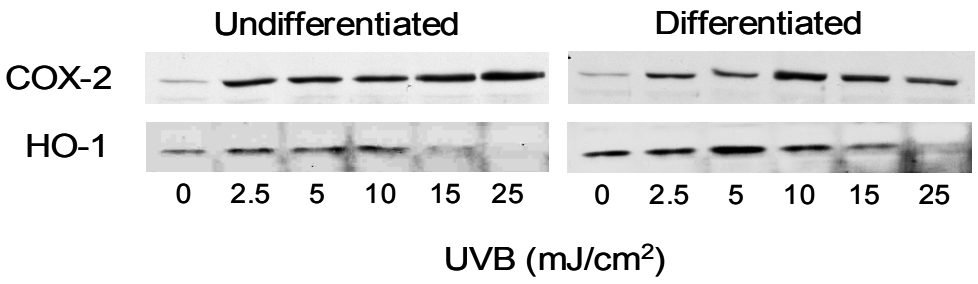
Undifferentiated
Differentiated
COX-2
HO-1
0 2.5 5 10 15 25
0 2.5 5 10 15 25
UVB (mJ/cm2)

Figure 9. Effects of UVB on antioxidant gene expression in keratinocytes.

Undifferentiated and differentiated keratinocytes were treated with UVB light (0 - 25 mJ/cm^2). After 24 hours, cells were lysed and analyzed for gene expression of antioxidant enzymes by realtime PCR (n = 3-6, ± SE).

Figure 9

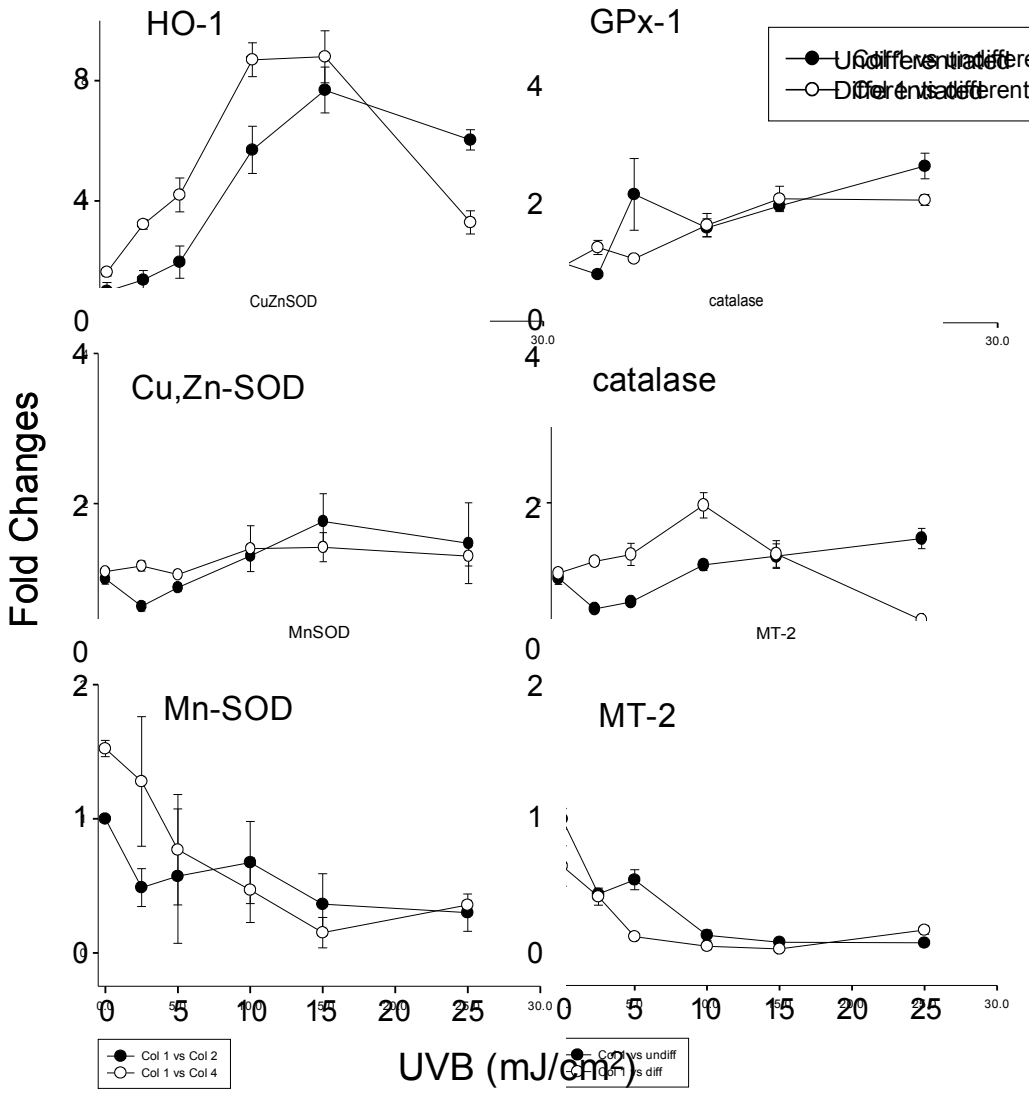
HO-1
GPx-1
CuZnSOD
catalase
Cu,Zn-SOD
catalase
MnSOD
MT-2
Mn-SOD
MT-2
Fold Changes
UVB (mJ/cm2)
Col 1 vs Col 2
Col 1 vs Col 4

Figure 10. Effects of UVB on GST expression in keratinocytes.

Undifferentiated and differentiated keratinocytes were treated with UVB (0 - 25 mJ/cm^2). After 24 hours, cells were lysed and analyzed for gene expression of cytosolic and microsomal GST's by realtime PCR (n = 3-6, ± SE).

Figure 10

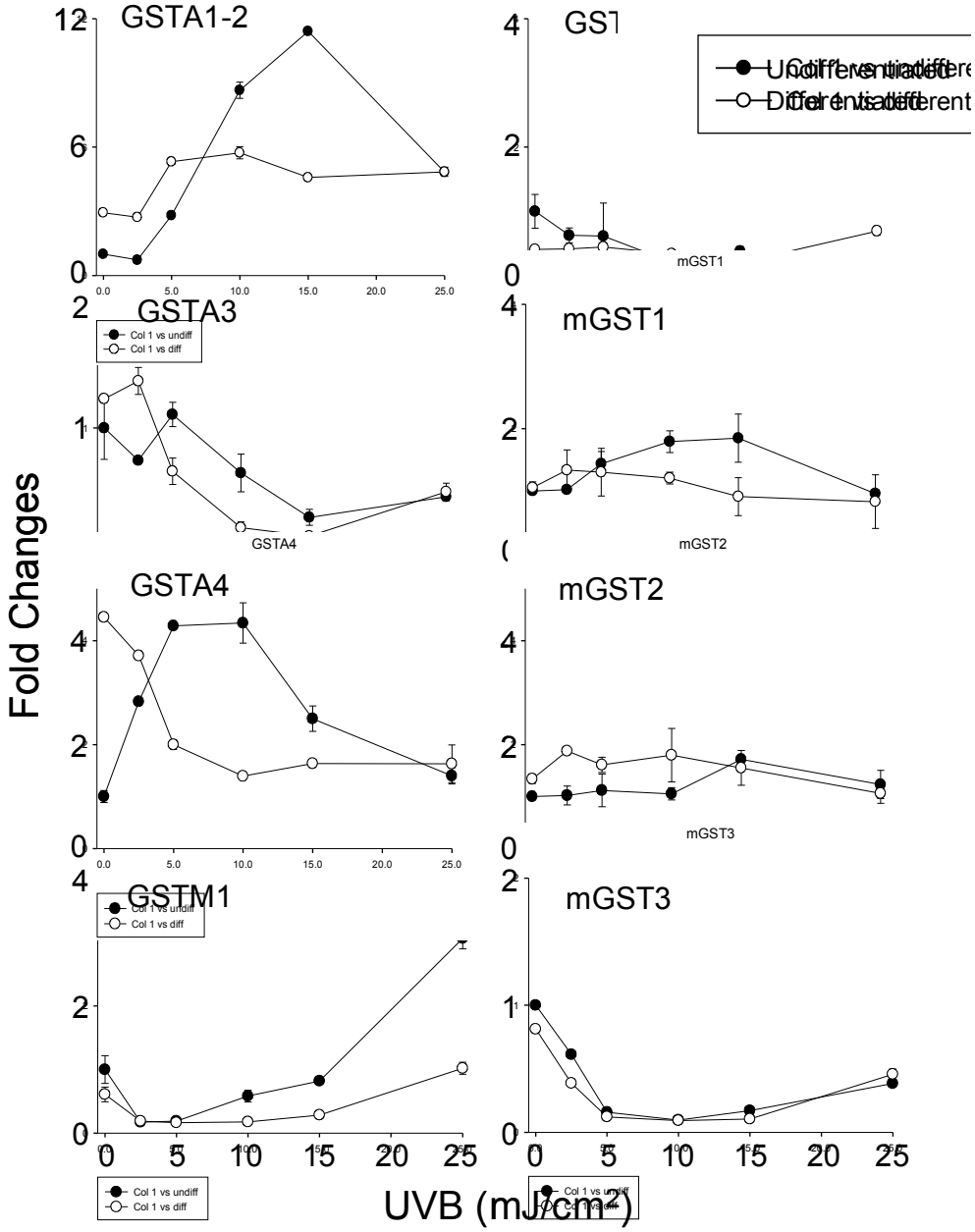
GSTA1-2
GST
mGST1
GSTA3
mGST1
GSTA4
mGST2
GSTA4
mGST2
mGST3
GSTM1
mGST3
Col 1 vs undiff
Col 1 vs diff
Fold Changes
UVB (mJ/cm2)

Figure 11. Activation of the MAP kinases by UVB light in primary mouse keratinocytes. Undifferentiated (U) and differentiated (D) keratinocytes were exposed to UVB light at the indicated doses. At 15 minutes post-UVB exposure, the cells were lysed and analyzed for protein expression by Western blotting. The blots were probed for the total and phosphorylated forms of the p38, JNK and ERK 1/2 MAP kinases.

Figure 11

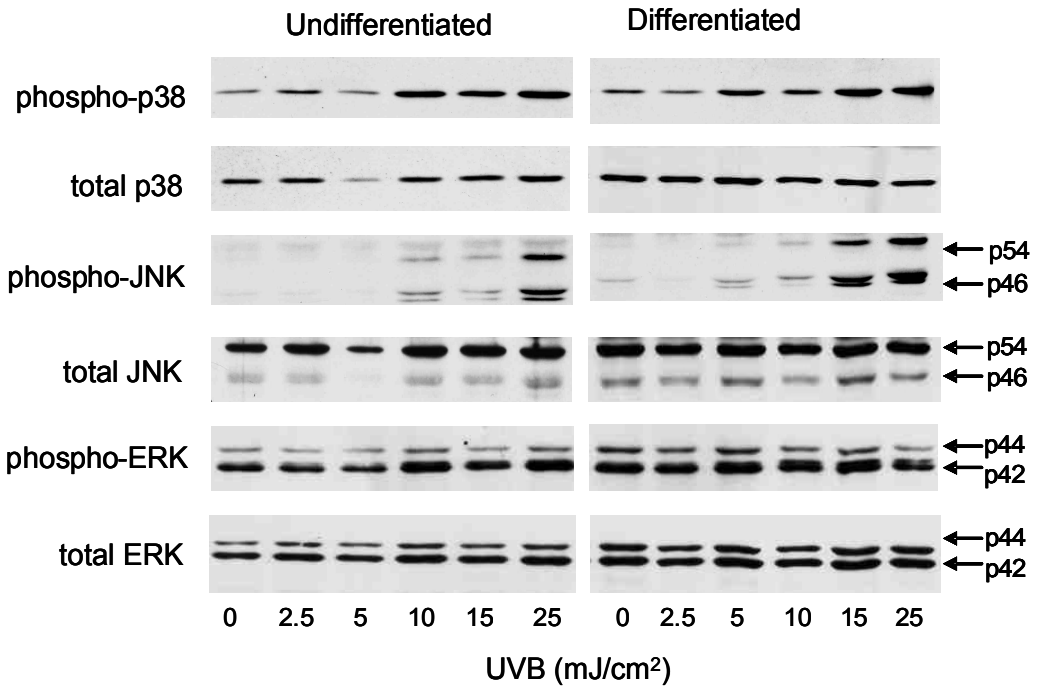
Undifferentiated
Differentiated
phospho-p38
total p38
phospho-JNK
total JNK
phospho-ERK
total ERK
p54
p46
p54
p46
p44
p42
p44
p42
0 2.5 5 10 15 25 0 2.5 5 10 15 25
UVB (mJ/cm²)

Figure 12. Effects of p38 and JNK MAP kinase inhibitors on UVB-induced expression of GSTA1-2, GSTA4 and HO-1 mRNA.

Undifferentiated and differentiated keratinocytes were incubated with SB203580 (10 μM), a p38 MAP kinase inhibitor, or SP600125 (20 μM), a JNK MAP kinase inhibitor, for 3 hours and then exposed to UVB at the indicated doses. After 24 hours, cells were analyzed for mRNA expression by real-time PCR (n = 3-6, ± SE).

Figure 12

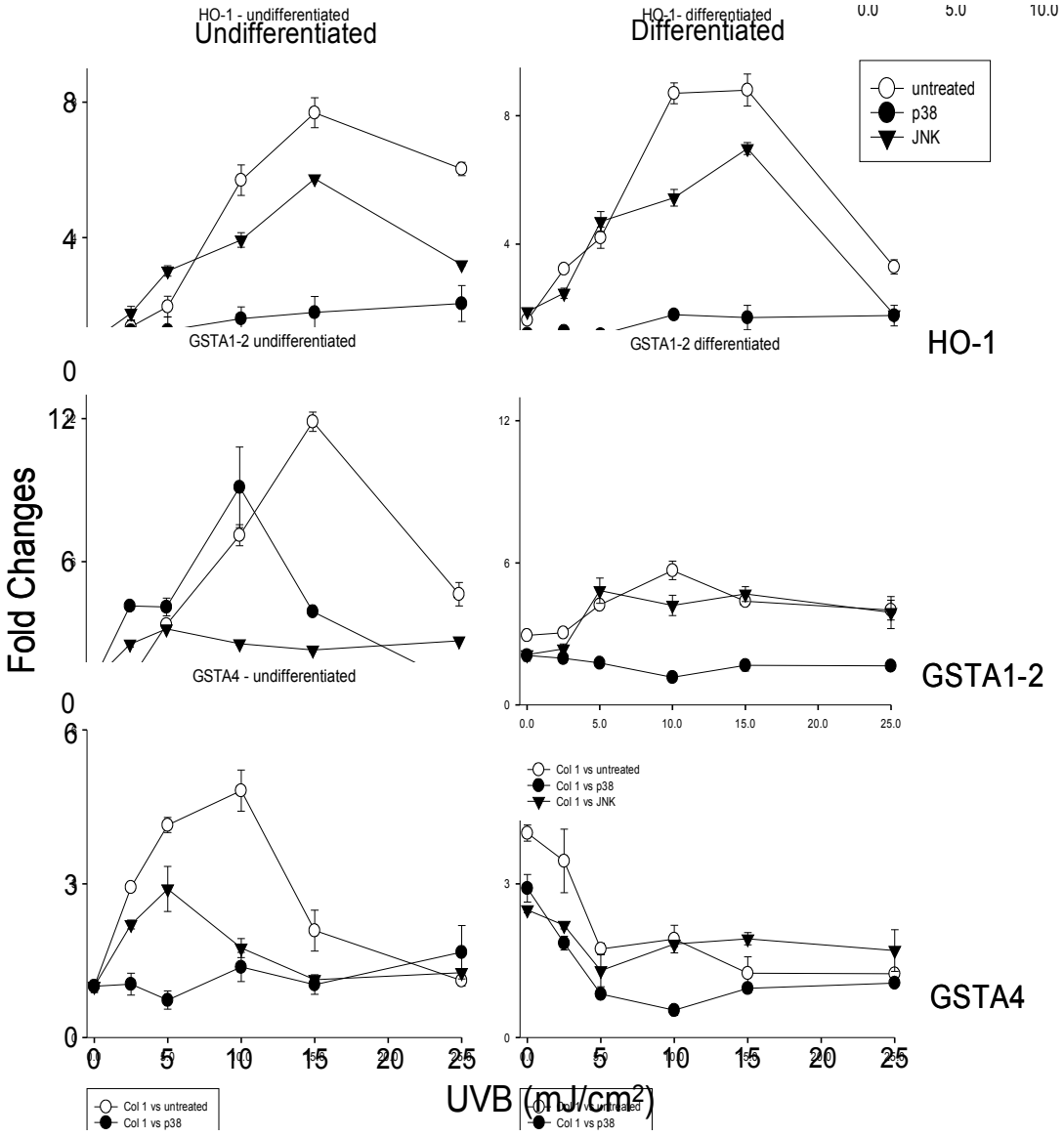
HO-1 - undifferentiated
Undifferentiated
HO-1 - differentiated
Differentiated
untreated
p38
JNK
GSTA1-2 undifferentiated
GSTA1-2 differentiated
HO-1
Fold Changes
GSTA4 - undifferentiated
GSTA1-2
Col 1 vs untreated
Col 1 vs p38
Col 1 vs JNK
GSTA4
UVB (mJ/cm2)

Figure 13. Paraquat redox cycling produces reactive oxygen intermediates.

Paraquat is reduced to the paraquat radical through the oxidation of NAD(P)H to $NAD(P)^+$ by NAD(P)H oxidase (Reaction 1). The paraquat radical is then immediately oxidized to the parent compound with the transfer of an electron to oxygen, forming superoxide anion (Reaction 2).

Figure 13

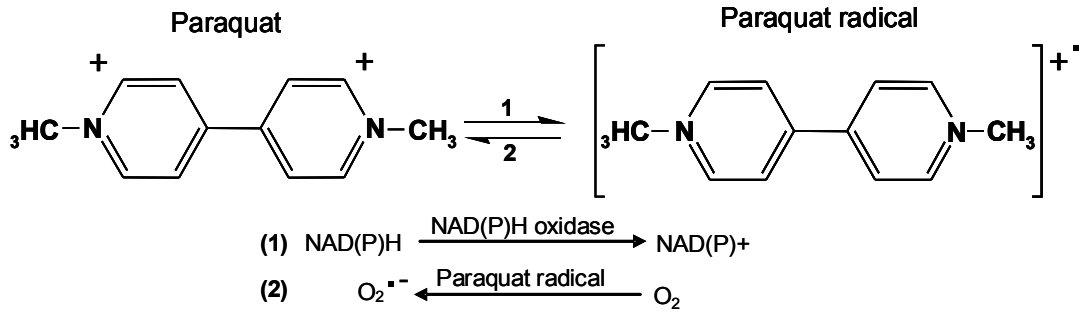
Paraquat
Paraquat radical
1
2
(1) NAD(P)H
NAD(P)H oxidase
NAD(P)+
(2)
Paraquat radical
O2
O2

Figure 14. Paraquat redox cycling produces superoxide anion in keratinocytes.

Lysates prepared from undifferentiated and differentiated keratinocytes were mixed with paraquat (100 μM), NADPH (0.5 mM) dihydroethidium (40 μM) and incubated for 1 hour at 37°C. After methanol was added to stop the reactions, the samples were analyzed by HPLC. The detection of 2-hydroxyethidium indicates the formation of superoxide anion. CuZnSOD (350 U/ml) was used to confirm that the 2-hydroxyethidium peak was due to superoxide anion generation.

Figure 14

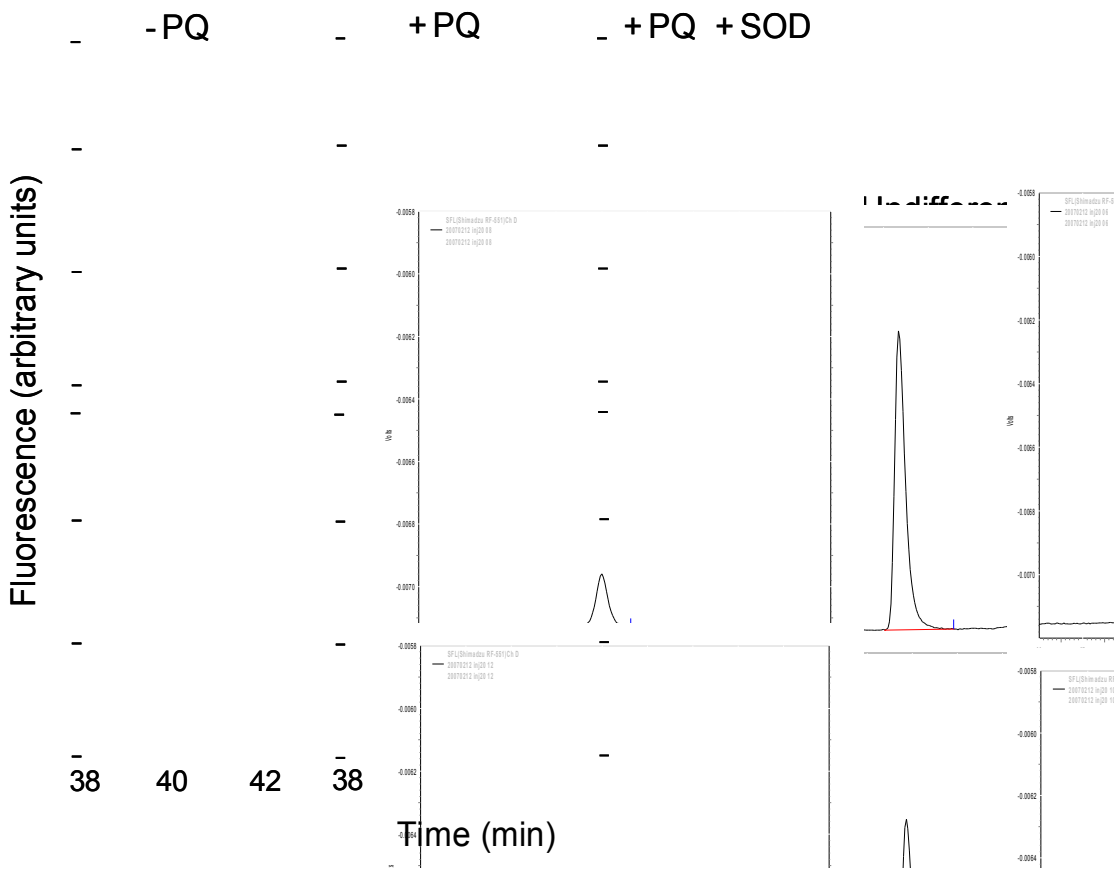
- PQ
+ PQ
+ PQ + SOD
Fluorescence (arbitrary units)
38
40
42
38
Time (min)

Figure 15. Redox cycling of paraquat by keratinocytes.

Reaction mixes contained lysates from undifferentiated and differentiated keratinocytes, 0.05 mM NADPH and increasing concentrations of paraquat. Production of hydrogen peroxide was quantified using the Amplex Red assay. Panels A and B: Effects of increasing concentrations of paraquat on hydrogen peroxide formation in undifferentiated and differentiated cells, respectively. Panel C: Comparison of paraquat (100 μM)-induced hydrogen peroxide formation in lysates from undifferentiated and differentiated cells. Panel D: Concentration-dependent increase in hydrogen peroxide formation in lysates from undifferentiated and differentiated cells. Assays were run for 30 minutes.

Figure 15

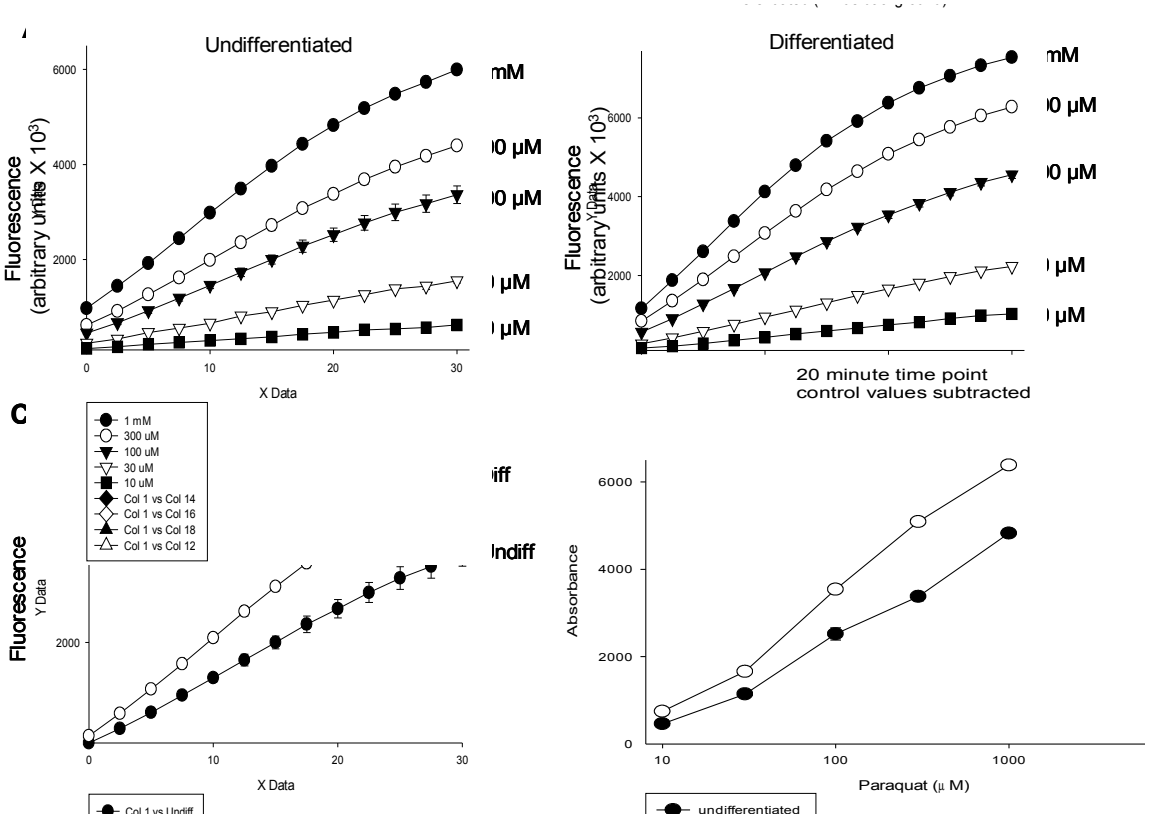
Undifferentiated
Differentiated
Fluorescence
(arbitrary units X 10³)
X Data
20 minute time point
control values subtracted
1 mM
300 uM
100 uM
30 uM
10 uM
Col 1 vs Col 14
Col 1 vs Col 16
Col 1 vs Col 18
Col 1 vs Col 12
Absorbance
Paraquat (μ M)
undifferentiated

Figure 16. Depletion of NADPH during paraquat redox cycling.

Lysates prepared from undifferentiated and differentiated keratinocytes were mixed with paraquat (100 μM) and NADPH (100 μM) in a 1 ml cuvette. Absorbance (340 nm) was recorded every 2.5 minutes for 3 hours using a UV/VIS spectrophotometer.

Figure 16

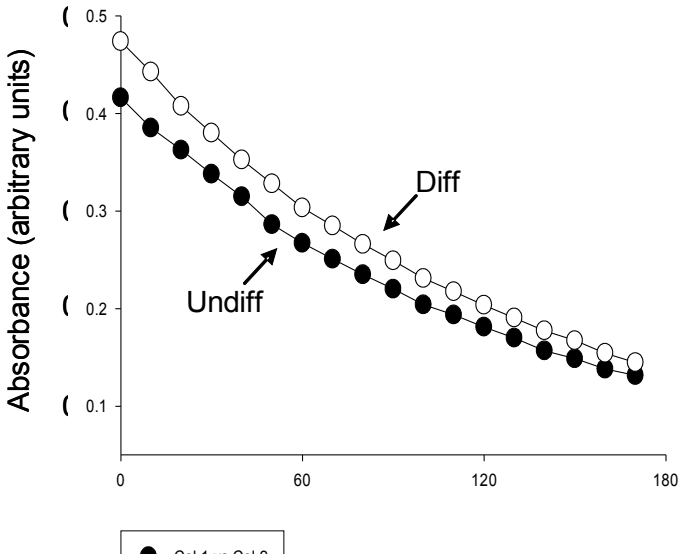
Absorbance (arbitrary units)
0.5
0.4
0.3
0.2
0.1
0
60
120
180
Diff
Undiff

Figure 17. Effects of DPI and dicoumarol on redox cycling of paraquat.

Standard enzyme reactions containing cell lysates from undifferentiated (upper panel) and differentiated (lower panel) keratinocytes were run in the presence and absence of dicoumarol (100 μM) or DPI (10 μM). Hydrogen peroxide formation was determined using Amplex Red. Assays contained 100 μM paraquat (PQ) and 0.05 mM NADPH.

Figure 17

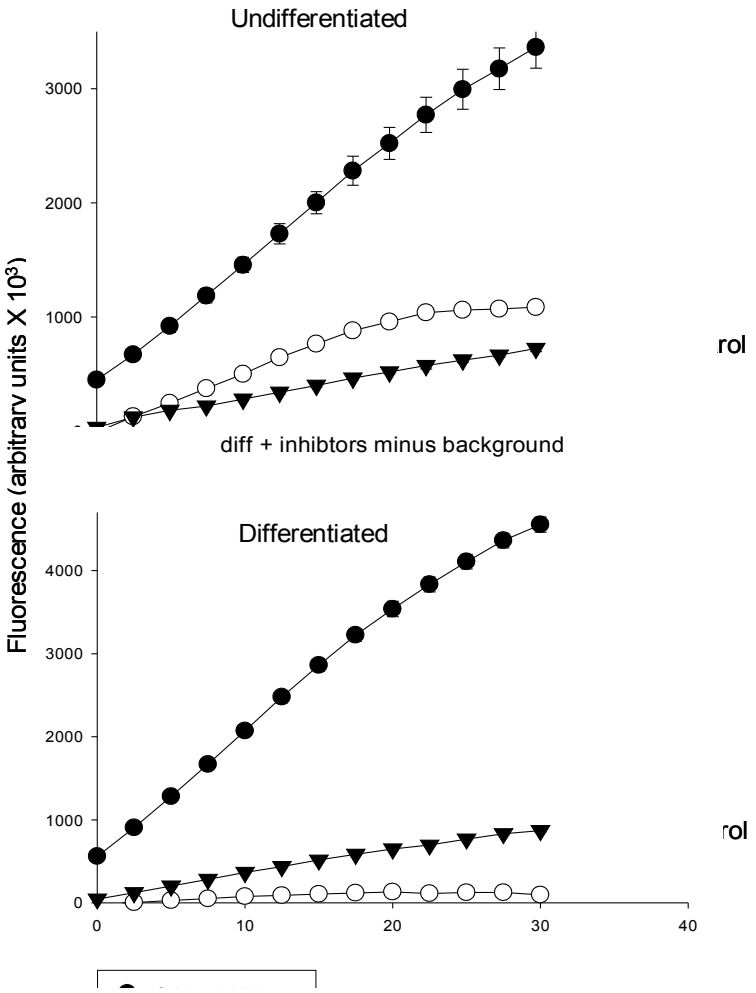
Undifferentiated
3000
2000
1000
Fluorescence (arbitrarv units X 10³)
diff + inhibtors minus background
Differentiated
4000
3000
2000
1000
0
0
10
20
30
40

Figure 18. Production of the paraquat radical in keratinocytes extracts.

Cell lysates from undifferentiated and differentiated keratinocytes were mixed with paraquat (500 μM) and NADPH (3 mM) in a sealed cuvette and placed in a UV/VIS spectrophotometer. After 120 minutes, anaerobic conditions were established and readings were recorded every 2.5 minutes. The paraquat radical has a peak absorbance peak of 604 nm . The inset shows the formation of the paraquat radical over time.

Figure 18

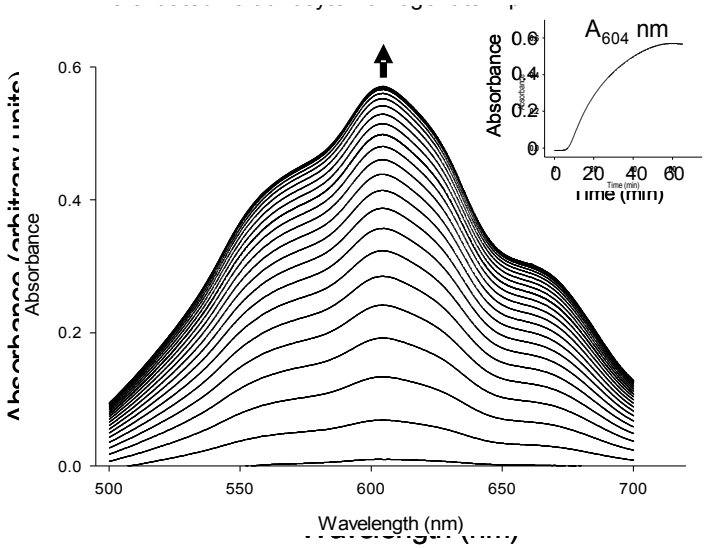
Absorbance
0.6
0.4
0.2
0.0
500
550
600
650
700
Wavelength (nm)
A604 nm
Absorbance
0.6
0.4
0.2
0
0
20
40
60
Time (min)

Figure 19. Cellular oxidative stress in paraquat-treated keratinocytes.

Undifferentiated and differentiated keratinocytes were incubated in medium in the absence and presence of 100 μM paraquat (PQ). After 24 hours, carbonyl groups within the cell lysates were derivatized with 2,4-dinitrophenylhydrazine (DNPH) to 2,4-dinitrophenylhydrazone (DNP-hydrazone). Using the OxyBlot Protein Oxidation Detection Kit, DNP-modified carbonyl groups were detected by Western blotting. Quantification of carbonyl formation was used as an indicator of protein oxidation.

Figure 19

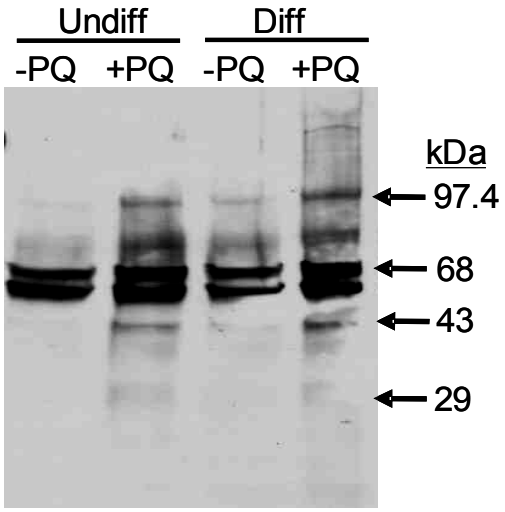

Figure 20. Effects of paraquat on expression of antioxidant enzymes.

Undifferentiated (U) and differentiated (D) keratinocytes were treated with 100 μM paraquat or buffer control. After 24 hours, mRNA was extracted and analyzed for gene expression by realtime PCR (n = 3-6, ± SE) or lysates prepared for Western blotting. Panel A: Expression of mRNA of antioxidant genes. * $p < 0.03$, paraquat-treated undifferentiated versus paraquat-treated differentiated cells. Panel B: Protein expression of HO-1.

Figure 20

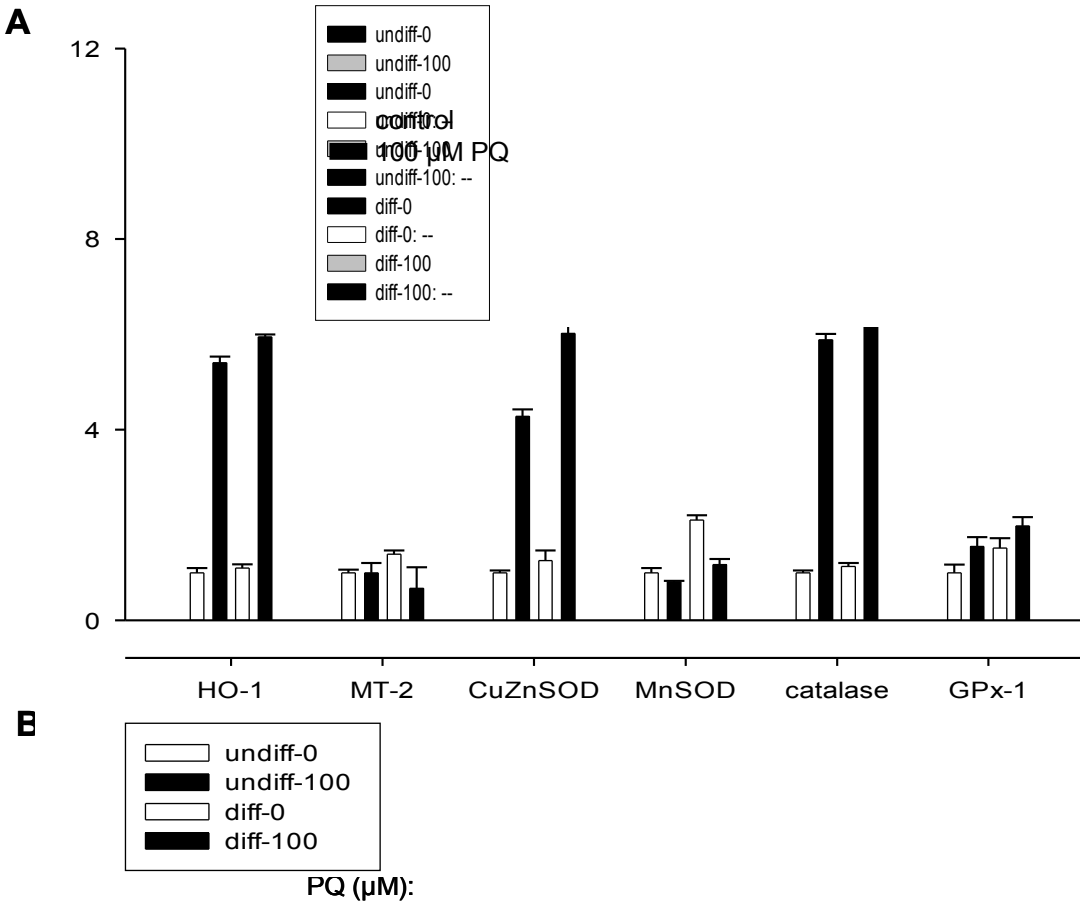
A
12
8
4
0
undiff-0
undiff-100
undiff-0
undiff-0: --
undiff-100
undiff-100: --
diff-0
diff-0: --
diff-100
diff-100: --
control
100 µM PQ
HO-1
MT-2
CuZnSOD
MnSOD
catalase
GPx-1
B
undiff-0
undiff-100
diff-0
diff-100
PQ (µM):

Figure 21. Effects of paraquat on keratinocyte expression of glutathione-S-transferases (GST).

Expression of the mRNA of the GST enzymes was assayed in undifferentiated (U) and differentiated (D) keratinocytes by realtime PCR (n = 3-6, ± SE) 24 hours after treatment with 100 μM paraquat. Panel A: Effects of paraquat on mRNA expression of GSTA1-2, GSTA3 and GSTA4. * $p < 0.01$, ** $p < 0.02$, paraquat-treated undifferentiated versus paraquat-treated differentiated cells. Panel B: Effects of paraquat on mRNA expression of GSTM1 and GSTP1.

Figure 21

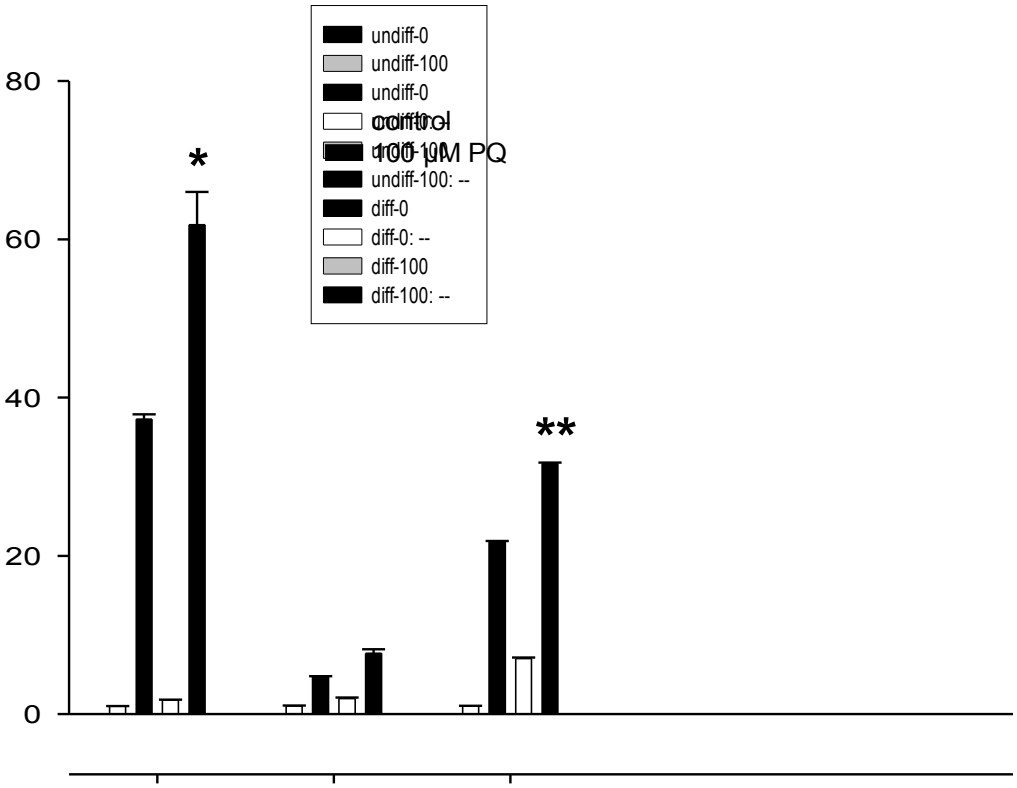
undiff-0
undiff-100
undiff-0
undiff-100
undiff-100: --
diff-0
diff-0: --
diff-100
diff-100: --
100 µM PQ
80
60
40
20
0
*
**

Figure 22. Production of prostaglandins is mediated by UVB light in keratinocytes. Keratinocytes were exposed to UVB (25 mJ/cm^2). After 24 hours, arachidonic acid (10 μM) was added to the medium, the cells were incubated for 20 minutes, methanol was added and the supernatants collected. The samples were fluorescence derivatized and prostaglandin production was detected using HPLC analysis.

Figure 22

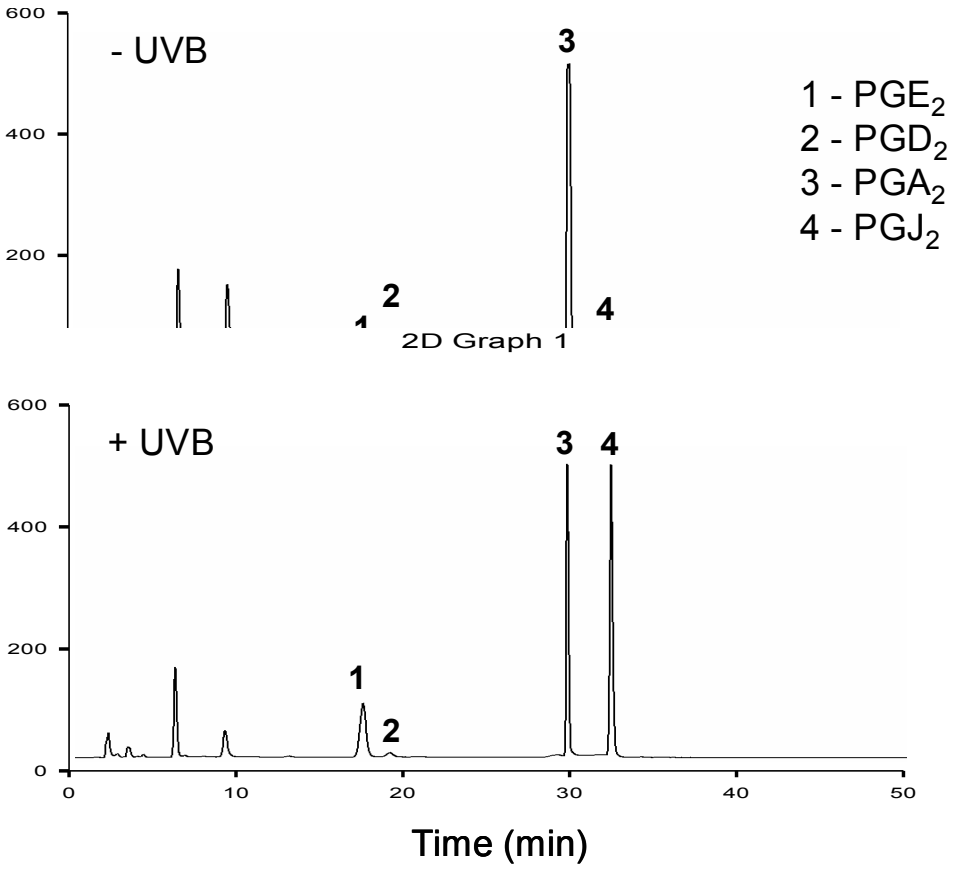
600
400
200
- UVB
3
2
4
1 - PGE2
2 - PGD2
3 - PGA2
4 - PGJ2
2D Graph 1
600
400
200
0
+ UVB
3
4
1
2
0
10
20
30
40
50
Time (min)

Figure 23. Effects of UVB light on expression of $cPLA_2$, PLCβ1, DAG lipase and MAG lipase mRNA in keratinocytes.

Undifferentiated and differentiated keratinocytes were exposed to UVB light at the indicated doses. After 24 hours, cells were analyzed for by realtime PCR (n = 3-6, ± SE) for mRNA expression of $cPLA_2$, PLCβ1, DAG lipase and MAG lipase.

Figure 23

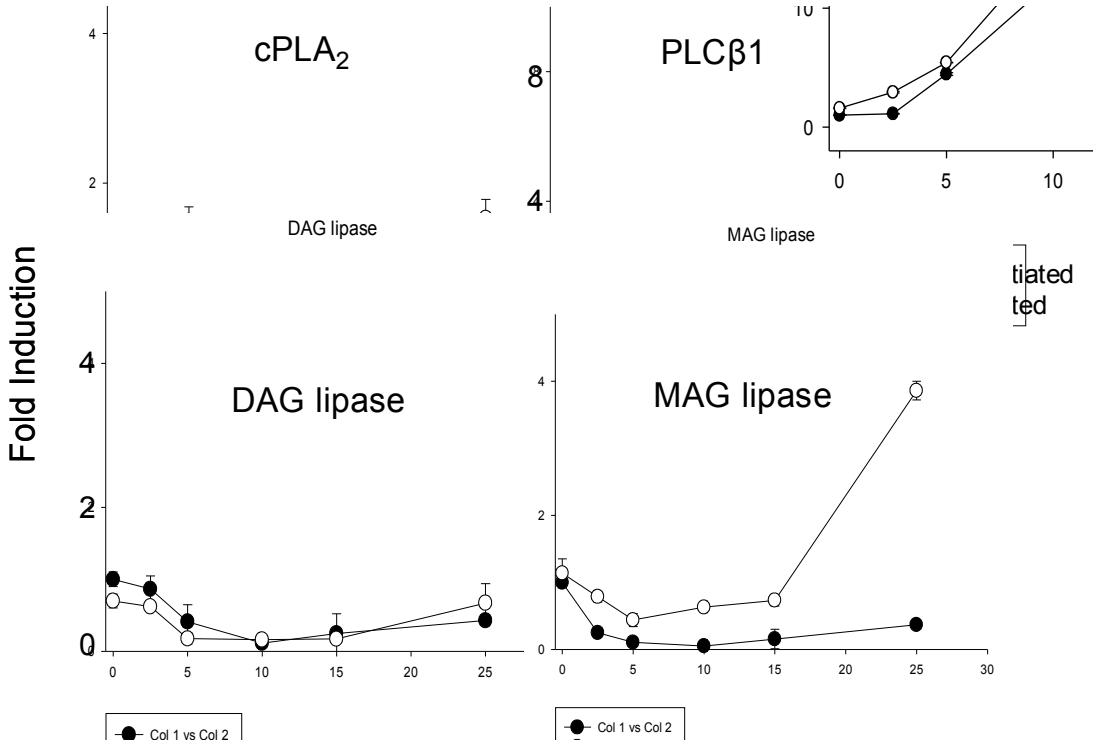
cPLA2
PLCβ1
DAG lipase
MAG lipase
Fold Induction
tiated
ted
DAG lipase
MAG lipase
Col 1 vs Col 2
Col 1 vs Col 2

Figure 24. Effects of UVB light on expression of COX-1 in keratinocytes.

Undifferentiated and differentiated keratinocytes were exposed to UVB light at the indicated doses. After 24 hours, cells were analyzed for COX-1 mRNA expression by realtime PCR (n = 3-6, ± SE).

Figure 24

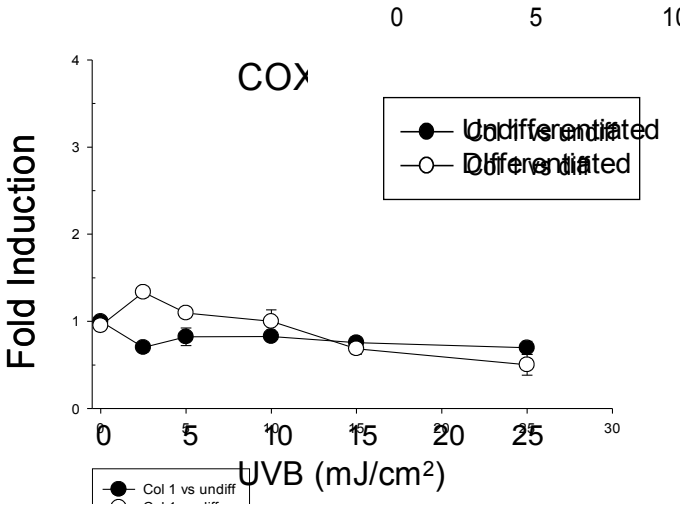
0
5
1(
COX
Undifferentiated
Differentiated
Fold Induction
0
1
2
3
4
0
5
10
15
20
25
30
UVB (mJ/cm²)
Col 1 vs undiff

Figure 25. Effects of UVB light on mRNA expression of the prostanoid synthases. Undifferentiated and differentiated keratinocytes were exposed to UVB light at the indicated doses. After 24 hours, mRNA expression of mPGES-1, mPGES-2, PGDS, PGFS, PGIS and TXAS was determined using real-time PCR (n = 3-6, ± SE).

Figure 25

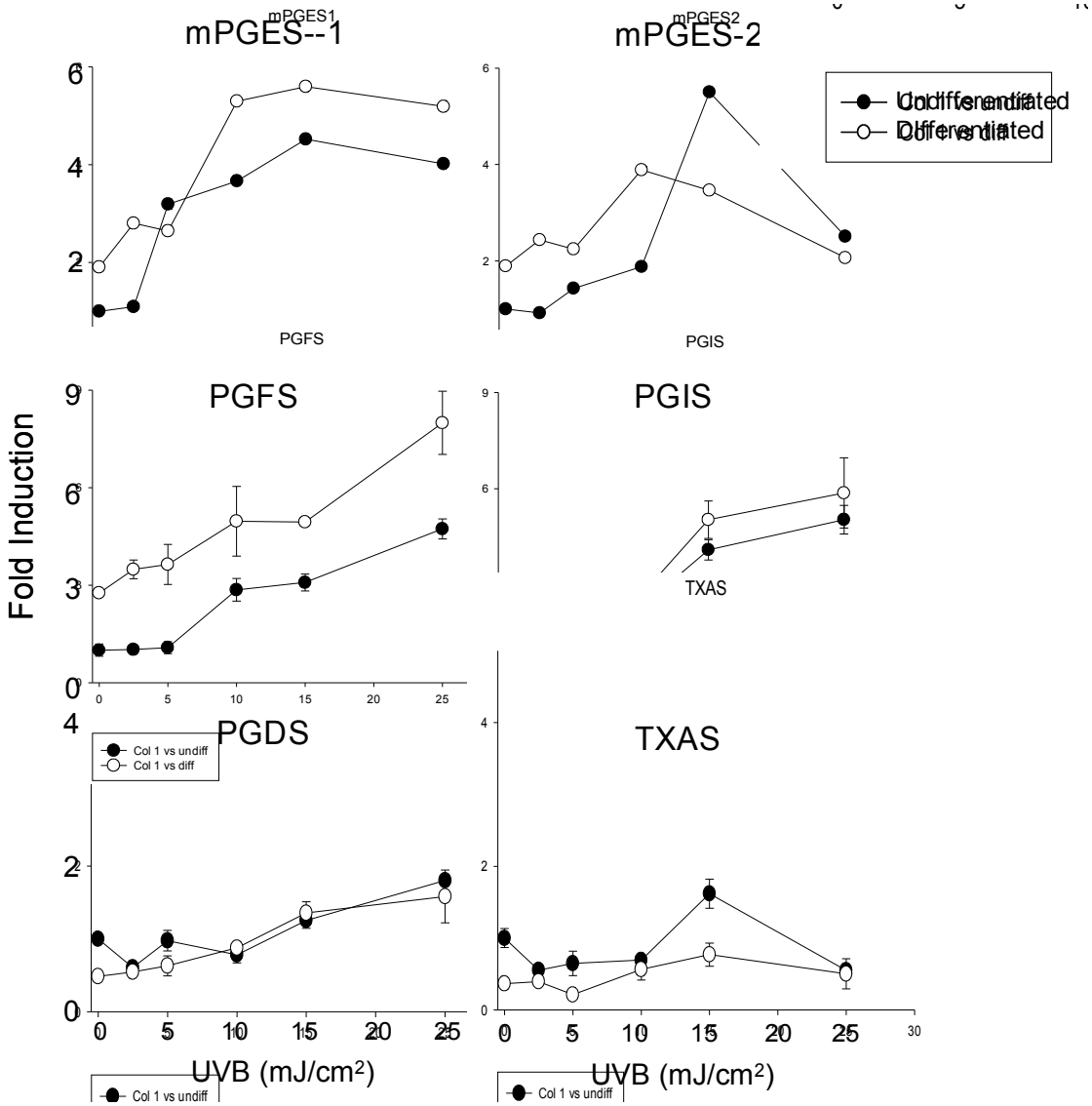
mPGES1
mPGES--1
mPGES2
mPGES-2
Col 1 vs undiff
Col 1 vs diff
PGFS
PGIS
Fold Induction
PGFS
PGIS
TXAS
PGDS
TXAS
Col 1 vs undiff
Col 1 vs diff
UVB (mJ/cm²)
UVB (mJ/cm²)
Col 1 vs undiff

Figure 26. Effects of UVB light on expression of the prostaglandin E_2 receptors.

Undifferentiated and differentiated keratinocytes were exposed to UVB light at the indicated doses. After 24 hours, cells were analyzed for mRNA expression of the PGE_2 receptors, EP1, EP2, EP3 and EP4, by realtime PCR (n = 3-6, ± SE).

Figure 26

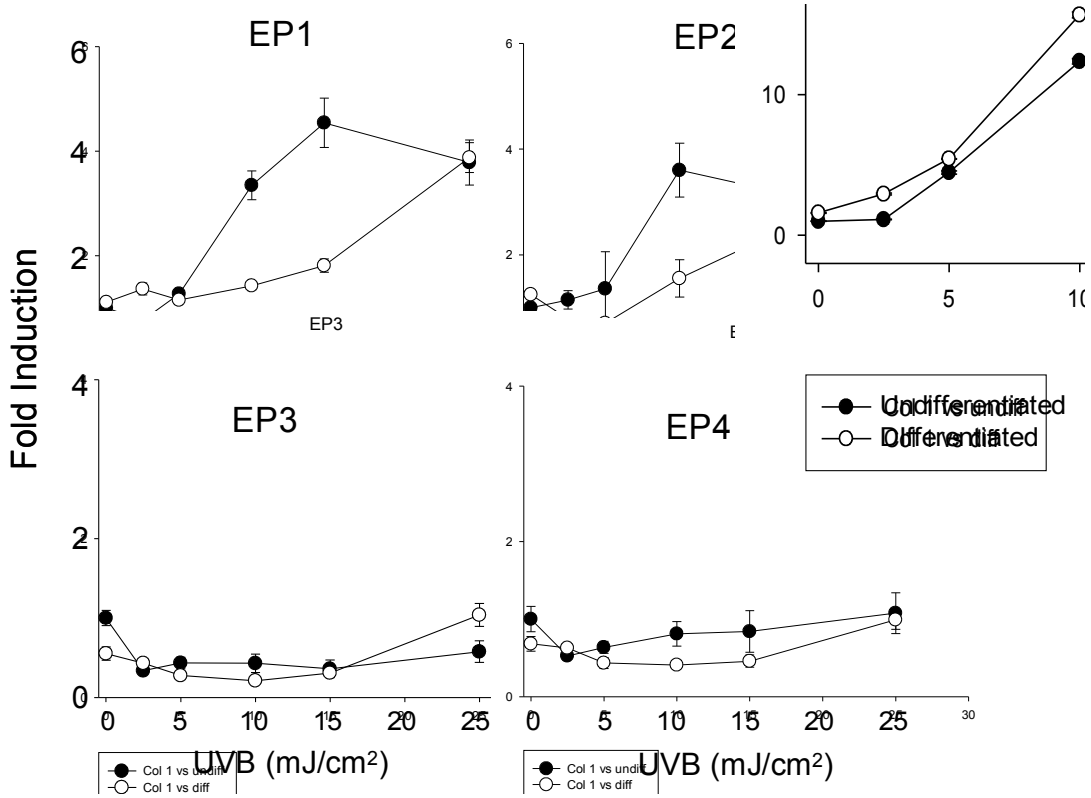
EP1
EP2
EP3
EP4
Fold Induction
UVB (mJ/cm²)
Col 1 vs undiff
Col 1 vs diff
Undifferentiated
Differentiated

Figure 27. Effects of UVB light on expression of the prostaglandin D_2, F_2, and I_2 and thromboxane A_2 receptors.

Undifferentiated and differentiated keratinocytes were exposed to UVB light at the indicated doses. After 24 hours, cells were analyzed for mRNA expression of the PGD_2 receptors, DP and CRTH2; PGF_2 receptor, FP; PGI_2 receptor, IP; and TXA_2 receptor, TP by realtime PCR (n = 3-6, ± SE).

Figure 27

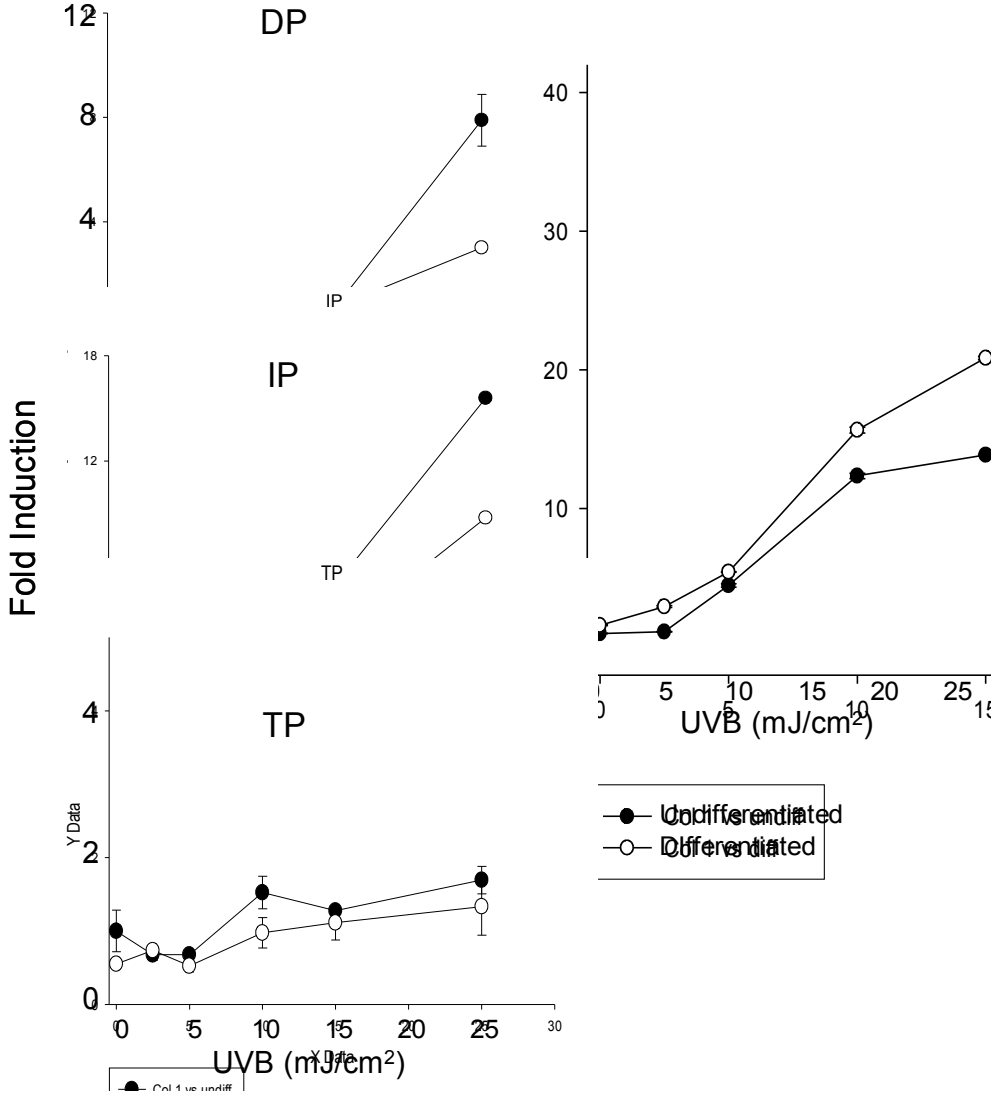
DP
IP
TP
Fold Induction
UVB (mJ/cm²)
Y Data
Undifferentiated
Differentiated

Figure 28. Effects of UVB light on expression of the lipoxygenases.

Undifferentiated (U) and differentiated (D) keratinocytes were exposed to UVB light at the indicated doses. After 24 hours, cells were analyzed for mRNA expression of FLAP, 5-LOX, 8-LOX, 12-LOX epidermal and platelet types and 15-LOX by real-time PCR ($n = 3\text{-}6, \pm SE$).

Figure 28

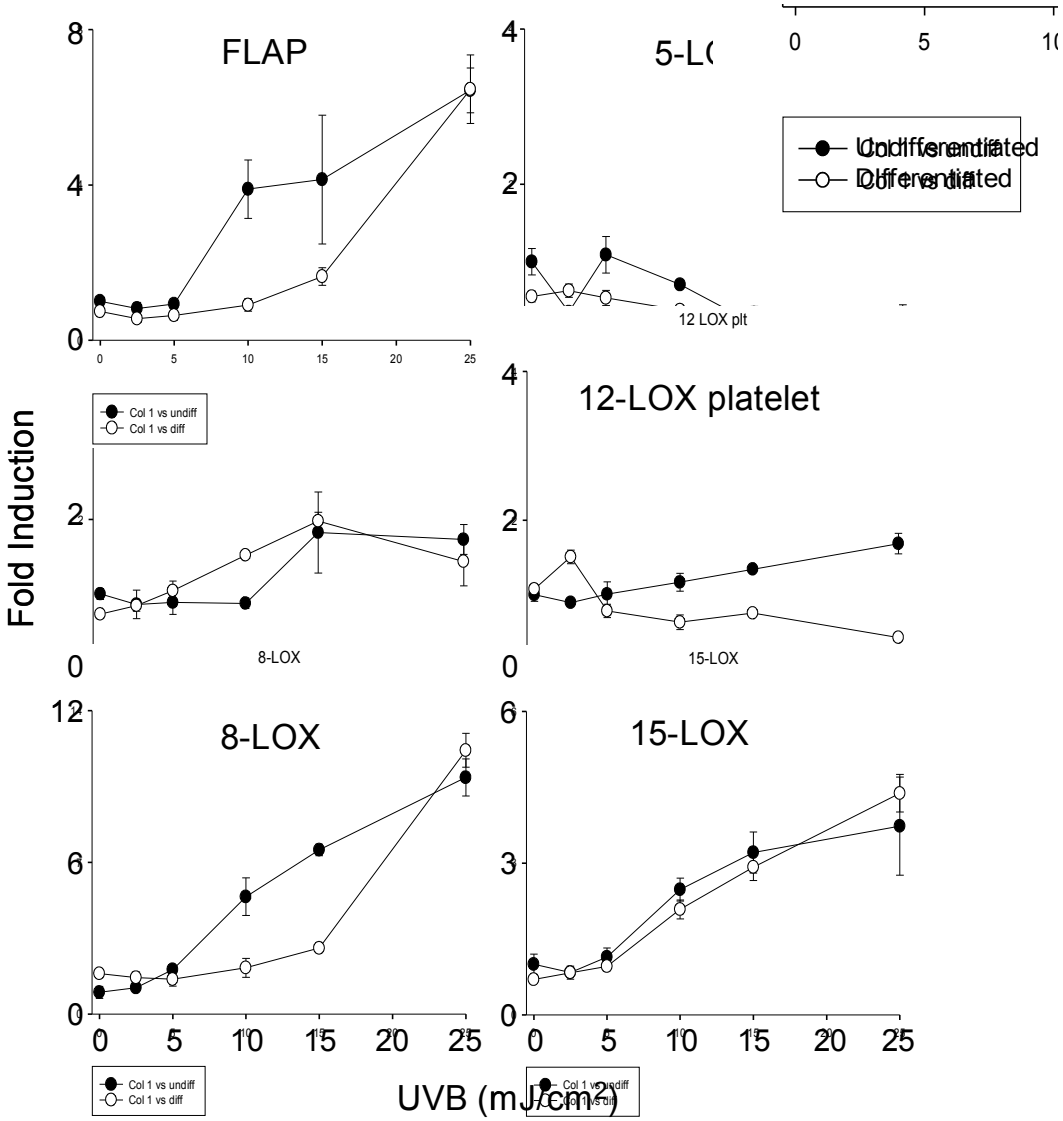
FLAP
5-LO
12 LOX plt
12-LOX platelet
8-LOX
15-LOX
Col 1 vs undiff
Col 1 vs diff
Fold Induction
UVB (mJ/cm2)

Figure 29. Effects of UVB light on expression of the leukotriene synthesis enzymes. Undifferentiated (U) and differentiated (D) keratinocytes were exposed to UVB light at the indicated doses. After 24 hours, cells were analyzed for mRNA expression of LTA_4 hydrolase and LTC_4 synthase by real-time PCR (n = 3-6, ± SE).

Figure 29

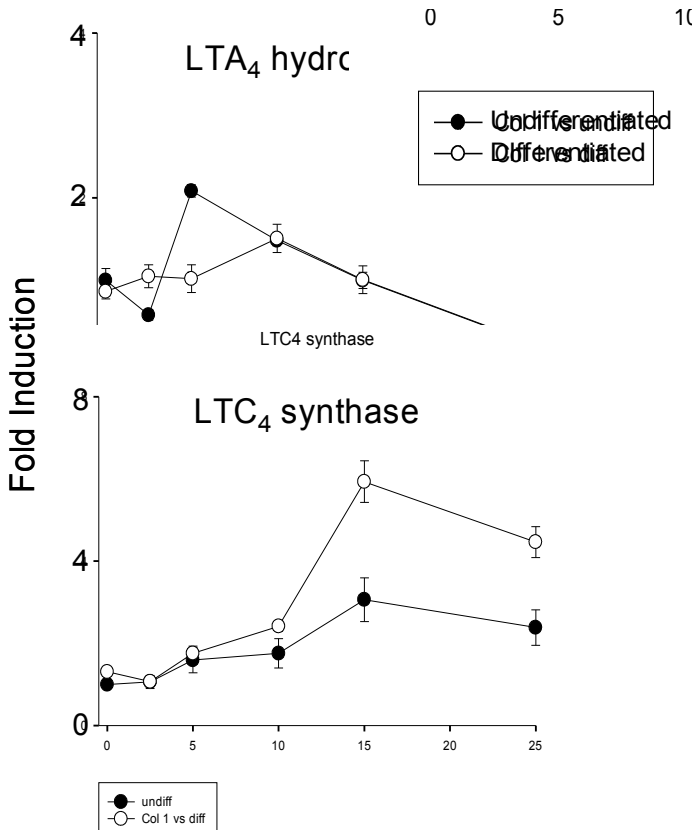
0
5
10
4
LTA4 hydrc
Undifferentiated
Differentiated
2
LTC4 synthase
Fold Induction
8
LTC4 synthase
4
0
0
5
10
15
20
25
undiff
Col 1 vs diff

Figure 30. Effects of UVB light on expression of the leukotriene receptors.

Undifferentiated and differentiated keratinocytes were exposed to UVB light at the indicated doses. After 24 hours cells were analyzed for mRNA expression of the LTB_4 receptors, BLT1 and BLT2, and the cysteinyl leukotriene receptors, CysLT1 and CysLT2, by realtime PCR (n = 3-6, ± SE).

Figure 30

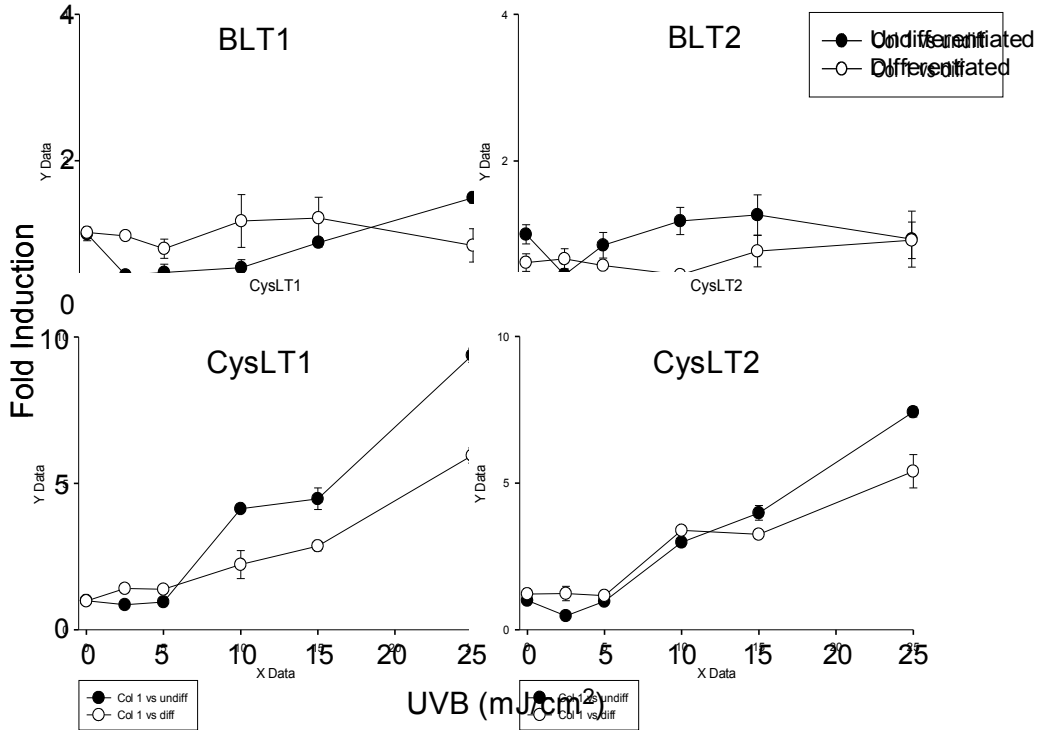
BLT1
BLT2
CysLT1
CysLT2
Undifferentiated
Differentiated
Col 1 vs undiff
Col 1 vs diff
Y Data
X Data
Fold Induction
UVB (mJ/cm2)

Figure 31. Effects of UVB light on mRNA expression of the MAPEG family enzymes. Undifferentiated and differentiated keratinocytes were exposed to UVB light at the indicated doses. After 24 hours, cells were analyzed for FLAP, mPGES-1, LTC_4 synthase, mGST1, mGST2 and mGST3 mRNA expression by real-time PCR (n = 3-6, ± SE).

Figure 31

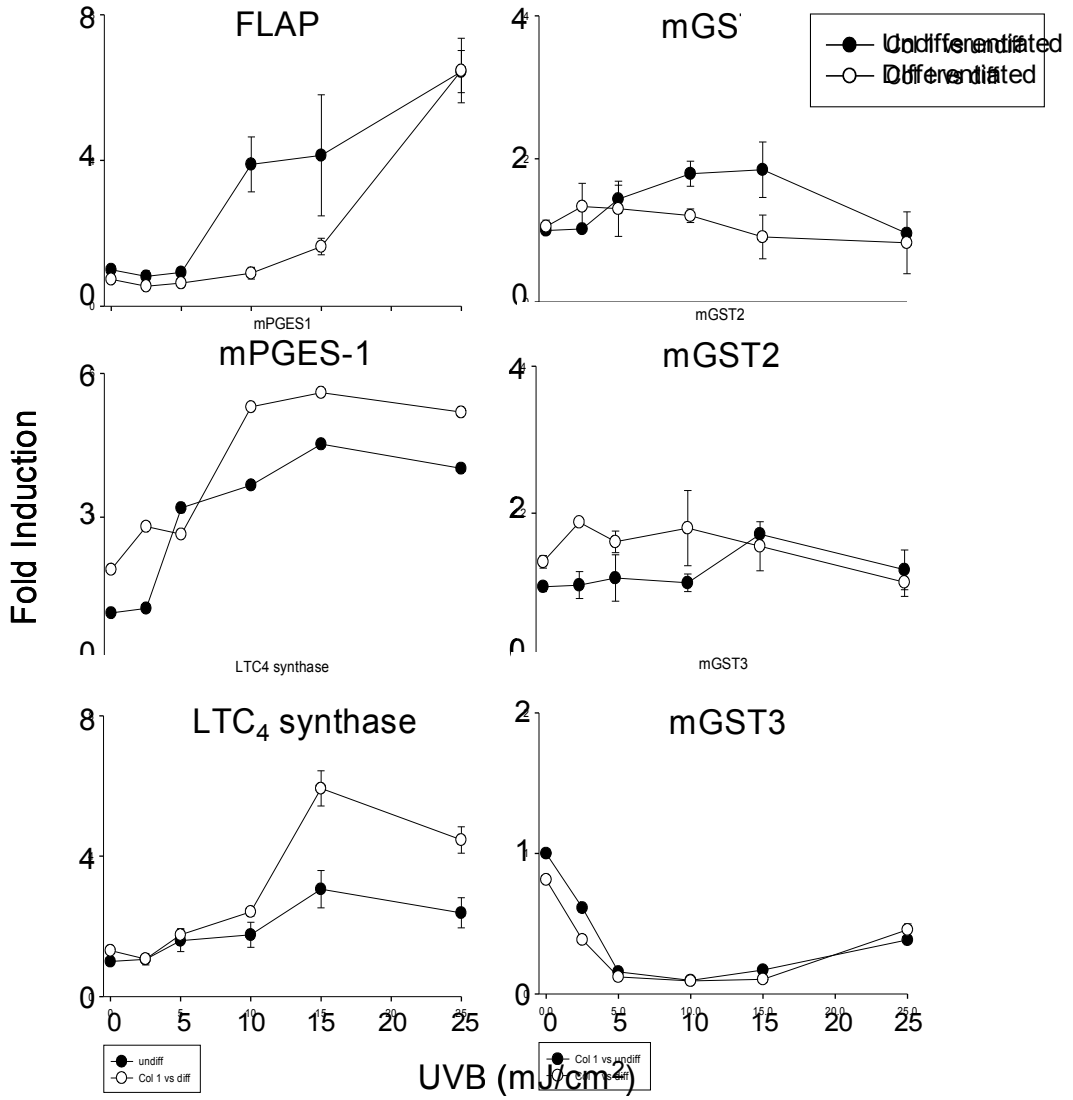
FLAP
mGS
mPGES1
mGST2
mPGES-1
mGST2
LTC4 synthase
mGST3
LTC4 synthase
mGST3
Fold Induction
UVB (mJ/cm2)
undiff
Col 1 vs diff
Col 1 vs undiff

Figure 32. Effects of MAP kinase inhibitors on UVB induction of COX-2, mPGES-1 and PGIS expression.

Undifferentiated and differentiated keratinocytes were incubated with SB203580 (10 μM), a p38 MAP kinase inhibitor or SP600125 (20 μM), a JNK MAP kinase inhibitor, for 3 hours and then exposed to UVB light at the indicated doses. After 24 hours, cells were analyzed for mRNA expression by real-time PCR (n = 3-6, ± SE).

Figure 32

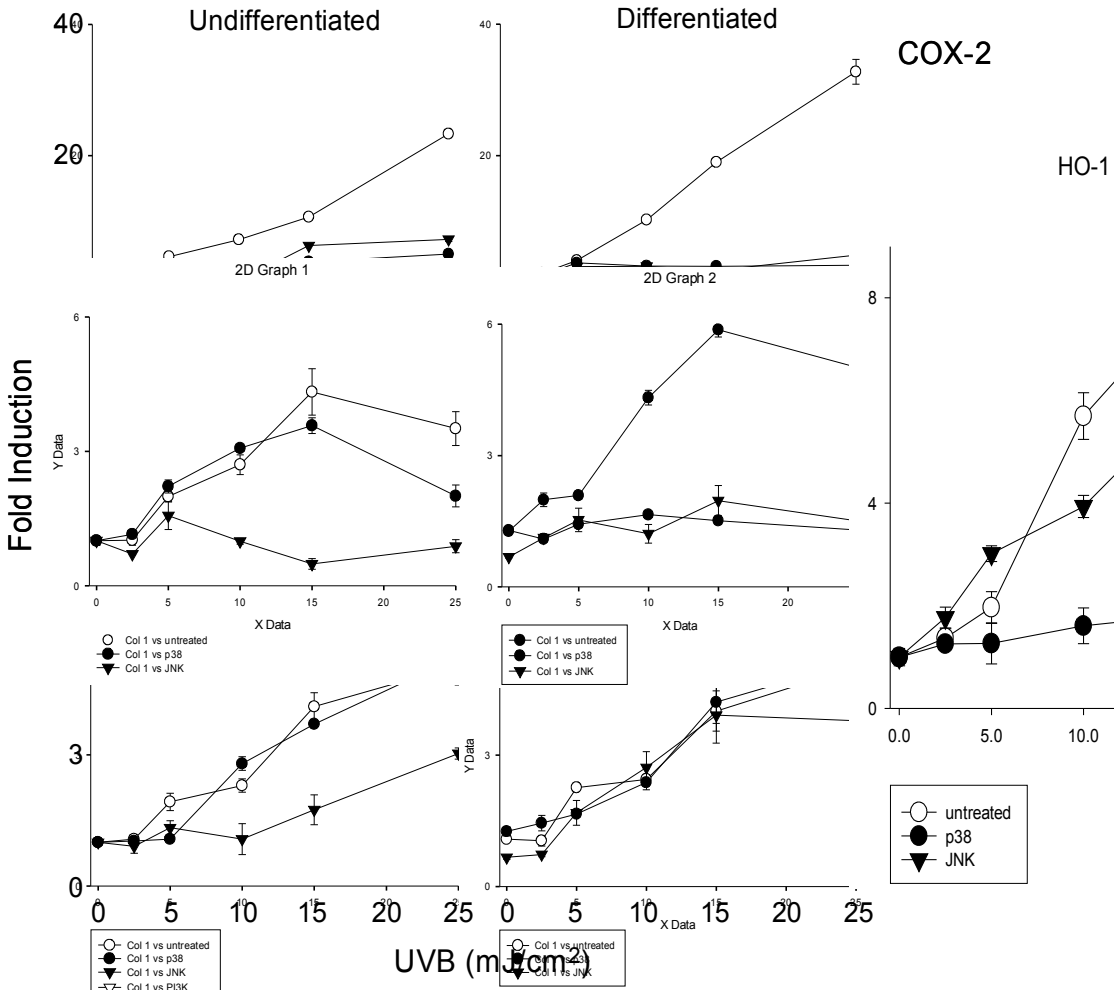
Undifferentiated
Differentiated
COX-2
HO-1
2D Graph 1
2D Graph 2
Fold Induction
Y Data
X Data
Col 1 vs untreated
Col 1 vs p38
Col 1 vs JNK
Col 1 vs PI3K
untreated
p38
JNK
UVB (mJ/cm2)

Figure 33. Effects of MAP kinase inhibitors on UVB induction of 8-LOX and 15-LOX expression.

Undifferentiated and differentiated keratinocytes were incubated with SB203580 (10 μM), a p38 MAP kinase inhibitor or SP600125 (20 μM), a JNK MAP kinase inhibitor, for 3 hours and then exposed to UVB light at the indicated doses. After 24 hours, cells were analyzed for mRNA expression by real-time PCR (n = 3-6, ± SE).

Figure 33

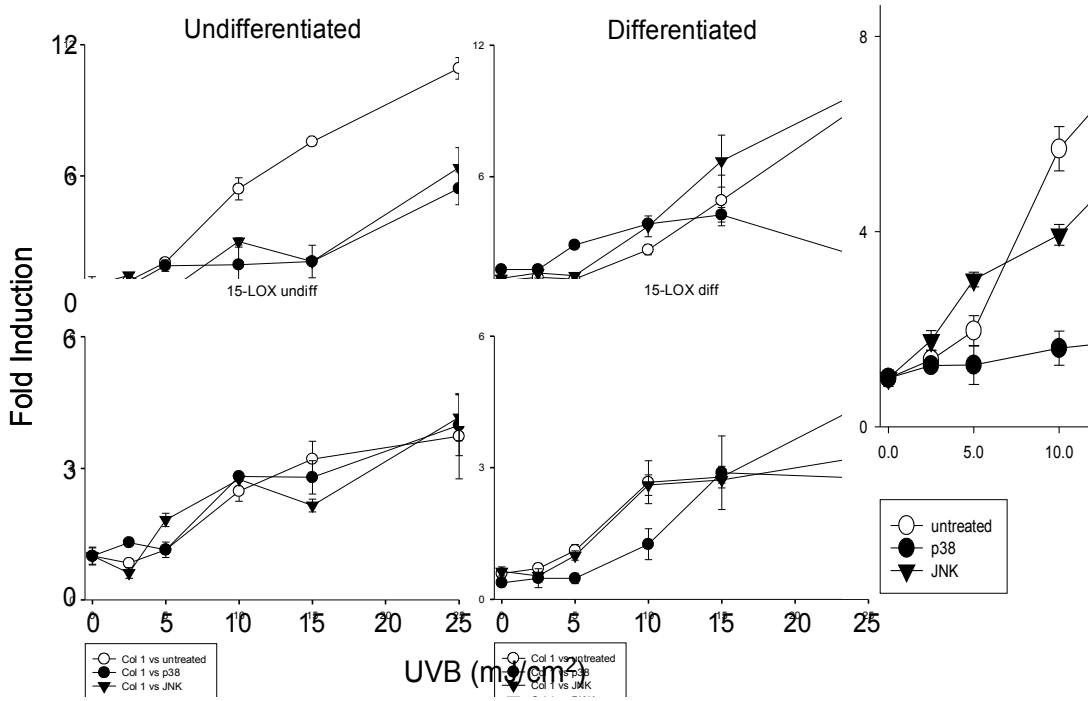
Undifferentiated
Differentiated
15-LOX undiff
15-LOX diff
Fold Induction
UVB (mJ/cm2)
Col 1 vs untreated
Col 1 vs p38
Col 1 vs JNK
untreated
p38
JNK

Figure 34. UVB light activates Akt in keratinocytes.

Undifferentiated and differentiated keratinocytes were exposed to UVB light at the indicated doses. At 15 minutes post-UVB exposure, the cells were lysed and analyzed for protein expression by Western blotting. The blots were probed for the total and phosphorylated forms of Akt kinase.

Figure 34

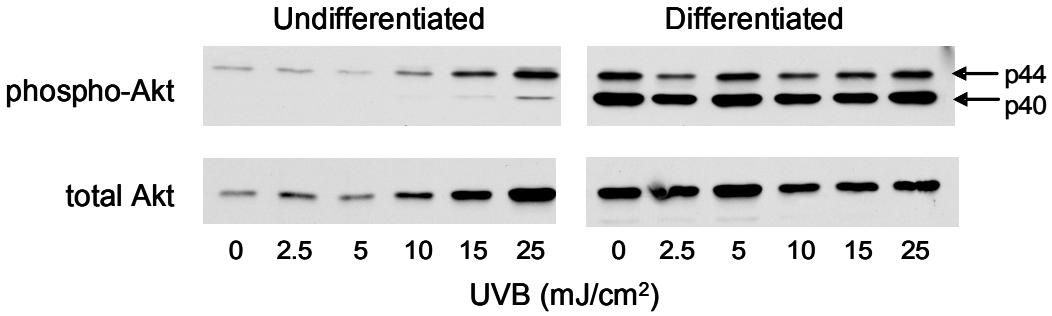
Undifferentiated
Differentiated
phospho-Akt
total Akt
p44
p40
0 2.5 5 10 15 25 0 2.5 5 10 15 25
UVB (mJ/cm2)

Figure 35. UVB mediates COX-2, mPGES-1 and PGIS expression through activation of Akt kinase.

Undifferentiated and differentiated keratinocytes were incubated with Wortmannin (0.1 μM), a PI3-kinase inhibitor, for 3 hours and then exposed to UVB light at the indicated doses. After 24 hours, cells were analyzed for mRNA expression by real-time PCR (n = 3-6, ± SE).

Figure 35

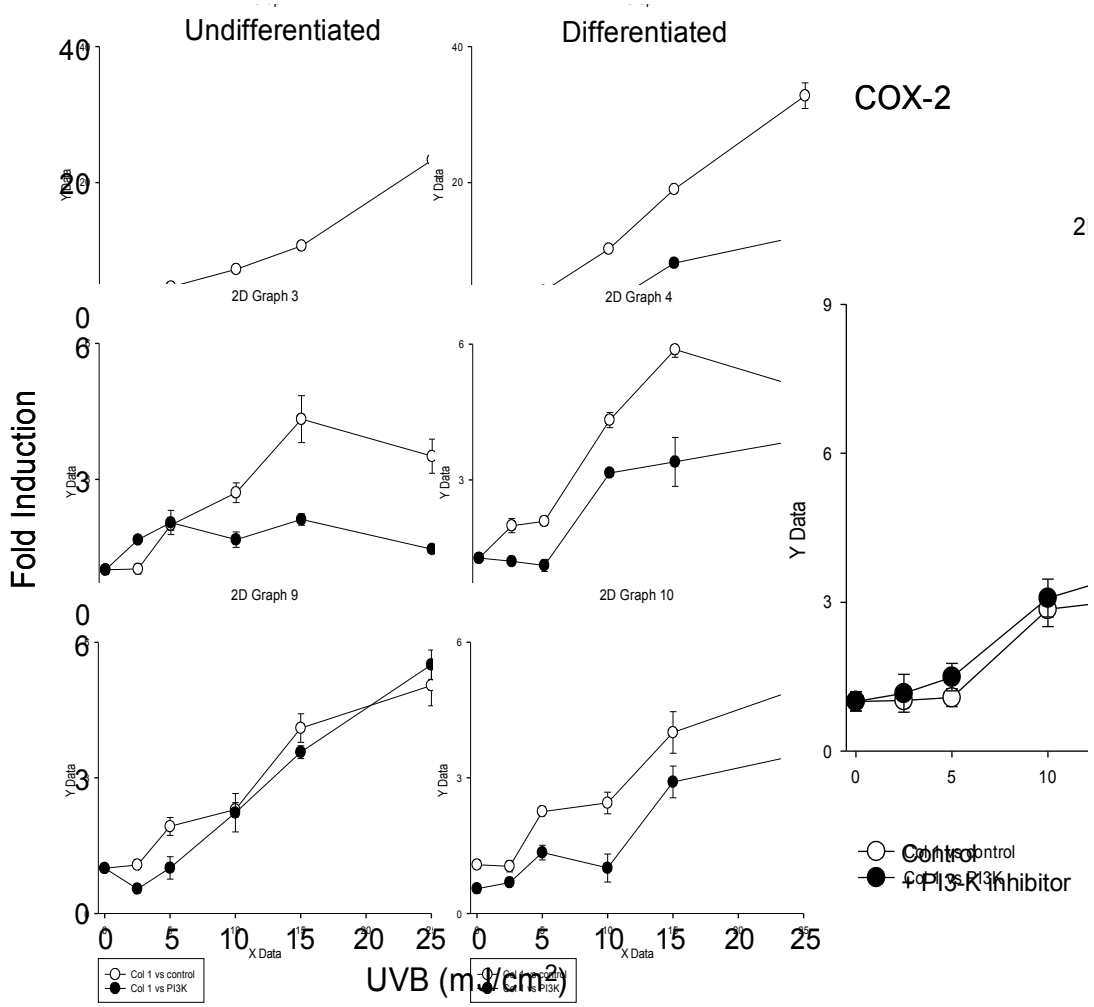
Undifferentiated
Differentiated
COX-2
2D Graph 3
2D Graph 4
2D Graph 9
2D Graph 10
Y Data
X Data
Fold Induction
UVB (mJ/cm2)
Col 1 vs control
Col 1 vs PI3K
Control
+PI3-K Inhibitor

Figure 36. UVB light-induced expression of 8-LOX and 15-LOX is mediated by Akt kinase.

Undifferentiated and differentiated keratinocytes were incubated with Wortmannin (0.1 μM), a PI3-kinase inhibitor, for 3 hours and then exposed to UVB light at the indicated doses. After 24 hours, cells were analyzed for mRNA expression of 8-LOX and 15-LOX by real-time PCR (n = 3-6, ± SE).

Figure 36

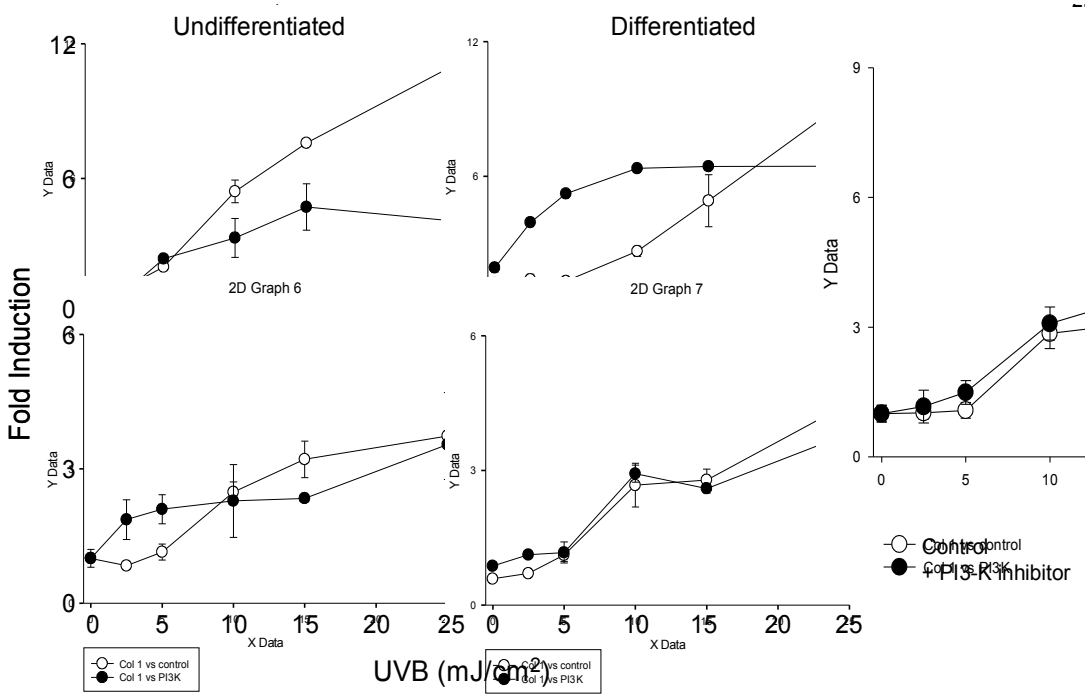
Undifferentiated
Differentiated
Fold Induction
Y Data
X Data
2D Graph 6
2D Graph 7
Col 1 vs control
Col 1 vs PI3K
UVB (mJ/cm2)
Control
+ PI3-K inhibitor

Figure 37. Effects of paraquat on mRNA expression of $cPLA_2$, COX-1 and COX-2. Undifferentiated (U) and differentiated (D) keratinocytes were treated with paraquat (100 μM). After 24 hours, cells were analyzed for mRNA and protein expression by realtime PCR (n = 3, ± SE) and Western blotting, respectively. Panel A: mRNA expression of $cPLA_2$, COX-1 and COX-2. Panel B: Protein expression of COX-2.

Figure 37

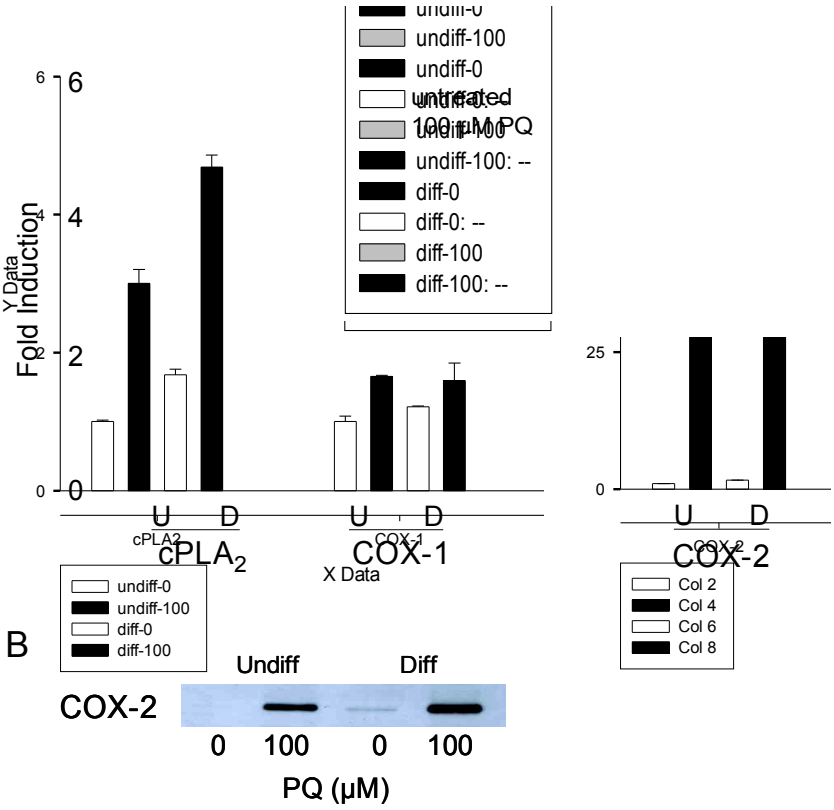
undiff-0
undiff-100
undiff-0
untreated
100 µM PQ
undiff-100: --
diff-0
diff-0: --
diff-100
diff-100: --
Y Data
Fold Induction
6
4
2
0
U
D
cPLA2
COX-1
cPLA2
COX-1
X Data
25
COX-2
Col 2
Col 4
Col 6
Col 8
B
undiff-0
undiff-100
diff-0
diff-100
Undiff
Diff
COX-2
0
100
0
100
PQ (µM)

Figure 38. Effects of paraquat on mRNA expression of the prostanoid synthases.

Undifferentiated (U) and differentiated (D) keratinocytes were treated with paraquat (100 μM). After 24 hours, mRNA expression of mPGES-1, mPGES-2, PGDS, PGFS, PGIS and TXAS was determined using real-time PCR (n = 3, ± SE).

Figure 38

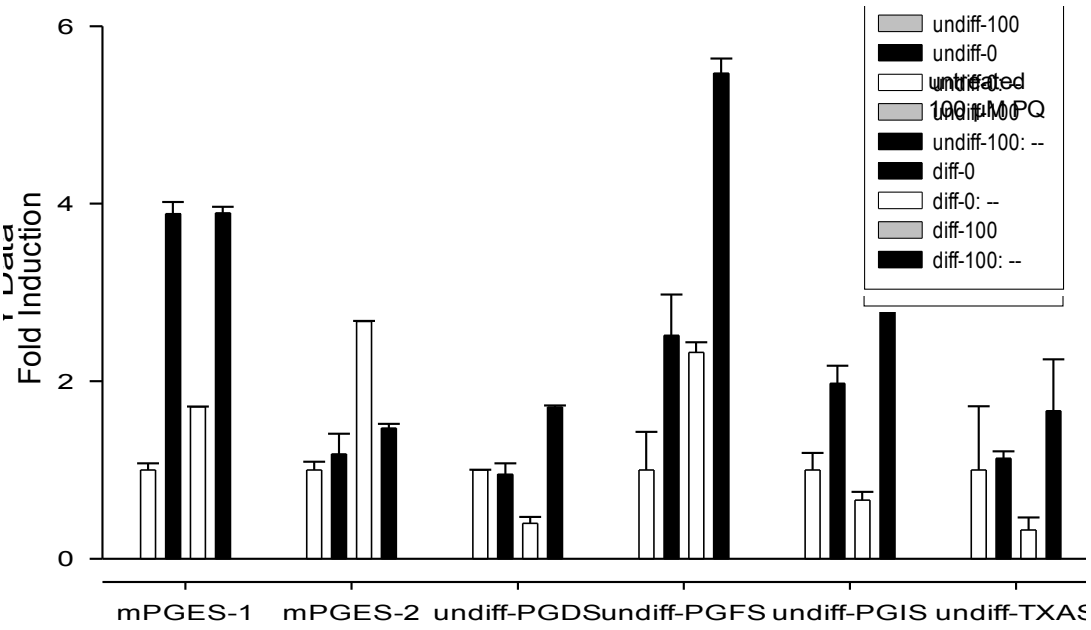
Fold Induction
6
4
2
0
undiff-100
undiff-0
untreated
100 µM PQ
undiff-100: --
diff-0
diff-0: --
diff-100
diff-100: --
mPGES-1
mPGES-2
undiff-PGDS
undiff-PGFS
undiff-PGIS
undiff-TXAS

Figure 39. Effects of paraquat on mRNA expression of lipoxygenase pathway enzymes. Undifferentiated (U) and differentiated (D) keratinocytes were treated with paraquat (100 μM). After 24 hours, mRNA expression of 5-LOX, FLAP, 8-LOX, 12-LOX platelet and epidermal types, 15-LOX, LTA_4 hydrolase and LTC_4 synthase was determined using real-time PCR (n = 3, ± SE).

Figure 39

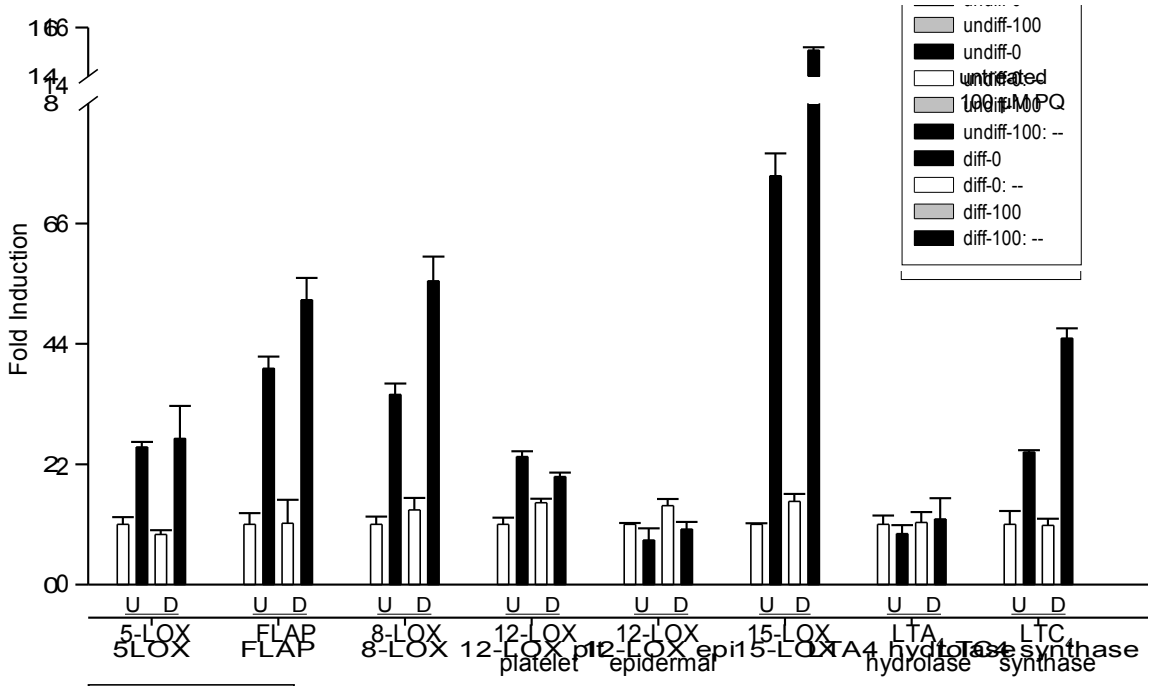
Fold Induction
undiff-100
undiff-0
undiff-0: --
undiff-100
undiff-100: --
diff-0
diff-0: --
diff-100
diff-100: --
U D
5-LOX
FLAP
8-LOX
12-LOX platelet
12-LOX epidermal
15-LOX
LTA4 hydrolase
LTC4 synthase
5LOX
FLAP
8-LOX
12-LOX pl
12-LOX epi
15-LOX
LTA4 hydrolase
LTC4 synthase

Figure 40. Effects of paraquat on mRNA expression of MAPEG enzymes.

Undifferentiated (U) and differentiated (D) keratinocytes were treated with paraquat (100 μM). After 24 hours, mRNA expression of mPGES-1, FLAP, LTC_4 synthase, mGST1, mGST2 and mGST3 was determined using real-time PCR (n = 3, ± SE).

Figure 40

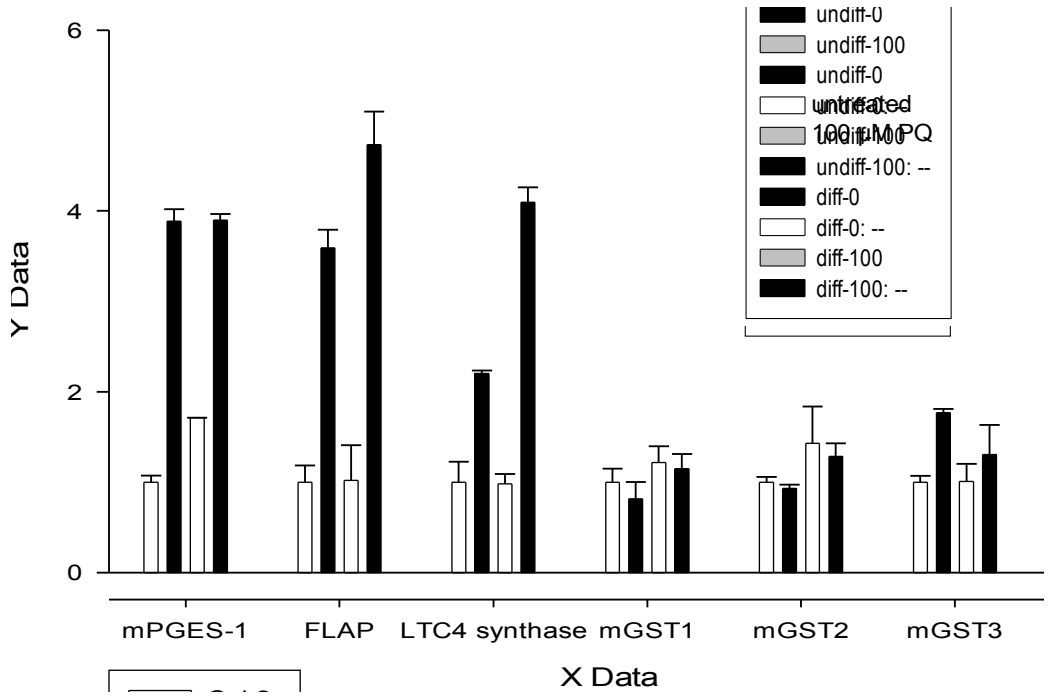
undiff-0
undiff-100
undiff-0
untreated
100 µM PQ
undiff-100: --
diff-0
diff-0: --
diff-100
diff-100: --
6
4
2
0
Y Data
mPGES-1
FLAP
LTC4 synthase
mGST1
mGST2
mGST3
X Data

Table 1. Realtime PCR primer sequences.

Gene	Forward (5'→3')	Reverse (5'→3')
β-actin	TCACCCACACTGTGCCCATCTACGA	GGATGCCACAGGATTCCATACCCA
catalase	ACCAGGGCATCAAAAACTTG	GCCCTGAAGCTTTTTGTCAG
BLT1	AATGGGCAACAGAGACAGGG	CCTGCAGCACCTTGTTCTCC
BLT2	GGCTTTCTTCAGTTCCAGCG	CCCGCAGTGAAGACATAGAGC
COX-1	GTCCCAGAACCAGGGTGTCT	CACTGGTAGTTGTCGAGGCCA
COX-2	CATTCTTTGCCCAGCACTTCAC	GACCAGGCACCAGACCAAAGAC
CRTH2	GTCACACTGAAGCCGCTCTG	TGGAAGCTGGACCATCTCCT
CysLT1	TGTACATTGCCTCTCCGTGTG	GAGCCACTTGCCTTTGTGAAC
CysLT2	CATGCTCAACCTGGCCACTT	AAGGGCAAGGTGCTGATGAA
DAG lipase	TTCGCCGAGTTCATTGACAG	TCTCAGGCACCATCATGCA
DP	TAAAGGAACTGCTGCCTGCC	AGGCGAACGTTTCGCATAAC
EP1	CTGGGCCTAACCAAGAGTGC	CCGGGAACTACGCAGTGAAC
EP2	GTTTCACGTGCTGGTAACGGA	CAGGTTCCCAGCAGGTCAGT
EP3	ATGGGAAAGGAGAAGGAGTGC	AGCCAGGCGAACTGCAATTA
EP4	TTTGCGAATTTCCGAGACCT	CTCTCAGAGTCCTGGCCCTG
FLAP	GGTGGAGCATGAAAGCAAGG	CCGGTCCTCTGGAAGCTTC
FP	TCCAAGCAGCCAGTGTCTCC	GCAGGTTGTGTTTGCCATGA
IP	TGGGTCTTCATCCTTTTCCG	CCAGAACTTGAGGCGTTGGA
mGST1	GCTTTGGCAAGGGAGAGAATG	CCTTCTCGTCAGTGCGAACA
mGST2	TGCAGCCTGTCTGGGTCTC	CAGAAATACTTGTGACGGGCG
mGST3	GGAGGTGTACCCTCCCTTCC	TGGTAAACACCTCCCACCGT
GSTA1-2	CAGAGTCCGGAAGATTTGGA	CAAGGCAGTCTTGGCTTCTC
GSTA3	GCAAGCCTTGCCAAGATCAA	GGCAGGGAAGTAACGGTTCC
GSTA4	CCCTTGGTTGAAATCGATGG	GAGGATGGCCCTGGTCTGT
GSTM1	CCTACATGAAGAGTAGCCGCTACA	TAGTGAGTGCCCGTGTAGCAA
GSTP1	CCTTGGCCGCTCTTTGG	GGCCTTCACGTAGTCATTCTTACC
GPx-1	GGTTCGAGCCCAATTTTACA	TCGATGTCGATGGTACGAAA
HO-1	CCTCACTGGCAGGAAATCATC	CCTCGTGGAGACGCTTTACATA
hydrolase	CTCACGGTCCAGTCACAGGA	TGTGTCCAAAGTCAGGCTGC
synthase	GGACGAAGTGGCTCTTCTGG	TGCAACAGAACTCCCACGAG
5-LOX	AGGGAGAAGCTGTCCGAGT	GCAGAGGCCGTGAAGATCAC
8-LOX	TGTTTGCACACTGGCAGGAA	CATTTAGGAACTGGGAGGCG
12-LOX epi	AAGTTCCTTGGCAGACGCC	TCTTTATGCTGCCCCAGGG
12-LOX plt	ACCAGCAAGGACGACGTGAC	ATCAGGTAGCGACCCCATCA
15-LOX	TCGGAGGCAGAATTCAAGGT	CAGCAGTGGCCCAAGGTATT
MAG lipase	TGCTTTGGCATACAGCTGCT	CATTGCTCGCTCCACTCTTG
MT-2	TGCAGGAAGTACATTTGCATTGTT	TTTTCTTGCAGGAAGTACATTTGC
$cPLA_2$	AGCCATCCAGGCATCAAAGA	TGCCCTATCCCATCTTTGCA

Gene	Forward (5'→3')	Reverse (5'→3')
PLCβ1	CTCCAAGCGAAACCAGGACA	CGGTGTGATTCACCCCATTC
PGDS	CTGCTCTGAGCAAATGGCTG	AGGACCAAACCCATCCACAG
mPGES-1	GGCCTTTCTGCTCTGCAGC	GCCACCGCGTACATCTTGAT
mPGES-2	AGCCCCTGGAAGAGGTCATC	CATTCATGGCCTTCATGGGT
PGFS	GAGGAAGTAGGGCTGGCCAT	CCTCACAGTGCCATCAGCAA
PGIS	ATCTGCTGCTCCCCAAACTG	CTTTATCCCCCGCTGACAAG
CuZn-SOD	ACCAGTGCAGGACCTCATTTTAA	TCTCCAACATGCCTCTCTTCATC
Mn-SOD	CACATTAACGCGCAGATCATG	CCAGAGCCTCGTGGTACTTCTC
TNFα	AAATTCGAGTGACAAGCCGTA	CCCTTGAAGAGAACCTGGGAGTAG
TP	TACAGTGTGCAGTACCCCGG	CTGTGTCCCGAGTGTCAGGA
TXAS	CCCCAAGCCTTCTCCTTTTG	AAACCCTGGCGGAAAAACAT

VITA

ADRIENNE T. BLACK

1982.86	Cook College, Rutgers University B.S., Biology
1986.88	Laboratory Technician Sera-Tec Biologicals North Brunswick, New Jersey
1988.2002	Medical Technologist Robert Wood Johnson University Hospital New Brunswick, New Jersey
1991-94	Cook College, Rutgers University B.S., Environmental Science
1994-97	Rutgers University M.S., Environmental Science
2004.5	Teaching Assistant Department of Pharmacology and Toxicology Rutgers University New Brunswick, New Jersey
2005.7	Predoctoral Fellow New Jersey Commission on Cancer Research Rutgers University-UMDNJ Piscataway, New Jersey
2002-07	Rutgers University Ph.D, Toxicology